1.0 | 45 | 2.8 | 2.5
| 50 | 3.2 | 2.2
| 56 | 3.6 |
| 03 | 40 | 2.0
1.1 | | | 1.8
1.25 | 1.4 | 1.6

MICROCOPY RESOLUTION TEST CHART
NATIONAL BUREAU OF STANDARDS-1963-A

AFOSR-TR. 85-0087

FINAL REPORT

"RESEARCH ON THERMIONIC PLASMAS"

Prepared for

United States Air Force Office of Scientific Research
Contract Number AFOSR-83-0048
Contract Period: January 15, 1983 to June 30, 1984

Prepared by

G. L. Main and S. H. Lam

Principal Investigator
Sau-Hai Lam
Department of Mechanical and Aerospace Engineering
Princeton University
Princeton, New Jersey 08544

June 1984

DTIC
ELECTE
FEB 2 7 1985
A

SECURITY CLASSIFICATION OF THIS PAGE

REPORT DOCUMENTATION PAGE

1a. REPORT SECURITY CLASSIFICATION	1b. RESTRICTIVE MARKINGS	
Unclassified		
2a. SECURITY CLASSIFICATION AUTHORITY	3. DISTRIBUTION/AVAILABILITY OF REPORT	
	Approved for public release; distribution unlimited.	
2b. DECLASSIFICATION/DOWNGRADING SCHEDULE		
4. PERFORMING ORGANIZATION REPORT NUMBER(S)	5. MONITORING ORGANIZATION REPORT NUMBER(S)	
1662-MAE	AFOSR-TR- 85-0087	

6a. NAME OF PERFORMING ORGANIZATION	6b. OFFICE SYMBOL (If applicable)	7a. NAME OF MONITORING ORGANIZATION
Princeton University		AFOSR/NA
6c. ADDRESS (City, State and ZIP Code)		7b. ADDRESS (City, State and ZIP Code)
Department of Mechanical & Aerospace Engineering, Princeton University, Princeton, New Jersey 08544		Bolling AFB DC 20332-6448

8a. NAME OF FUNDING/SPONSORING ORGANIZATION	8b. OFFICE SYMBOL (If applicable)	9. PROCUREMENT INSTRUMENT IDENTIFICATION NUMBER		
AFOSR	NA	AFOSR-83-0048		
8c. ADDRESS (City, State and ZIP Code)		10. SOURCE OF FUNDING NOS.		

		PROGRAM ELEMENT NO.	PROJECT NO.	TASK NO.	WORK UNIT NO.
AFOSR Bolling AFB 20332					
11. TITLE (Include Security Classification) Research on Thermionic Plasmas		61102F	2301	K2	

12. PERSONAL AUTHOR(S)
G. L. Main and S. H. Lam

13a. TYPE OF REPORT	13b. TIME COVERED	14. DATE OF REPORT (Yr., Mo., Day)	15. PAGE COUNT
Final	FROM 1/15/83 TO 6/30/84	1984 June 13th	157

16. SUPPLEMENTARY NOTATION

17. COSATI CODES			18. SUBJECT TERMS (Continue on reverse if necessary and identify by block number)
FIELD	GROUP	SUB. GR.	Energy Conversion Thermionic Plasma Theory
20.13			Thermionic Emissions
20.09			Sheath

19. ABSTRACT (Continue on reverse if necessary and identify by block number)

Emitter sheath phenomena are important in thermionic energy convertors because the emitter sheath forms the boundary conditions for the plasma in the gap and controls both the ion loss rate and the loss rate of hot (3000 K) plasma electrons to the emitter. This thesis examines three expected emitter sheath phenomena and their effects on convertor performance: 1) reflection of ions coming from the plasma; 2) ions trapped in the

20. DISTRIBUTION/AVAILABILITY OF ABSTRACT	21. ABSTRACT SECURITY CLASSIFICATION	
UNCLASSIFIED/UNLIMITED ☒ SAME AS RPT. ☒ DTIC USERS ☐	Unclassified	
22a. NAME OF RESPONSIBLE INDIVIDUAL	22b. TELEPHONE NUMBER (Include Area Code)	22c. OFFICE SYMBOL
LEONARD H CAVENY, Program Manager	(202) 767-4937	NA

DD FORM 1473, 83 APR   EDITION OF 1 JAN 73 IS OBSOLETE.   Unclassified

SECURITY CLASSIFICATION OF THIS PAGE

double emitter sheath; and 3) surface emission ions. Inclusion of these three phenomena combined with the elimination of previous sheath approximations requires careful analysis and calculation of the sheath structure. It is shown that the "Bohm" matching condition must be generalized to insure that self-consistency prevails throughout the entire sheath and not just at the plasma-sheath interface. Further, it is shown that plasma ion distribution coming into that sheath must have its low energy ions "cut off" to produce a self-consistent collisionless sheath, and that each of these emitter sheath phenomena reduce the normalized (by plasma density) net ion loss rate to the emitter.

Each of these phenomena also raise the normalized plasma density adjacent to the emitter. The higher plasma density at the emitter causes a greater increase in the loss of hot plasma electron energy to the emitter than the corresponding decrease in the loss of ionization energy (carried by the ions) to the emitter. Therefore these emitter sheath phenomena increase arc-drop. Within the limitations of the current thermionic convertor formulation, all three of these phenomena (which become significant at low currents) steepen the current-voltage characteristic. At low current densities, the present theory shows that the collector sheath height decreases, resulting in a larger electron diffusion velocity than can be justified for the continuum model used in the plasma region. The result of lower performance at lower current is in agreement with experimental studies, but the limitation imposed by the formulation prevent theoretical examination of the lower current region in which a plateau of improved performance is found.

TABLE OF CONTENTS

Accession For

NTIS CRA&I

DTIC TAB

Unannounced

Justification

Distribution/

Availability Codes

Avail and/or

Dist   Special

DTIC
COPY
INSPECTED
6

SUMMARY OF WORK

This document contains a complete reproduction of the Ph.D. dissertation of G. L. Main. The following paragraphs outline (chapter by chapter) the results of the research carried out under this contract.

Chapter 1 develops the basic principles of the thermionic convertor and its formulation. Since the formulation uses many approximations out of computational necessity, we present an overview of these approximations and the reasoning behind them. The fluid mechanical nature of the formulation yields some fundamental insight into how the sheath affects the convertor's performance, and gives some quantitative results on performance.

Chapter 2 carries out the formulation of the convertor for the general case and then for the isothermal electron case. These results are entirely conventional. We center on the isothermal electron case for its simplicity in explaining emitter sheath effects.

Chapter 3 on sheaths advances collisionless sheath theory to

cover the sheath phenomena under consideration. Previous sheath formulations have contained several mathematical simplifications which are incompatible with the study of these sheath phenomena. The simplifications are 1) monoenergetic ions from the plasma, 2) monoenergetic emitted electrons, and 3) that the sheath potential drop is large. Further, for these corrections, it is shown that the "Bohm" criterion for matching the sheath to the plasma must be generalized.

Chapter 4 presents isothermal results for the thermionic convertor including the effects of surface emission, trapped ions and reflected ions. The general result found here is that, contrary to intuition, a higher plasma density at the emitter increases arc-drop. All three emitter sheath phenomena produce a lower net ion loss rate and yield higher plasma density at the emitter.

Chapter 5 presents the results of non-isothermal calculations using an implicit numerical algorithm to confirm the isothermal results with ion reflection. However, detailed non-isothermal calculations with trapped ions surface emission ions are not carried out because the combination of the non-isothermal algorithm and the full collisionless sheath algorithm would require large amounts of CPU time.

Chapter 6 presents the conclusions of this work.

LIST of SYMBOLS

Symbol	First Use and Definition
a_e	II-13
a_E	II-13
a_i	II-18
A	II-19
C	II-19
d	I-10
f_{plasma}	III-21
f_{sur}	III-21
f_{tr}	III-21
$F(x)$	III-5
$F_e(x)$	III-12
$F_i(x)$	III-12
$F_{plasma}(x)$	III-12
$F_{sur}(x)$	III-12
$F_{tr}(x)$	III-12
h	II-4
j	II-13
j_i	II-16
J	I-8
J_{BS}	II-15
J_{cs+}	I-11
J_R	I-8
J_E	II-13
k	I-8

·

CHAPTER 1: INTRODUCTION

1.1 The Cesium Diode Convertor

1.2 Formulation for the Convertor

1.3 Emitter Sheath Effects

The thermionic energy convertor is perhaps the simplest and most direct heat engine in existence. It converts heat directly into electrical power by thermionic emission. The device essentially consists of two electrodes separated by a gap (typically .25 mm) containing cesium vapor at a low pressure (typically 1 torr). One of the two plates (the emitter) is heated by an external source to 1500 - 1750 K and the other (the collector) is kept at 750 - 800 K by an external sink. The hotter of the two plates emits electrons thermionically with a greater average velocity and a far greater density than the cooler plate. Because of the difference in emitted density and velocity, a potential rise develops from the emitter to the collector. Consequently, electrical power is generated directly. The convertor could operate with a vacuum gap; however a vacuum

gap is impractical because an extremely small gap (on the order

of 1 micron or less) would be required to prevent the build up

of a space charge of electrons which limits current density. [1]

Cesium is introduced into the gap to overcome the space charge

effects because cesium ionizes easily (a first ionization energy

of 3.89 eV). The cesium diode convertor, in its ignited mode, [2]

maintains a plasma electron temperature of approximately 3000 K

which supports the ionization of the cesium.

Emitter sheath phenomena are important in thermionic energy

convertors because the emitter sheath forms the boundary

conditions for the plasma in the gap and controls both the ion

loss rate and the loss rate of hot (3000 K) plasma electrons to

the emitter. This thesis examines three expected emitter sheath

phenomena and their effects on convertor performance: [3] 1)

reflection of ions coming from the plasma, 2) ions trapped in the

double emitter sheath, and 3) surface emission ions. Inclusion

of these three phenomena combined with the elimination of

previous sheath approximations requires careful analysis and

calculation of the sheath structure. It is shown that the "bohm"

----

[1] At 1 micron approximately 5 amps/cm^2 could pass through the
convertor under typical conditions.

[2] By ignited mode, we mean a plasma arc in which the electron
temperature is greater than the temperatures of the electrodes
bounding the plasma.

[3] The collector sheath does not have similar effects of any
significance because its low temperature makes it essentially
non-emitting.

matching condition must be generalized to insure that self-consistancy prevails throughout the entire sheath and not just at the plasma-sheath interface. Further, it is shown that plasma ion distribution coming into that sheath must have its low energy ions "cut off" to produce a self-consistant collisionless sheath, and that each of these emitter sheath phenomena reduce the normalized (by plasma density) net ion loss rate to the emitter.

Each of these phenomena also raise the normalized plasma density adjacent to the emitter. The higher plasma density at the emitter causes a greater increase in the loss of hot plasma electron energy to the emitter than the corresponding decrease in the loss of ionization energy (carried by the ions) to the emitter. Therefore these emitter sheath phenomena increase arc-drop. Within the limitations of the current thermionic converter formulation, all three of these phenomena (which become significant at low currents) steepen the current-voltage characteristic. At low current densities, the present theory shows that the collector sheath height decreases, resulting in a larger electron diffusion velocity than can be justified for the continuum model used in the plasma region. [*] The result of lower performance at lower current is in agreement with experimental studies, but the limitation imposed by the formulation prevent theoretical examination of the lower current region in which a

- - - - - - - - - - - - - - - - - - - -

[*] The limitations of the present formulation result from the asymptotic division of the plasma into a neutral plasma and a collisionless sheath.

plateau of improved performance is found.

The remainder of this chapter develops the basic principles of the thermionic convertor and its formulation. Since the formulation uses many approximations out of computational necessity, we present an overview of these approximations and the reasoning behind them. The fluid mechanical nature of the formulation yields some fundamental insight into how the sheath affects the convertor's performance, and gives some quantitative results on performance.

Chapter 2 carries out the formulation of the convertor for the general case and then for the isothermal electron case. These results are entirely conventional. We center on the isothermal electron case for its simplicity in explaining emitter sheath effects.

Chapter 3 on sheaths advances collisionless sheath theory to cover the sheath phenomena under consideration. Previous sheath formulations have contained several mathematical simplifications which are incompatible with the study of these sheath phenomena. The simplifications are 1) monoenergetic ions from the plasma, 2) monoenergetic emitted electrons, and 3) that the sheath potential drop is large. Further, for these corrections, it is shown that the "Bohm" criterion for matching the sheath to the plasma must be generalized.

Chapter 4 presents isothermal results for the thermionic convertor including the effects of surface emission, trapped ions

and reflected ions. The general result found here is that, contrary to intuition, a higher plasma density at the emitter increases arc-drop. All three emitter sheath phenomena produce a lower net ion loss rate and yield higher plasma density at the emitter.

Chapter 5 presents the results of non-isothermal calculations using an implicit numerical algorithm to confirm the isothermal results with ion reflection. However, detailed non-isothermal calculations with trapped ions surface emission ions are not carried out because the combination of the non-isothermal algorithm and the full collisionless sheath algorithm would require large amounts of CPU time.

Chapter 6 presents the conclusions of this thesis.

1.1 The Cesium Diode Convertor

Figure 1.1.1 is a schematic diagram of the cesium diode convertor. The emitter is heated externally to temperature T_E which is typically 1750 K and the collector is cooled to temperature T_C which is typically 750 K. The gap space, d, or convertor length, which is typically .25 mm, seperates the emitter from the collector. The cesium reservoir, which is sometimes imbedded in the collector, is kept at temperature, T_R, to maintain the desired cesium pressure (typically 1 torr) in the gap. The electrical load is connected across the emitter and collector to produce power. Figure 1.1.2 is an experimental
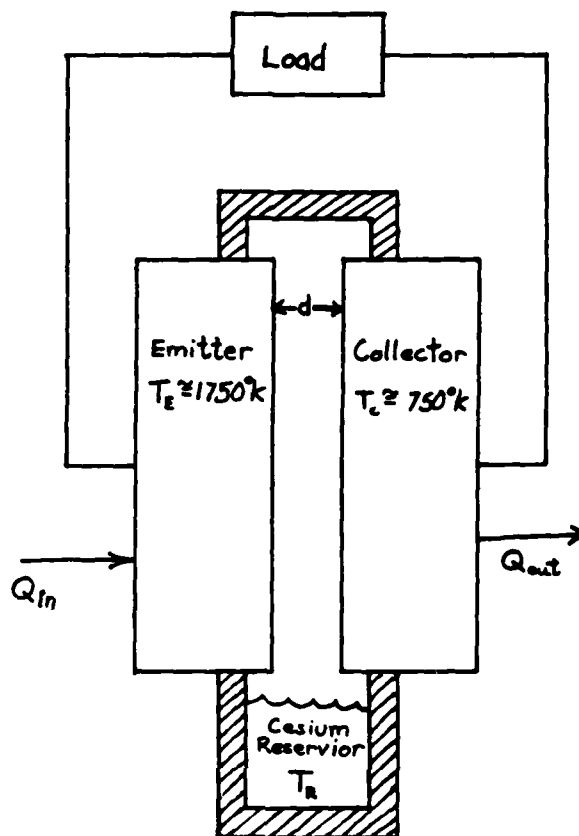
Figure 1.1.1 The Cesium Diode Convertor

result showing actual thermionic convertor performance under
these conditions. [s] It should be noted that at reasonable output

current densities (10 amp/cm^2), the output voltage is on the
order of 0.5 volts. A basic understanding of the thermionic
convertor output is gained by developing the ideal thermionic
convertor (no space charge effects) in fig. 1.1.3. In the

- - - - - - - - - - - - - - - - - - -

[s] The experimental device shown here is swept through voltage
from -0.4 to 0.8 volts by an external sine wave generator at 60
Hz. What is shown as output voltage is the applied voltage. The
convertor is producing power when the output voltage is greater
than zero.
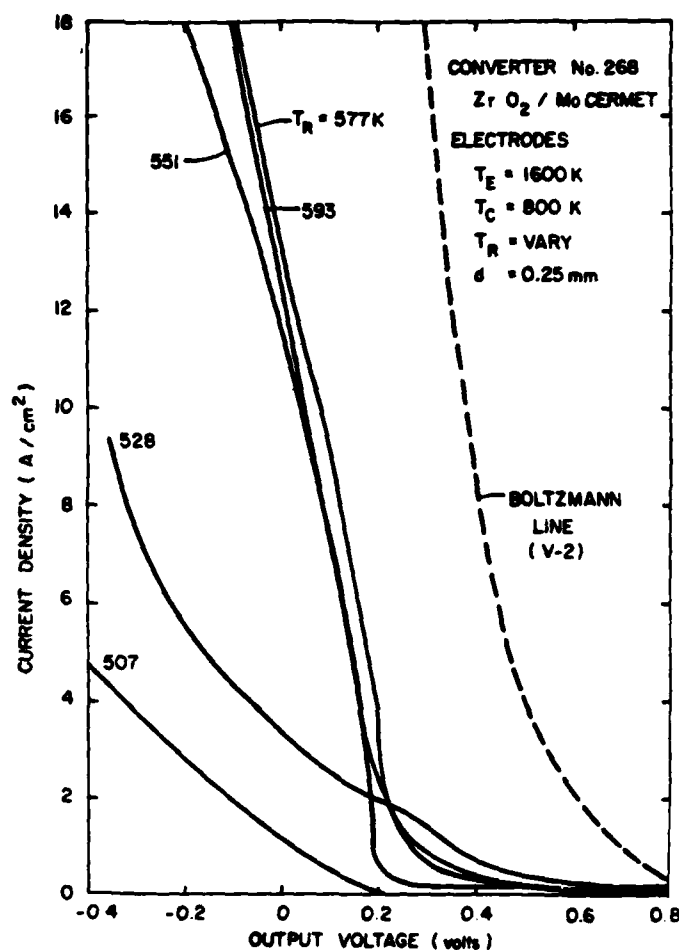
Figure 1.1.2 Actual Thermionic Convertor Performance

from Thermo-Electron Progress Report No. 48

ideal case, potential varies linearly across the gap because the

Poisson equation in the absence of space charge is $d^2\phi/dx^2 = 0$.
Case a is current saturation in which all electrons escaping the

emitter (the emitter work function is ϕ_E) arrive at the

collector (the collector work function is ϕ_C). The quantity

V_{out} is the output voltage. In case b the potential is flat and
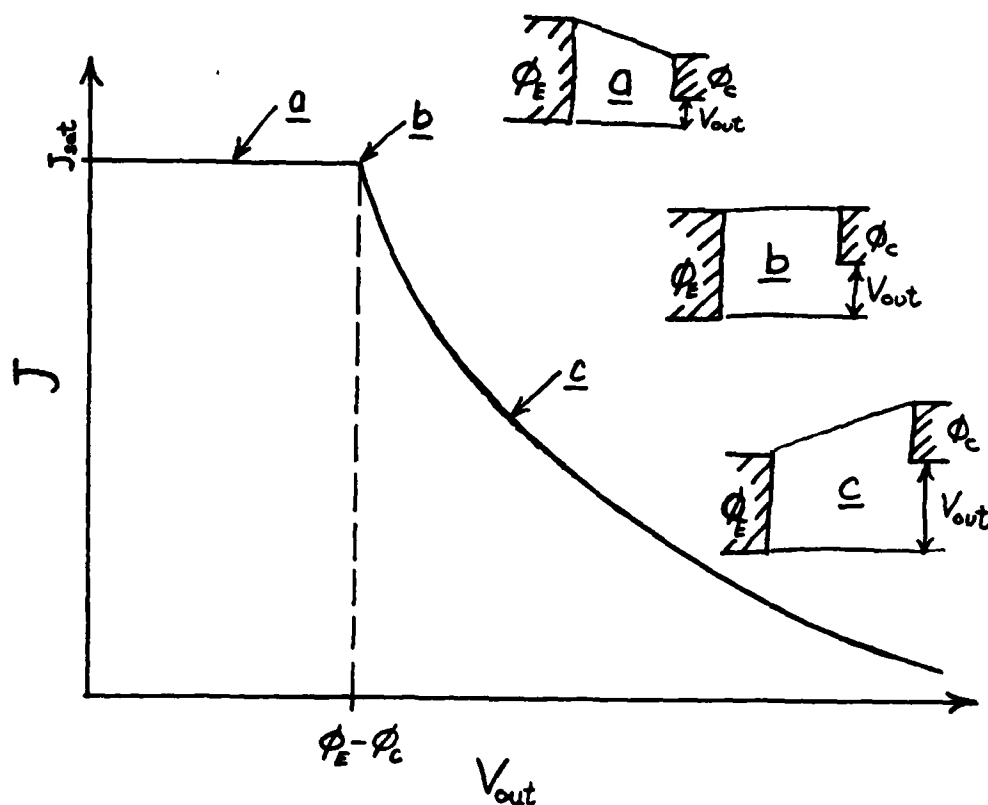
Figure 1.1.3 The Ideal Convertor

the current is still at saturation. In case c the convertor is
operating in the Boltzmann region. This region is so named
because the net current density drops off exponentially with
increasing output voltage. In the Boltzmann region the net
current density as a function of output voltage is:

$$J = J_R e^{\frac{\phi_E - \phi_c - V_{out}}{kT_E}} \quad , \quad V_{out} \geq \phi_E - \phi_c \qquad (1)$$

while in the saturation region:

$$J = J_R \quad , \quad V_{out} \leq \phi_E - \phi_c \qquad (2)$$

where J_R is the Richardson emitted current,

$$J_R = A T_E^2 e^{-\phi_E / k T_E} \tag{3}$$

and where

$$A = 120 \ \text{amps/cm}^2 \, k^2. \tag{4}$$

If, for instance, $T_E = 1500$ K and $\phi_E = 2.12$ eV then $J_R = 20$ amp/cm^2. We have assumed the collector emits no electrons, and therefore a lower collector work function always improves performance. This assumption is very good under the usual conditions in the thermionic convertor ($\phi_C = 1.6$ eV, $T_C = 750$ K) because the collector emitted current is 10^5 times smaller then the emitter's emitted current.

The experimental results clearly show the Boltzmann region, except 1) the curve is steeper than exponential, 2) there is sometimes a plateau at the base of the Boltzmann region, and 3) the output voltage is lower than ideal because of plasma losses known as arc-drop. Previous work [6] has shown that part of the steepness can be explained by the ionization kinetics of the plasma. In this work we show that part of the steepness can be explained by the sheath effects. All three of the emitter sheath phenomena considered here increase arc-drop and decrease output voltage. Since all three phenomena become more significant at

----

[6] Lawless, J.L., The Plasma Dynamics and Ionization Kinetics of The..ionic Energy Conversion, Ph.D. Thesis, Princeton University, 1981.

low current densities, a steeper curve results. We had also
wished to explain the plateau region theoretically because of its
locally lower arc-drop. It is believed that the plateau, which
sometimes occurs at low current density, results from the
collapse of the plasma arc and is the result of surface emission
as the source of ions for the plasma. Unfortunately, our
theoretical calculations cannot be carried into this region
because the formulation (the asymptotic division of the plasma
into a collisionless sheath and a neutral continuum plasma region
) breaks down.

1.2 Formulation for the Convertor

Best performance from the thermionic convertor is obtained
experimentally when the following empirical relationship is
satisfied:

$$p_{cs}d = 10 \text{ mil-torr}, \tag{1}$$

where p_{cs} is the neutral cesium pressure and d is the gap. This
corresponds to about 15 ion mean free paths in the gap. Also,
under this condition, the convertor operates in an ignited mode
with the plasma electrons at approximately 3000 K (the energy
necessary to maintain the plasma electrons at a higher
temperature than the emitter temperature is supplied by the arc-
drop). At this electron temperature (or lower temperature when
the convertor is not ignited such as in the plateau), the
ionization is about 10%. This can be seen from the Saha equation

for equilibrium plasma density,

$$\frac{n_i^2}{n_n} = 2.4 \times 10^{15} T_e^{3/2} e^{-V_{fi}/kT_e} \qquad (2)$$

where

n_n = neutral density $(1/cm^3)$,

n_i = ion density $(1/cm^3)$,

V_{fi} = first ionization energy, and

T_e = plasma electron temperature.

Under the conditions, p_{cs} = 1 torr, T_e = 3000 K and V_{fi} = 3.89 eV, we have

n_n = 6.44 X 10^{15} $(1/cm^3)$, and

n_i = 8.63 X 10^{14} $(1/cm^3)$.

Since the convertor is only 15 mean free paths long, the plasma does not attain its equilibrium plasma density and recombination is usually negligible. Therefore the ions are generated by the high electron temperature in the gap and are lost to the emitter and collector by diffusion. Surface emission of ions is generally not a factor in supporting the plasma as can be seen from the Saha-Langmuir equation,

$$J_{cs+} = \frac{\beta n_{cs}}{\sqrt{2\pi}} \sqrt{\frac{kT_E}{M_{cs}}} \frac{1}{1 + 2 e^{\frac{V_{ci} - \phi_E}{kT_E}}} \qquad (3)$$

where

J_{cs+} = surface emission ion current,

n_{cs} = neutral cesium number density, and

M_{cs} = cesium atom mass.

Under the previously used conditions,

J_{cs+} = 1.6 X 10^{-5} amps/cm^2.

In the convertor, Debye length,

$$\lambda_D = \sqrt{\frac{kT_\epsilon}{4\pi q^2 n_{plasma}}} \qquad (4)$$

which is length scale for charge seperation in the plasma and therefore the sheath length scaling, is small compared to both the electron and ion mean free paths,

$$\lambda_D << \lambda_i, \ \lambda_e << d. \qquad (5)$$

Therefore, we divide the convertor into a neutral plasma region terminated by collisionless sheaths at the electrodes. Figure 1.2.1 is potential distribution in the convertor (definitions of terms are detailed in chap. 2). Based on the asymptotic matching of the neutral plasma region to the collisionless sheaths, the sheath results produce boundary conditions for the neutral plasma. The plasma region is treated as fluid (with a source term for ionization) with conservation of mass, momentum, and energy. Conservation of mass requires a boundary condition for the ion loss rate which is found from the sheath net ion flux rate. Conservation of momentum results in a net change in potential through the plasma region which is added to the change through the sheaths. And conservation of energy (which is dominated by electron energy) requires boundary conditions on plasma electron temperature. Examination of fig. 1.2.1 shows that ions leaving the plasma for the emitter (at 0^+) can be reflected by the back of the sheath if Δx_s is greater than zero. Ions entering the sheath are accelerated by the front sheath and decelerated by the back sheath. Those ions entering the sheath
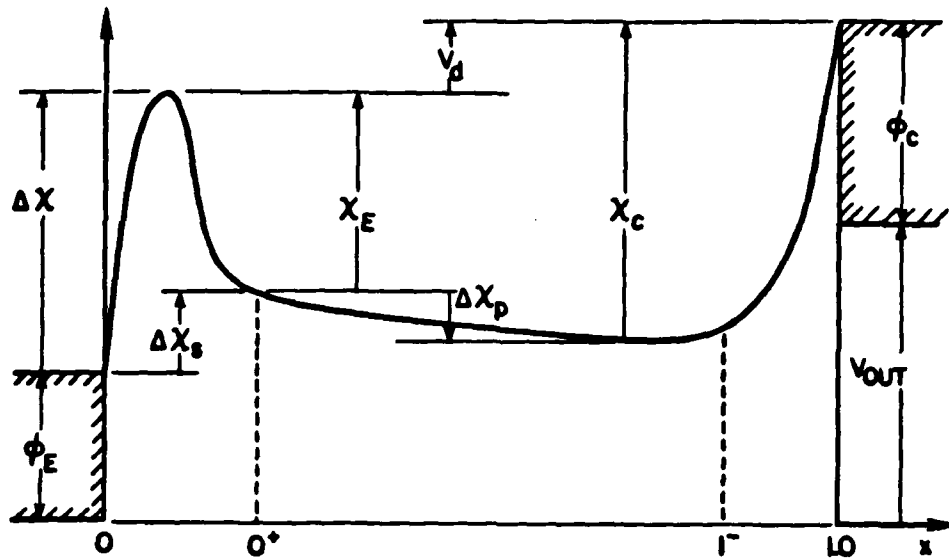
Figure 1.2.1 Potential in the Convertor

with energies less than Δx_s reflected back through the sheath into the plasma region again. Figure 1.2.2 is plasma density in the convertor gap normalized by net current, J, and electron speed of sound, c, for different ion reflection conditions at the emitter. The higher curves are of little or no ion reflection and the lower curves result from ion reflection.

1.3 Emitter Sheath Effects
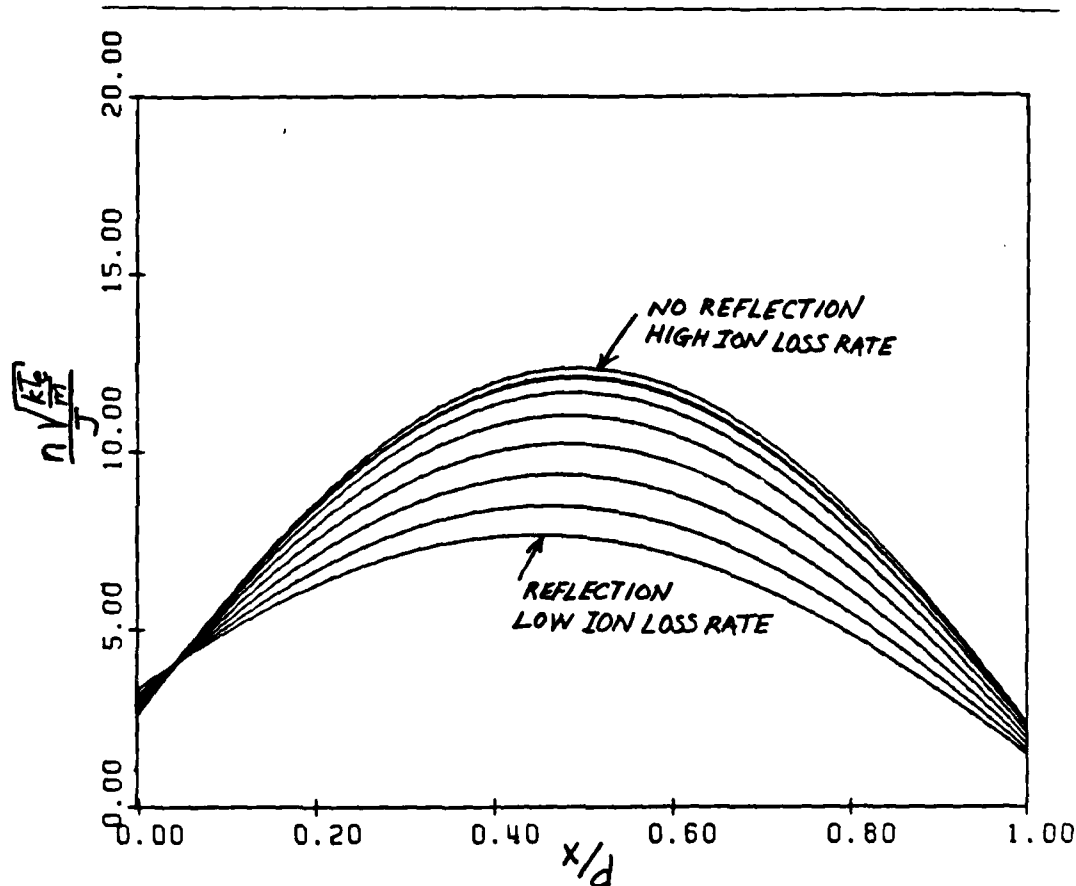
Figure 1.2.2 Typical Plasma Density in the Convertor

Emitter sheath effects on thermionic convertor performance can be divided into two categories: 1) changes in net ion flux rate into the sheath which affect plasma density directly, and 2) changes in sheath potential distribution which affect the exchange of "hot" plasma electrons for "cold" emitter ions directly. A decreased influx of ions into the sheath, which occurs for all three emitter sheath phenomena, increases the plasma density at the neutral plasma- emitter sheath interface. Theoretical intuition suggests that an increased plasma density at the emitter would benefit performance by reducing resistance

through the plasma and therefore reducing arc-drop. However, this is not the case. While the plasma density at the emitter increases slightly, plasma density at the collector decreases. Consequently total resistance increases.

CHAPTER 2: THERMIONIC CONVERTOR FORMULATION

2.1 General Formulation

2.2 Isothermal Formulation

In this chapter we develop the formulation for the quasi-
neutral plasma region of the thermionic convertor and the
boundary conditions for it. The boundary conditions contain
fluxes of electrons and ions that must be determined from the
sheaths and therefore the sheath is critical to the formulation.
Sheaths are considered in detail in the next chapter. The first
section is the general formulation for the non-isothermal plasma
electron case (finite electron thermal conductivity), and the
second section is specialized to the isothermal case. The
general formulation follows closely the notation of Lawless [1] and
the isothermal formulation follows closely the notation of Lam.
[2] However, the isothermal formulation has been generalized to

----

[1] Lawless, J.L., The Plasma Dynamics and Ionization Kinetics of
Thermionic Energy Conversion, Ph.D. Thesis, Princeton University,
1981, chap. 2.

eliminate the assumption of high sheaths which has previously been used to simplify the electron dynamics. Lawless developed an explicit unsteady numerical scheme for the general non-isothermal case. However, the explicit scheme is slow because stability requires small time steps. In appendix C we develop an implicit numerical scheme which eliminates the stability constraint and speeds up the Lawless scheme by the number of space grids squared. Even the implicit scheme is slow and it is also difficult to gain physical insight from direct numerical results. Therefore we develop the isothermal formulation which is faster and easier to analyse. Most of the results in this thesis are based on the isothermal formulation. Appendix B contains the isothermal programs.

2.1 General Formulation

In this section, which follows the notation of Lawless (chap.2), we develop the general non-isothermal formulation for the quasi-neutral region of the thermionic convertor. We assume that the convertor is one-dimensional since convertors typically have a gap of .25 mm while the plates are 10 cm in diameter. Following Lawless, we present the conservation equations, then reduce them to convenient and useful forms. We next present and discuss the approximations to be used, and resulting parabolic P.D.E.s (first order in time and second order in space) which

----

[2] Lam, S.H., Preliminary Report on Plasma Arc-Drop in Thermionic in Thermionic Energy Converters. Princeton Unversity, 1976.

are used to carry out the numerical calculations. Finally, we
discuss the boundary conditions for these equations whose flux
rates (electrons and ions) are derived from the sheaths.

The conservation equations we develop are: mass of ions and
electrons, momentum of ions and electrons, and energy of
electrons.

Conservation of mass of ions and electrons is:

$$\frac{\partial n_e}{\partial t} = S^{(n)} - \frac{\partial \Gamma_e}{\partial x} \quad , \quad \frac{\partial n_i}{\partial t} = S^{(n)} - \frac{\partial \Gamma_i}{\partial x} \tag{1}$$

where

$\Gamma_e = n_e u_e$ = electron flux,

$\Gamma_i = n_i u_i$ = ion flux,

u_e = mean electron velocity,

u_i = mean ion velocity,

n_e = electron number density,

n_i = ion number density,

$S^{(n)}$ = net rate of ionization.

Conservation of momentum for ions and electrons is:

$$m n_e \frac{D_e u_e}{D_e t} = -\frac{\partial p_e}{\partial x} - n_e \frac{\partial}{\partial x} (q \psi) + S_{ea}^{(p)} + S_{ei}^{(p)}$$

$$M n_i \frac{D_i u_i}{D_i t} = -\frac{\partial p_i}{\partial x} + n_i \frac{\partial}{\partial x} (q \psi) + S_{ia}^{(p)} - S_{ei}^{(p)} \tag{2}$$

where

m = electron mass,

M = ion mass,

p_e = electron pressure,

p_i = ion pressure,

q = electron charge,

ψ = potential,

$S_{ea}^{(p)}$ = exchange of momemtum from neutrals to electrons,

$S_{ei}^{(p)}$ = exchange of momemtum from ions to electrons,

$S_{ia}^{(p)}$ = exchange of momemtum from neatrals to ion.

Note: in this thesis, potentials, ϕ, Φ, χ, are defined such that increasing potential repels electrons. This is in contrast to the usual convention and is done so because electrons are of principal interest.

Conservation of electron energy is:

$$\frac{\partial}{\partial t}(n\varepsilon) + \frac{\partial}{\partial x}(\Gamma_e h) + \frac{\partial q_e}{\partial x} + \Gamma_e \frac{\partial}{\partial x}(q\psi) = S^{(\varepsilon)} + \varepsilon S^{(n)} \quad (3)$$

where

$$\varepsilon = mu_e^2/2 + 3kT_e/2 = \text{stagnation energy,}$$

$$h = \varepsilon + p_e/n_e = \text{stagnation enthalpy,}$$

$S^{(E)}$ = collisional and ionization energy source term,

q_e = electron heat conduction flux.

Other useful conservation equations can be derived from eqs.1,2 and 3. Also, from this point forward we invoke the quasi-neutral approximation, $n = n_e = n_i$. From conservation of mass (eq.1) we have

$$\frac{\partial J}{\partial x} = 0 \tag{4}$$

where

$$J = q(\Gamma_e - \Gamma_i) = \text{net current density.}$$

Equation 4 results from subraction of eqs.1 and using the quasi-neutral approximation to equate the time derivatives of density. From conservation of momentum for ions and electrons, we have

$$Mn\frac{D_e u_e}{D_e t} + Mn\frac{D_i u_i}{D_i t} = -\frac{\partial p}{\partial x} + S_{ea}^{(p)} + S_{ia}^{(p)} \tag{5}$$

where

$$p = p_e + p_i = \text{total plasma pressure.}$$

We have added the two momentum equations and consequently have eliminated the terms, $S_{ei}^{(p)}$ and $n\partial(q\psi)/\partial x$, which represent

exchange of momentum between electrons and ions and the momentum
exchanged with the field. From electron energy conservation, we
derive

$$\frac{\partial}{\partial t}\left[n(\varepsilon + g\psi)\right] + \frac{\partial}{\partial x}\left[\Gamma_e(h + g\psi) + g_e\right] = n\frac{\partial}{\partial t}(g\psi) + S^{(\varepsilon)}$$
$$+ (\varepsilon + g\psi)S^{(n)} \tag{6}$$

by differentiation of a product. Finally, the electric potential
term can be eliminated from the energy equation by subtracting
the electron momentum equation multiplied by u_e:

$$\frac{\partial}{\partial t}(n\varepsilon) + \frac{\partial}{\partial x}(\Gamma_e\varepsilon) + \frac{\partial g_e}{\partial x} + p_e\frac{\partial u_e}{\partial x} = S^{(\varepsilon)} + \varepsilon\, S^{(n)} \tag{7}$$
$$+ m\Gamma_e'\frac{D_e u_e}{D_e t} - u_e\left(S_{ea}^{(p)} + S_{ei}^{(p)}\right).$$

These three conservation equations, which are just the first
three moments of the Boltzmann equation, cannot be solved without
constitutive equations for pressure, heat flux and the
collisional terms.   In order to produce the necessary
constitutive relations, we assume that the electron and ion
distributions in the plasma are near-Maxwellian and therefore we
can approximate (ideal gas laws),

$$p_e = nkT_e$$
$$p_i = nkT_i \tag{8}$$

where

$$T_e = \text{plasma electron temperature,}$$

$$T_i = T_n = \text{ion and neutral temperature,}$$

$$k = \text{Boltzmann's constant.}$$

Also, because of the near-Maxwellian assumption, we can make the first order approximation,

$$q_e = -k_e \frac{\partial T_e}{\partial x} \tag{9}$$

where

$$k_e = \text{electron thermal conductivity.}$$

The previous two models (electron heat flux and electron pressure) are not totally consistant since eq.8 assumes an isotropic Maxwellian electron distribution while the existence of an electron heat flux requires a non-isotropic distribution.

For the collision terms, we assume momentum transfer is proportional to the difference of mean species velocity,

$$S_{ea}^{(p)} = -m\nu_{ea}\Gamma_e$$
$$S_{ei}^{(p)} = -m\nu_{ei}(\Gamma_e - \Gamma_i) \tag{10}$$
$$S_{ia}^{(p)} = -M\nu_{ia}\Gamma_i$$

where

$$\nu_{ea} = \text{electron-atom collision frequency,}$$

$$\nu_{ei} = \text{electron-ion collision frequency,}$$

$$\nu_{ia} = \text{ion-atom collision frequency.}$$

The quantities ν_{ea}, ν_{ei}, ν_{ia} and k_e must be determined. This is covered extensively by Lawless. One further assumption is used, namely, that the substantial time derivatives in the momentum equations (Du/Dt) are small. This is justified for two reasons: first, $\partial u/\partial t$ is small because the mean time between collisions is on the order of 10 nsec while all characteric time scales in the equations are much greater, and second, $u\partial u/\partial x$ is small when the Mach number is small (electron or ion). The first part is always easily satisfied. The second part is not well satisfied near the electrodes for the ions, and not well satisfied near the electrodes for the electrons when the sheath heights are low.

We now introduce the definition of ambipolar flux and resulting equations:

$$\Gamma = \Gamma_i + \frac{\mu_i}{\mu_{ea}} \Gamma_e \tag{11}$$

where

$$\mu_i = \frac{1}{M\nu_{ia}} \quad , \quad \mu_{ea} = \frac{1}{m\nu_{ea}} \; . \tag{12}$$

The quantity Γ is called ambipolar flux and μ_i and μ_{ea} are called mobilities. With these definitions and assumptions we can write eq.5 (ion and electron momentum) as

$$0 = -\frac{\partial P}{\partial x} - \frac{\Gamma}{\mu_i} \; . \tag{13}$$

Similarly, we can write conservation of mass as

$$\left(1+\frac{\mu_i}{\mu_{ea}}\right)\frac{\partial n}{\partial t} = \frac{\partial}{\partial x}\left(\mu_i\frac{\partial P}{\partial x}\right) + \left(1+\frac{\mu_i}{\mu_{ea}}\right)S^{(n)} + \Gamma_e\frac{\partial}{\partial x}\left(\frac{\mu_i}{\mu_{ea}}\right) \tag{14}$$

and conservation of energy as

$$\frac{3}{2} n \frac{\partial}{\partial t} \left(kT_e \right) = \frac{\partial}{\partial x} \left(k_e \frac{\partial T_e}{\partial x} \right) - \frac{3}{2} \Gamma_e \frac{\partial (kT_e)}{\partial x}$$

$$- nkT_e \frac{\partial}{\partial x} \left(\Gamma_e / n \right) + \frac{\Gamma_e^2}{n \mu_{ea}} + \Gamma_e \frac{\Gamma_e - \Gamma_i}{n \mu_{ei}} \, . \tag{15}$$

Two final approximations are used to close these equations:

$$S^{(E)} = -E_0 S^{(n)} \tag{16}$$

and

$$S^{(n)} = \left(\alpha N_0 - \beta n_e^2 \right) n_e \tag{17}$$

The first states that ionization is the only volume source term for electron energy where E_0 is first ionization energy. The second is a model for ionization and recombination. The quantity α called the ionization coefficient, β is the recombination coefficient and N_0 is the neutral density. Again, the choice of this model and its coefficients is covered in Lawless.

Now that the conservation equations and the constitutive relations are established, we can derive boundary conditions for mass and energy. These boundary conditions contain fluxes of electrons and ions which are obtained from the sheath results. The boundary conditions for mass come from eq.13,

$$\Gamma_0 = -\mu_i \frac{\partial P}{\partial x} \bigg|_0 = -n_0 u_i \left(1 + \frac{\mu_i}{\mu_{ea}} \right) + \frac{\mu_i}{\mu_{ea}} J/q \, ,$$

$$\Gamma_l = -\mu_i \frac{\partial P}{\partial x} \bigg|_l = n_l u_i \left(1 + \frac{\mu_i}{\mu_{ea}} \right) + \frac{\mu_i}{\mu_{ea}} J/q \, . \tag{18}$$

The quantities u_i and J are the fluxes through the sheaths. The

subscripts 0 and 1 denote the emitter and collector plasma-sheath interfaces respectively. The boundary conditions for electron energy are

$$-k_e \frac{\partial T_e}{\partial x}\bigg|_o = -2\Gamma_E \left(kT_{e_o} - kT_E\right) + \Gamma_e \left(qV_E - \frac{kT_{e_o}}{2}\right),$$

$$-k_e \frac{\partial T_e}{\partial x}\bigg|_1 = \Gamma_e \left(qV_C - \frac{kT_{e_1}}{2}\right) \tag{19}$$

where

Γ_E = flux of electrons from the emitter into the plasma,

T_E = emitter temperature,

V_E = emitter sheath height,

V_C = collector sheath height.

We have assumed the collector emits nothing.

2.2 Isothermal Formulation

In this section the corrected isothermal model, based on the isothermal model of Lam, and including ion reflection at the emitter, is developed. Since we encounter both low emitter and low collector sheath heights as a consequence of ion reflection and trapped ions, the assumption of Boltzmann plasma electron distributions at the plasma-sheath interface must be abandoned. At both the emitter and collector the low sheaths return few plasma electrons, leaving the distributions largely one sided.

Furthermore, at the emitter sheath emitted electrons must be taken into account. Thus the ratio of electrons moving toward the sheath to the total density of electrons at the sheath edge is not 1/2, as in the Boltzmann assumption.
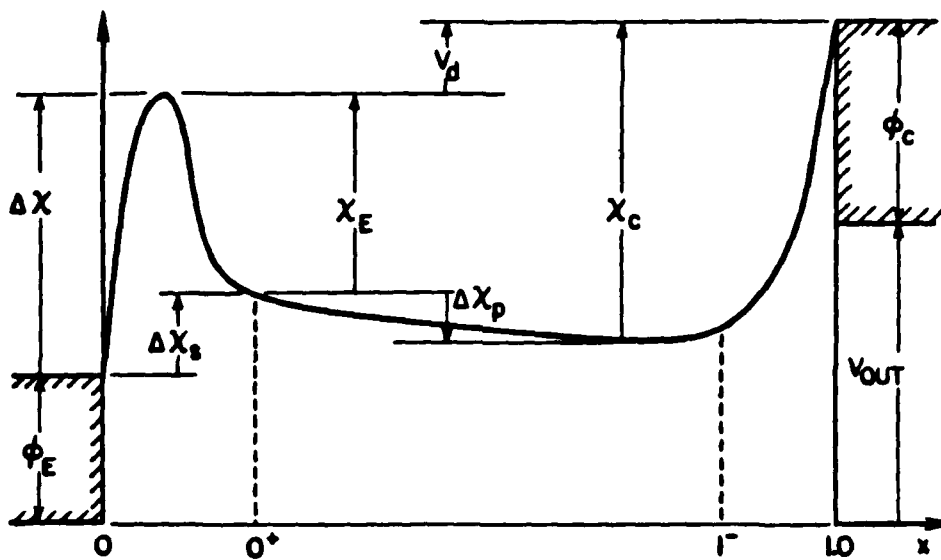

Figure 2.2.1 The Potential Distribution in the Convertor

In fig. 2.2.1 we define the potentials in the convertor. All of the potentials are nondimensionalized by emitter temperature as follows:

$$\chi = \frac{q\phi}{kT_E} \qquad (1)$$

where

$$\chi = \text{nondimensional potential,}$$

$$\phi = \text{potential,}$$

$$q = \text{electron charge,}$$

$$k = \text{Boltzmann's constant,}$$

$$T_E = \text{emitter temperature.}$$

We also use the following terminology for various potentials in the convertor:

$$\phi_E = \text{emitter work function,}$$

$$\Delta\chi = \text{back sheath height,}$$

$$\Delta\chi_s = \text{reflective potential,}$$

$$\chi_E = \text{emitter sheath height,}$$

$$\Delta\chi_p = \text{plasma potential drop,}$$

$$V_d = \text{arc-drop,}$$

$$\chi_C = \text{collector sheath height,}$$

$$\phi_C = \text{collector work function,}$$

$$V_{out} = \text{convertor output voltage.}$$

Inspection of fig. 2.2.1 yields immediately the following relations which will be useful later:

$$V_d = V_{out} - (\Phi_E - \Phi_c) - \Delta\chi, \qquad (2)$$

$$V_d = (\chi_c - \chi_E) - \Delta\chi_p. \qquad (3)$$

Some further preliminary definitions are also needed. We have the Richardson current density of electrons from the emitter,

$$J_R \left(\frac{amps}{cm^2}\right) = 120\, T_E^2\, (k^2)\, exp\, (-\bar{\Phi}_E) \qquad (4)$$

The emitted current density which crosses the emitter sheath potential peak into the convertor plasma region is

$$J_E = J_R\, e^{-\Delta\chi}, \quad \Delta\chi > 0,$$

$$J_E = J_R \qquad , \quad \Delta\chi \leq 0. \qquad (5)$$

We also define the net current density through the convertor, J, and the normalized current density,

$$j = J/J_E \qquad (6)$$

Electron temperature is nondimensionalized as

$$\tau = T_e / T_E \qquad (7)$$

where T_e is the plasma electron temperature which, in this section, is constant by the isothermal assumption. Finally we have the thermal speeds,

$$a_e = \sqrt{\frac{8kT_e}{\pi m}}, \qquad (8)$$

$$q_E = \sqrt{\frac{8 k T_E}{\pi m}} \ . \tag{9}$$

The isothermal formulation is developed from here in the same way as the general formulation except that we take full advantage of the isothermal assumption by looking only at the global conservation equations instead of the local ones used in the general formulation. We then assume that the transport properties, collision frequencies, and the ionization source coefficient are constant across the convertor because of the isothermal assumption. Also we find only the steady state solution. We carry out this development by deriving the global conservation equations for the isothermal case (current, momentum, and electron energy) and then reducing these to a set of three simultaneous equations in the variables τ, x_E, and x_C. [3] These equations are nonlinear and solved numerically using a positive definite Newton's method explained in appendix B.

First we consider conservation of current. The collector is assumed to emit nothing, therefore at the collector plasma-sheath interface we have

$$J = \frac{q_e \, \alpha_1 \, n(1)}{2} \, e^{-x_c/\tau} \tag{10}$$

where α_1 is the fraction of the total plasma density at the

----

[2] In some cases the the actual calculations are carried out using different variables when x_E or x_C are small or zero. In the case, for instance, of a single ion repelling emitter sheath we use j because x_E is zero.

collector sheath which is moving toward the collector and n(1) is
the total plasma density at the plasma-collector sheath
interface. Because we continue to assume that the plasma
electron distribution there is Maxwellian, we can write α_1 as

$$\alpha_1 = \frac{1}{1 + \frac{2}{\sqrt{\pi}} \int_0^{\sqrt{\frac{x_1}{T}}} e^{-u^2} du} \tag{11}$$

which takes into account the plasma electrons reflected by the
collector sheath. We still assume that the plasma electron
distribution coming into the collector sheath is Maxwellian and
that it does not have any velocity shift because the sheath is
expected to be electron repelling. In the limit of a high
collector sheath, $\alpha_1 = 1/2$ and we have a fully Boltzmann
distribution of electrons at the collector sheath edge. The
situation at the emitter is more complex because the emitted
electrons must be taken into account. We have the back scattered
current density, J_{BS}, which is the plasma electron current
density moving into the emitter,

$$J_{BS} = \frac{n(0) \, q_e \, \overline{u}_0}{2} \, e^{-x_e/T} \tag{12}$$

where n(0) is the total plasma density at the emitter sheath-
plasma interface and α_0 is the fraction of total plasma density
at the interface moving toward the emitter.

Continuity of electron current demands

$$J_E = J_{BS} + J \tag{13}$$

which can be written as

$$J_E = J\left(1 + \frac{n(0)}{n(1)}\frac{\alpha_0}{\alpha_1}\exp\left(\frac{\chi_c - \chi_E}{\tau}\right)\right). \tag{14}$$

This can be rewritten using eqs.3 and 6 as

$$j = \frac{1}{1 + \frac{n(0)}{n(1)}\frac{\alpha_0}{\alpha_1}\exp\left(\frac{V_d + \Delta\chi}{\tau}\right)} . \tag{15}$$

The quantity α_0 can be written as

$$\alpha_0 = \sqrt{\frac{\pi}{2}}\, Q\left(\frac{1}{j} - 1\right)e^{\chi_E/\tau} \tag{16}$$

where

$$Q = \frac{(u_e)_0}{\sqrt{\frac{kT_e}{m}}}$$

is the electron Mach number at the emitter. This is just an application of eq.13.

Electron energy conservation is developed by considering energy exchange with the emitter and collector and energy lost to ionization. Power carried into the plasma by emitted electrons is

$$P_E = J_E\left(2 + \Phi_E + \Delta\chi\right)\frac{kT_E}{q} . \tag{17}$$

Power returned to the emitter is

$$P_{BS} = (J_E - J)\left(2\tau + \Phi_E + \Delta\chi\right)\frac{kT_E}{q} . \tag{18}$$

Power flowing into the collector is

$$P_c = J\left(2\tau + \Phi_E + \Delta\chi + V_d\right)\frac{kT_E}{q} . \tag{19}$$

Ionization power loss is

$$P_{ion} = J_{ion} V_{fi} \frac{kT_E}{q} , \tag{20}$$

where J_{ion} is the total ion current into both the emitter and collector, and V_{fi} is the first ionization energy. Conservation of electron energy is

$$P_E = P_{BS} + P_c + P_{ion} \tag{21}$$

this can be reduced to

$$\tau = 1 - \frac{1}{2} j V_d - \frac{1}{2} j_i V_{fi} \tag{22}$$

where $j_i = J_{ion}/J_E$. In the ignited mode τ is generally about 2 (T_E = 1500 K and T_e = 3000 K), consequently the arc-drop, V_d, is negative. In other words the high plasma electron temperature is generated by resistance heating.

Finally, we consider electron and ion momentum. From electron momentum conservation, we find the potential drop in the plasma region. By adding the electron and ion momentum equations as in the general case, we find our diffusion equation and boundary conditions to which the sheaths contribute flux terms. When we introduce the ionization source term into this, we have the complete formulation. Electron momentum conservation is

$$0 = -\frac{dp_e}{dx} - qn\frac{d\psi}{dx} - \frac{q_e mn u_e}{\lambda_e} , \tag{23}$$

where λ_e is electron mean free path. Using $p_e = nkT_e$ and $J = qnu_e$, we can rearrange eq.23 into

$$J = -\frac{q\lambda_e}{ma_e} \left(kT_e \frac{dn}{dx} + nq \frac{d\psi}{dx} \right). \tag{24}$$

This can be further reduced by dividing by J_E and using $\xi = x/d$ where d is the convertor gap thickness:

$$j \doteq -\frac{\pi}{4} \frac{\lambda_e}{d} \frac{1}{\sqrt{\tau} n_E} \left\{ \tau \frac{dn}{d\xi} + n \frac{d\chi}{d\xi} \right\}. \tag{25}$$

Integration of this equation from the emitter sheath interface to the collector sheath interface yields

$$\Delta\chi_p = \tau \ln\left(\frac{n(1)}{n(0)}\right) + jR \tag{26}$$

where

$$R = \frac{4}{\pi} \frac{d}{\lambda_e} \sqrt{\tau} \int_0^1 \frac{n_E}{n(\xi)} d\xi. \tag{27}$$

The quanity R is the normalized plasma resistance.

The ion and electron momentum equations can be written

$$kT_e \frac{dn}{dx} = -\gamma n \frac{d\phi}{dx} - \frac{mn u_e a_e}{\lambda_e}$$

$$kT_i \frac{dn}{dx} = \gamma n \frac{d\phi}{dx} - \frac{Mn u_i a_i}{\lambda_i} \tag{28}$$

where λ_i is ion mean free path and a_i is ion thermal speed,

$$a_i = \sqrt{\frac{8\pi T_E}{\pi M}}.$$

Addition of eqs.28 yields

$$(kT_e + kT_E) \frac{dn}{dx} = -\left(\frac{a_e m}{\lambda_e} u_e + \frac{a_i M}{\lambda_i} u_i\right) n, \tag{29}$$

which is ambipolar diffusion. Equation 29 is differentiated to become

$$(kT_e + kT_E) \frac{d^2 n}{dx^2} + \frac{a_e m}{\lambda_e} \frac{d}{dx}(n u_e) + \frac{a_i M}{\lambda_i} \frac{d}{dx}(n u_i). \tag{30}$$

At this point we assume recombination is negligible and the ionization source term is

$$\frac{d}{dx}(u_e n) = \frac{d}{dx}(u_i n) = Sn \, .$$

(31)

Using eqs.31 in eq.30 yields

$$\frac{d^2 n}{d\xi^2} + \left[\left(\frac{a_e m}{\lambda_e} + \frac{a_i M}{\lambda_i}\right)Sd^2\right]n = 0 \, .$$

(32)

Equation 29 taken at the boundaries of the plasma (at the emitter and collector sheath interfaces) forms the plasma boundary conditions

$$\left.\frac{dn}{d\xi}\right)_o = \beta_o n_o \, , \, \left.\frac{dn}{d\xi}\right)_l = -\beta_l n_l$$

(33)

where

$$\beta_o = \frac{-d}{kT_e + kT_E}\left(\frac{a_e m}{\lambda_e}u_{e_o} + \frac{a_i M}{\lambda_i}u_{i_o}\right),$$

$$\beta_l = \frac{d}{kT_e + kT_E}\left(\frac{a_e m}{\lambda_e}u_{e_l} + \frac{a_i M}{\lambda_i}u_{i_l}\right).$$

(34)

Equation 32 is written as

$$\frac{d^2 n}{d\xi^2} + A^2(\tau)\, n = 0$$

(35)

where

$$A^2(\tau) = d^2 S\left(\frac{a_e m}{\lambda_e} + \frac{a_i M}{\lambda_i}\right)$$

(36)

where $A(\tau)$ is the ionization coefficient and is found from consideration of ionization kinetics. Its solution for n is

$$n(\xi) = B\sin(A\xi + C)$$

(37)

where B and C are constants of integration and $A=A(\tau)$. The
quantities β_0 and β_1, which are the boundary conditions for
eq.37, can be written as functions of τ, x_E, x_C and Δx_s,

$$\beta_0 = \beta_0(\tau, x_E, x_c, \Delta x_s),$$
$$\beta_1 = \beta_1(\tau, x_E, x_c, \Delta x_s).$$
(38)

When there is no reflection, β_0 and β_1 are both large, i.e.,

$$\beta_0 = O\left(\frac{d}{\lambda_i}\right), \quad \beta_1 = O\left(\frac{d}{\lambda_i}\right).$$

Significant reflection on the emitter side reduces β_0 and it may
indeed attain negative values for sufficiently strong reflection.

The density equation (eq. 35) with the boundary conditions β_0
and β_1 is a linear eigenvalue problem; its solution yields A and
C as functions of β_0 and β_1. The calculated results are shown in
fig. 2.2.2. Since $A(\tau)$ is function of τ from the ionization
kinetics, the value of τ is thus determined by a function of β_0
and β_1. The plasma resistance, R, also can be expessed in terms
of functions of β_0 and β_1 through A and C using eq.27:

$$R = \frac{4}{\sqrt{2\pi}} \frac{d}{\lambda_e} \tau \frac{Q}{j} \frac{\sin C}{A} \ln\left(\frac{\tan\left(\frac{A+C}{2}\right)}{\tan\left(\frac{C}{2}\right)}\right).$$
(39)

Using the sheath results which provide j, Q, β_0 and β_1, the
isothermal formulation is complete. The results are summarized
below. The quantities β_0, β_1, Q and j are found from the sheath
calculations as functions of τ, x_E, x_C, and Δx_s, i.e.,

$$\beta_0 = \beta_0(\tau, x_E, x_c, \Delta x_s),$$
$$\beta_1 = \beta_1(\tau, x_E, x_c, \Delta x_s),$$
$$Q = Q(\tau, x_E, x_c, \Delta x_s),$$
$$j = j(\tau, x_E, x_c, \Delta x_s).$$
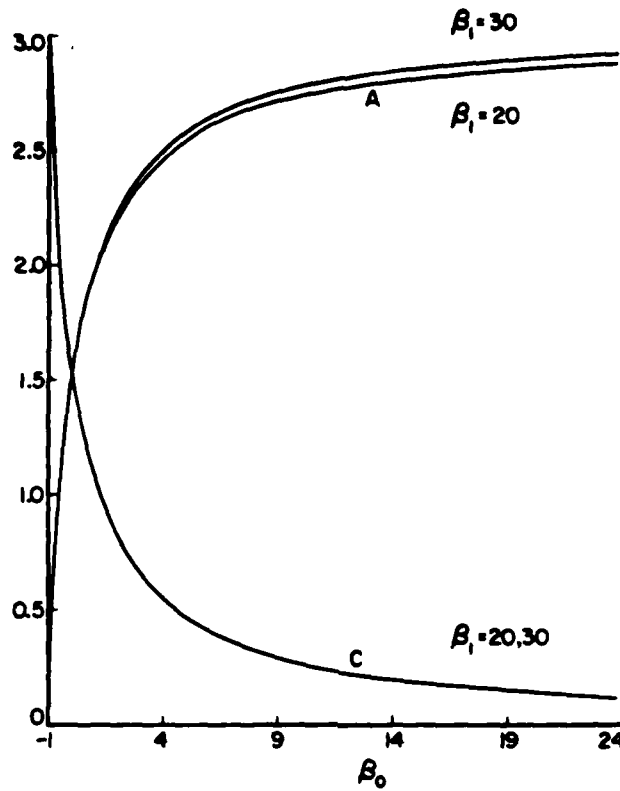
Figure 2.2.2 The Eigenvalue Problem

From the eigenvalue problem for the plasma density we then find

$$A(\tau) = A(\beta_o, \beta_1).$$

(40)

From the continuity equation for current we find

$$\chi_c - \chi_E = \tau \ln\left(\frac{\sin(A+C)}{\sin C}\right) + \tau \ln\frac{\alpha_1}{\alpha_o} + \tau \ln\left(\frac{1}{j}-1\right).$$

(41)

And from the electron momentum equation we find

$$\chi_c - \chi_E = \tau \ln\left(\frac{\sin(A+C)}{\sin C}\right) + jR + \frac{2(\tau-1)}{j} - \frac{j_i}{j}V_{fi}.$$

(42)

These three previous equations determine χ_E, χ_C and τ when $\Delta\chi_s$ is

given. This set of equations is valid for all Δx_s. Even in the case of $\Delta x_s <= 0$ when there is no reflection, the calculations differ from previous isothermal calculations because the Boltzmann assumption on the electrons is not used as indicated by the presence of α_0 and α_1.

CHAPTER 3: SHEATHS

3.1 Assumptions

3.2 General Solution Condition

3.3 Equations

3.4 Sheath Solutions

In this chapter the collisionless sheath formulation is developed. The sheath formulation and its results are essential to thermionic convertor formulation because two pieces of information are required from the sheath:

1) the potential change through the sheath, and

2) plasma density boundary conditions, and in the
   non-isothermal case, electron temperature
   boundary conditions.

Both of these have significant effects on predicted thermionic convertor performance, and therefore sheath formulation is of great interest. In addition to calculating more accurate sheath results than in previous sheath formulations, we examine three expected emitter sheath phenomena:

1) plasma ions reflected by the emitter sheath,

2) ions trapped in the double emitter sheath, and

3) surface emission ions from the emitter surface.

These three phenomena and more accurate results require generalizations to previous formulations along two lines. First, the assumption of cold ions (monoenergetic plasma ions) cannot be retained since ion reflection begins with the lowest energy plasma ions and reflects only the part of the ion distribution that has energies lower than the potential rise through the sheath. Second, previous formulations have idealized electron dynamics in the sheath under the assumption of a large sheath height. In fact the actual sheath heights are of order unity, and therefore this is a poor assumption. Complete calculation of the electron dynamics converts the simple algebraic equations of the large sheath height formulation to equations containing integrals over distribution functions that must be integrated numerically. By contrast, the finite temperature ion distribution causes theoretical difficulties which must be carefully considered. The cold ion formulation uses the Bohm criterion on ion kinetic energy to assure a self-consistant sheath solution. We show that a finite temperature plasma ion distribution must have its low energy tail cut off before it enters the collisionless sheath since otherwise no self-consistant sheath solution exists. We expect a transitional region to exist between the collisionless sheath and the neutral plasma since we are asymptotically matching the two. This region would be collisional but with relatively strong electric field

that would accelerate and depopulate the ion distribution of low velocity members. Therefore we cut off the low energy tail of the ion distribution. We show that the minimum ion distribution shift speed depends logarithimically on an arbitrarily chosen cut-off of low energy ions, thus we can therefore pick an order-of-magnitude cut-off with little effect on the physical outcome. In both the cold ion and finite temperature ion cases, self-consistantcy is critical at the plasma-sheath interface, and we develop a generalized self-consistancy condition which includes the original Bohm criterion as a special case.

When trapped ions and surface emission ions are considered, the point of critical self-consistancy moves away from the plasma-sheath interface into the sheath. The new generalized self-consistancy condition remains valid for this case. The amount of surface emission ions present in the sheath is determined by the Saha-Langmuir equation and thus by the temperature and work function of the electrode along with the neutral pressure next to the electrode. On the other hand, the amount of trapped ions is determined by the coll'sional processes (largely charge exchange) in the sheath. The amount of trapped ions cannot be easily calculated because of the complexity of the collisional processes. Threrefore, we estimate the amount of trapped ions and produce results for a range of values.

3.1 <u>Assumptions</u>

In this section we list and discuss the assumptions of the present sheath formulation and their justifications. The present formulation, which removes some previous idealizations, assumes:

1) the sheath is collisionless,

2) the electron distributions from the emitter and collector are Maxwellian with the emitter and collector temperatures respectively,

3) the plasma electrons are Maxwellian with the plasma electron temperature,

4) the ion distribution from the plasma has the neutral temperature, and is a shifted Maxwellian distribution,

5) at the plasma-sheath interface, charge neutrality exists,

6) at the plasma-sheath interface, the electric field is small (in the match-asymptotic sense),

7) the trapped ions have a Maxwellian distribution with the emitter temperature and an arbitrarily specified density, and

8) the surface emission ions are emitted with a Maxwellian distribution governed by the Saha-Langmuir equation.

In contrast, most previous formulations have assumed:

1) the ion distribution is cold,

2) the plasma electron density in the sheath is Boltzmann with potential, and

3) the emitter electron distribution is also cold.

These three assumptions simplified the mathematics considerably, but produce relatively large errors in the sheath results,

particularly for small sheath heights. Since the emitter sheath effects of interest here, namely reflection, trapped ions, and surface emission ions, produce smaller sheath heights, it is essential to remove these assumptions. Additionally, the cold ion assumption is totally incompatible with ion reflection.

We can formulate the sheath using the Poisson equation in one dimension,

$$\frac{d^2\phi}{dx^2} = 4\pi q \left(n_i(\phi) - n_e(\phi) \right) , \tag{1}$$

where ϕ is potential, x is distance into the sheath, q is unit charge, $n_i(\phi)$ is ion density, and $n_e(\phi)$ is electron density. The quantities $n_i(\phi)$ and $n_e(\phi)$ are only functions of ϕ by virtue of the collisionless assumption. In non-dimensional form, eq.1 becomes

$$\frac{d^2\chi}{d\xi^2} = F(\chi) , \tag{2}$$

where $\chi = (q\phi)/(kT_E)$, $\xi = x/\lambda_D$, and where

$$\lambda_D = \sqrt{\frac{kT_E}{4\pi q^2 n_o}} \tag{3}$$

which is the Debye length. The quantity n_0 is the plasma density at the plasma-sheath interface. The function $F(\chi)$ is

$$F(\chi) = \frac{n_i(\chi) - n_e(\chi)}{n_o} . \tag{4}$$

The collisionless assumption is used because the Debye length in the thermionic convertor is always at least an order of magnitude smaller than the mean free paths. In principle, a transitional layer must exist to buffer between the collisionless sheath and

the continuum plasma. This layer would also accelerate low energy ions and therefore cut off the bottom of the ion distribution. The cut-off is arbitrarily determined, but has a weak logarithimic effect on the sheath results (it raises ion distribution shift speed).

Assumptions 2 and 8 regarding the surface emission of electrons and ions are expected to be very good because the surface temperatures are high. The emitted distributions should be indistinguishable from Maxwellian distributions. The other assumptions regarding distributions, 3,4 and 7 are more tenuous. The ion distribution is assumed to have the neutral temperature because there is large charge-exchange collision cross-section between the ions and the neutrals. The shift in the ion distribution (assumption 4) is to be determined as the minimum shift required to construct a self-consistant sheath. The assumption that the trapped ions are at the neutral temperature is also based on the predominance of charge exchange collisions. The assumption that the plasma electrons are in a Maxwellian distribution with their own temperature is based on the length of the convertor plasma region (approx. 15 mean free paths). The convertor is long enough that the electrons have time to equilibrate with each other but not long enough to equibrate with the ions. [1]

----

[1] See, for instance, Montgomery, p.33.

3.2 The General Solution Condition

Before proceeding on to discuss the possible sheath configurations and their specific equations, we develop the general solution condition which applies to all collisionless sheaths to preclude consideration of non-self-consistant solutions. Asymptotically matching the collisionless sheath to the quasi-neutral plasma always requires some condition on the ion distribution function coming into the sheath from the plasma. In the past this had been the Bohm criterion which assumed cold plasma ions and required the monoenergetic plasma ion distribution to be shifted up in velocity to

$$ U_{mon.} = \sqrt{\frac{kT_e}{M}} $$

where T_e is plasma electron temperature, k is Boltzmann's constant and M ion mass. In this section it will be shown that a general condition for solving the collisionless sheath with a neutral plasma-sheath interface exists and that the Bohm criterion and other local (at the plasma-sheath interface) matching conditions are special cases of the general condition. We show that local matching is a necessary but not sufficient condition on the sheath solution. In the absence of trapped ions or surface emission ions, as is the case with most past calculations, local matching proves to be also sufficient. Further, we show, in the case of no trapped ions or surface emission ions, that for finite temperature the ion distribution must have no zero velocity ions when it enters the collisionless sheath.

A self-consistant sheath solution is found by integrating the nondimensional poisson equation from the last section,

$$\frac{d^2\chi}{d\xi^2} = F(\chi).$$

(1)

The specific forms of F(χ) are developed in the next section but we need not know them until we wish to evaluate specific cases. By convention $\chi = 0$ at the plasma-sheath interface and increasing χ repels electrons. To construct a non-trivial solution [2] we integrate eq.1 as follows,

$$\frac{d\chi}{d\xi}\frac{d^2\chi}{d\xi^2} = F(\chi)\frac{d\chi}{d\xi},$$

(2)

$$\frac{1}{2}\left(\frac{d\chi}{d\xi}\right)^2\Big|_{\xi_1}^{\xi_2} = \int_{\xi_1}^{\xi_2} F(\chi)\frac{d\chi}{d\xi}\,d\xi,$$

(3)

$$\frac{1}{2}\left(\frac{d\chi}{d\xi}\right)^2\Big|_{\xi_1}^{\xi_2} = \int_{\chi_1}^{\chi_2} F(\chi)d\chi.$$

(4)

Transforming eq.3 into eq.4 implicitly assumes $\chi(\xi)$ is monotonic on the domain (ξ_1,ξ_2). Since at the plasma-sheath interface, we assume charge neutrality and zero electric field, we have $F(0) = 0$ and $d\chi/d\xi = 0$. Therefore we can write,

$$\frac{1}{2}\left(\frac{d\chi}{d\xi}\right)^2 = \int_0^{\chi} F(\chi)d\chi$$

(5)

and,

$$\frac{d\chi}{\sqrt{2\int_0^{\chi} F(\chi)d\chi}} = \pm d\xi$$

(6)

- - - - - - - - - - - - - - - - - - - -

[2] Since $F(0) = 0$ by charge neurality, there is alway the trivial solution $\chi = 0$.

Equation 6 is the method for constructing non-trivial solutions. From eq.6 and our previous observation about converting eq.3 into eq.4 we can see that that inequality,

$$\int_0^x F(x)\,dx \geq 0 \quad , \quad 0 \leq x \leq x_m \tag{7}$$

must hold where x_m is the first maximum or minimum x reaches in the sheath since otherwise $x(\xi)$ is not monotonic. If we attempt to construct a solution which does not meet this condition, then eq.6 causes $x(\xi)$ to double back before reaching its full sheath height.

Shown below in figs. ... a) through 3.2.1(d) are the expected emitter ... ations and their solution conditions from eq. ... are arranged in the order that we expect them to ... current density through the convertor is reduced and the ratio of emitter Richardson current density to net current density increases. From the general solution condition (eq 7), we can derive necessary local (at the plasma-sheath interface) matching conditions, of which generalized Bohm criterion is a special case. We can expand $F(x)$ around $x=0$ as

$$F(x) = \sum_{n=1}^{\infty} a_n x^{n/2} - \sum_{n=2}^{\infty} b_n x^{n/2} \ln x \;, \tag{8}$$

since $F(x)$ may be represented asymptotically in this form for cases we intend to develop. Then eq.8 may be integrated,

$$\int_0^x F(x)\,dx = \sum_{n=1}^{\infty} \frac{a_n}{\frac{n}{2}+1} x^{n/2+1}$$

$$- \sum_{n=2}^{\infty} \frac{b_n}{\left(\frac{n}{2}+1\right)^2} x^{n/2+1} \left(\ln(x^{n/2+1}) - 1 \right) . \tag{9}$$
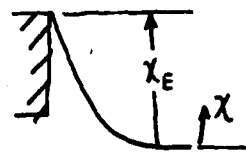
$$\int_0^X F(x)\,dx \geq 0 \;,\; 0 \leq X \leq X_E$$

Figure 3.2.1(a) Single Electron Repelling Sheath
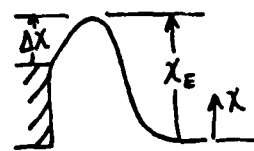
$$\int_0^X F(x)\,dx \geq 0 \;,\; 0 \leq X \leq X_E$$

Figure 3.2.1(b) Double Non Ion Reflecting Sheath
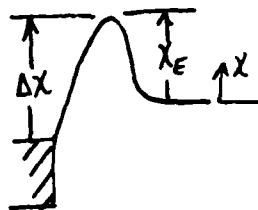
$$\int_0^X F(x)\,dx \geq 0 \;,\; 0 \leq X \leq X_E$$

Figure 3.2.1(c) Double Ion Reflecting Sheath
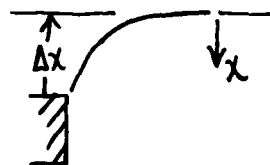
$$\int_0^X F(x)\,dx \leq 0 \;,\; 0 \leq X \leq \Delta X$$

Figure 3.2.1(d) Single Ion Repelling Sheath

The asymptopic order of the terms in this equation is $a_1\ b_2\ a_2\ b_3$ a_3 ... To insure that at least local matching is satisfied, the first non-zero term must be positive. We call this the

generalized Bohm criterion. The usual Bohm criterion assumes $F(X)$ is expandable as,

$$F(X) = 0 + \frac{\partial F}{\partial X}\bigg)_{X=0} X + \frac{\partial^2 F}{\partial X^2}\bigg)_{X=0} \frac{X^2}{2!} + \cdots \tag{10}$$

in which case the criterion is

$$a_2 = \frac{\partial F}{\partial X}\bigg)_{X=0} \geq 0. \tag{11}$$

When only cold ions are considered, the Bohm criterion (eq.11) is sufficient, but when finite temperature ions are considered, we must apply the generalized Bohm criterion. If trapped or surface emission ions are present, we find that local matching is not sufficient and that the full solution condition must be applied.

3.3 Equations

In this section we develop the sheath equations for the collisionless emitter sheath configurations shown in fig. 3.2.1 and for the collisionless collector sheath. In order to make the derivations as clear as possible, we divide this section into subsections for each of the cases listed previously and then follow a standard format in presenting the equations. We divide each subsection into the following order of presentation:

1. Sheath Configuration

2. $F_i(X)$ and $F_e(X)$

3. Integrals of $F_i(X)$ and $F_e(X)$

4. Equations: $F_i(0) = 1$,

$$F_e(0) = 1,$$

$$\min\left[\int_0^x F(x)dx \quad , \ 0 <= x <= x_E \right] = 0,$$

$$\int_0^{x_E} F(x)dx \quad = 0$$

5. Useful Resultant Quantities

We begin each subsection with the sheath configuration and appropriate definitions, and then derive the functions $F_i(x)$ and $F_e(x)$ accordingly. These functions are respectively the total ion and total electron densities as functions of sheath potential. The the third part of each subsection, we find the integrals of $F_i(x)$ and $F_e(x)$. The fourth part presents the equations which are solved simultaneously for the sheath. The equations $F_i(x) = 1$ and $F_e(x) = 1$ represent charge neutrality at the plasma-sheath interface: the charge densities there are both set equal to 1 because they are nondimensionalized by total plasma density, n_0, at the plasma-sheath interface. The third equation is the general solution condition, and the fourth equation is a condition which applies only in the case of a double sheath; it means that $d\phi/dx = 0$ at the sheath peak. This can be seen from eq. 3.2.5. These four equations are used to solve for the four variables:

N_i^- = density of ions moving toward the emitter

at the plasma-sheath interface,

N_E = density of electrons crossing the motive

peak (if any) coming from the emitter,

N_0^- = density of electrons moving toward the emitter

at the plasma-sheath interface, and

u_s = shift in the ion velocity distribution coming

from the plasma at the plasma-sheath interface.

The first three of these variables, denoted by capital N's are nondimensionalized by plasma density at the plasma-sheath interface, n_0. In the cases where no motive peak exists, the fourth equation does not apply since N_E is known. In general these equations must be solved numerically, and the numerical methods employed are straight forward. Therefore, no discussion of the methods is presented. Finally, in the fifth part of each subsection, we present the useful quantities that the sheath results produce.

a. single electron repelling sheath

1. Configuration
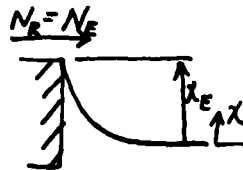
In this sheath, which occurs at high current densities, the Richardson emitted density, N_R, is equal to the emitted density, N_E, because no motive peak exists.

2. $F_i(x)$ and $F_e(x)$

The ion density is

$$F_i(x) = \frac{\int_{u_{cut}}^{\infty} e^{-(u-u_s)^2} \dfrac{u\,du}{\sqrt{u^2+x}}}{\int_{u_{cut}}^{\infty} e^{-(u-u_s)^2} du} \tag{1}$$

where u_s is the ion distribution shift speed and u_{cut} is the cut-off of low energy ions. Both u_s and u_{cut} are nondimensionalized by

$$u = \frac{U}{\sqrt{\dfrac{2kT_E}{M}}}$$

where U is velocity. The electron density is

$$F_e(x) = N_E \left\{ \frac{2}{\sqrt{\pi}} \int_o^{\infty} e^{-u^2} \frac{u\,du}{\sqrt{u^2+x}} \right\}$$

$$+ N_o^- \left\{ \frac{2}{\sqrt{\pi}} \int_{\sqrt{\frac{x}{\tau}}}^{\infty} e^{-u^2} \frac{u\,du}{\sqrt{u^2 - x/\tau}} + \frac{2}{\sqrt{\pi}} \int_{\sqrt{\frac{x}{\tau}}}^{\sqrt{\frac{x}{\tau}}} e^{-u^2} \frac{u\,du}{\sqrt{u^2 - x/\tau}} \right\} \tag{2}$$

where $N_E = N_R$ and both are the nondimensional emitted electron density at the plasma-sheath interface. The quantity τ is the nondimensional plasma electron temperature given by the ratio T_e/T_E. The first term in $F_e(x)$ represents the decreasing density contribution of emitted electrons as they accelerate down the sheath. The second term represents the density contribution of the plasma electrons which are decelerated as they climb the sheath.

3. Integrals of $F_i(x)$ and $F_e(x)$

These are just the integrals of eqs. 1 and 2. The integral of $F_i(\chi)$ is

$$\int_0^\chi F_i(\chi)d\chi = \int_{u_{cut}}^\infty e^{-(u-u_s)^2} 2u \left(\sqrt{u^2+\chi} - u\right) du. \qquad (3)$$

And, the integral of $F_e(\chi)$ is

$$\int_0^\chi F_e(\chi)d\chi = N_0^- \left\{ \tau(1- e^{-\chi/\tau}) + \tau \frac{2}{\sqrt{\pi}} \int_{\sqrt{\frac{\chi}{\tau}}}^{\sqrt{\frac{\chi_E}{\tau}}} e^{-u^2} 2u(u-\sqrt{u^2-\frac{\chi}{\tau}})\, du \right.$$
$$\left. + \tau \frac{2}{\sqrt{\pi}} \int_0^{\sqrt{\frac{\chi}{\tau}}} e^{-u^2} 2u^2 du \right\} \qquad (4)$$
$$+ N_E \left\{ \frac{2}{\sqrt{\pi}} \int_0^\infty e^{-u^2} \left(2u\sqrt{u^2+\chi_E} - 2u\sqrt{u^2+\chi_E-\chi}\right) du \right\}.$$

4. Equations

Charge neutrality for the ions, $F_i(0) = 1$, is immediately satified by eqs. 1 because no ions are reflected and therefore $N_i^- = 1$. Charge neutrality for the electrons is

$$1 = F_e(0) = N_E \left\{ \frac{2}{\sqrt{\pi}} \int_0^\infty e^{-u^2} \frac{u\,du}{\sqrt{u^2+\chi_E}} \right\} + N_0^- \left\{ 1 + \frac{2}{\sqrt{\pi}} \int_0^{\sqrt{\frac{\chi_E}{\tau}}} e^{-u^2} du \right\}. \qquad (5)$$

To complete the formulation, we apply local matching (the Bohm criterion) at the plasma-sheath interface. This can be done because 1) the fourth equation does not apply since there is no

motive peak in this sheath, and 2) local matching satisfies the general solution condition is this case. Local matching is sufficient because no trapped ions exist and we have assumed that there is no surface emission of ions in this case. The justification for assuming no surface emission and carrying out local matching in this case is that when this sheath occurs surface emission is entirely negligible. [3] Also, this case, because of simplicity, is used to explain the need for a cutoff of low energy ions in local Bohm matching. Local matching is done by asymptotically expanding $F(x) = F_i(x) - F_e(x)$ at $x = 0$. The lowest order terms are:

$$F(x) = 0 - x^{1/2}\left\{\begin{array}{l} 1 \text{ if } u_{cut} = 0 \\ 0 \text{ if } u_{cut} > 0 \end{array}\right\} \frac{e^{-u_s^2}}{\int_{u_{cut}}^{\infty} e^{-(u-u_s)^2} du} + O(x \ln x). \quad (6)$$

The $x^{1/2}$ term in this expansion comes entirely from the low energy ions entering the sheath. It represents the acceleration of zero velocity ions of finite velocity. Since local matching requires the lowest order term to be greater than or equal to zero (eq. 3.2.10), the cutoff of low energy ions, u_{cut} must be greater than zero. Otherwise, no self-consistant sheath solution can be constructed. We choose an arbitrary cut-off of

$$u_{cut} = (.1)u_{mono}$$

(u_{mono} is defined at the beginning of section 3.2) for two reasons: first, the effect of the cut-off on u_s, the ion

----

[3] At the high current densities corresponding to this sheath, surface emission ion density is 10^{-6} of total ion density.

distribution shift, is logarithmically weak (see fig. 3.4.3), and second, we expect an intermediate asymptotic region to exist between the collisionless sheath and the neutral plasma that would accelerate the ion distribution and depopulate it of low energy ions.

With this cutoff established, the expansion of F(x) is then:

$$F(\chi) = \chi \left\{ N_0 \frac{-2}{\sqrt{\pi}} \frac{1}{\tau} \left[1 + \int_0^{\sqrt{\frac{\chi_E}{\tau}}} e^{-u^2} du + \frac{1}{2\sqrt{\frac{\chi_E}{\tau}}} e^{-\chi_E/\tau} \right] \right.$$

$$- N_E \frac{2}{\sqrt{\pi}} \int_0^{\infty} e^{-u^2} \frac{\frac{1}{2} u \, du}{\sqrt{u^2 + \chi_E}^3}$$

$$\left. - \frac{\int_{u_{cut}}^{\infty} e^{-(u-u_s)^2} \frac{1}{2u^2} \, du}{\int_{u_{cut}}^{\infty} e^{-(u-u_s)^2} du} \right\} + O(\chi^2) , \qquad (7)$$

where the term in brackets is $\partial F/\partial \chi$ and the generalized Bohm criterion is

$$\left. \frac{\partial F}{\partial \chi} \right)_{\chi=0} \geq 0. \qquad (8)$$

Equations 8 and 5 written as,

$$1 = N_E C_2(\chi_E) + N_0^- C_1(\chi_E, \tau),$$

$$N_0^- C_5(\chi_E, \tau) = N_E C_6(\chi_E) + B(u_s), \qquad (9)$$

are solved numerically for u_s and N_0^- when N_E, τ, and χ_E are given.

5. Useful Resultant Quantities

The sheath solution provides the following functions to the rest of the thermionic convertor formulation:

$$\bar{u} = \bar{u}\,(\chi_E, T, N_E),$$
$$j = j\,(\chi_E, T, N_E),$$
$$Q = Q\,(\chi_E, T, N_E),$$
$$\alpha_0 = \alpha_0\,(\chi_E, T, N_E).$$

(10)

The first quantity, $\bar{u}$, is the net ion loss rate

$$\bar{u} = \frac{\int_{u_{cut}}^{\infty} u\, e^{-(u-u_s)^2}\, du}{\int_{u_{cut}}^{\infty} e^{-(u-u_s)^2}\, du}\,.$$

(11)

The second quantity, j, is normalized current

$$j = J/J_E$$

(12)

where J is net current density

$$J = \frac{N_E\, n_0\, a_E}{2} - \frac{N_0^-\, n_0\, a_e}{2}\, e^{-\chi_E/T}$$

(13)

and J_E is emitted current density

$$J_E = n_0\, N_E\, \sqrt{\frac{2kT_E}{\pi m}}$$

(14)

and where a_e and a_E are the thermal speeds

$$a_e = \sqrt{\frac{8kT_e}{\pi m}} \quad , \quad a_E = \sqrt{\frac{8kT_E}{\pi m}}\,.$$

The third quantity is electron Mach number

$$Q = \frac{J}{n_0\,\sqrt{\frac{kT_e}{m}}}\,.$$

(15)

And, the fourth quantity, α_0, is the ratio of electron density at

the plasma-sheath interface moving toward the emitter to the total electron density there,

$$\alpha_o = N_o^- = \frac{n_o^-}{n_o} \qquad (16)$$

b. and c. double sheath

1. Configuration
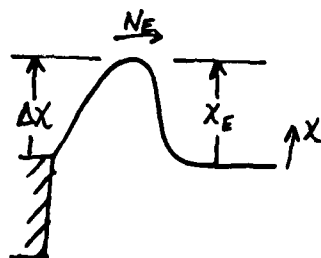
(Δx may be larger or smaller than x_E)

We develop cases b and c together because the differences are minimal. In this case the emitted density, N_R, is no longer the same as the emitted density crossing the motive peak, N_E, because the back sheath height, Δx, repels some of the emitted electrons.

2. $F_i(x)$ and $F_e(x)$

First, we consider $F_i(x)$. This is the most complicated of the two because we take into account three classes of ions: plasma ions (ions coming onto the sheath from the plasma), trapped ions, and surface emission ions. The surface emission ion density is known from the Saha-Langmuir equation and the plasma ion density is found in the usual way by setting $F_i(0) = 1$. However, the trapped ion density is not determined by anything in

the collisionless sheath theory; it is determined by the small number of collisions that do occur in the sheath. It is not known how to calculate the amount of trapped ions precisely, but clearly it should be less than the local equilibrium ("fully trapped") plasma density. The major source of trapped ions is expected to be plasma ions passing through the sheath having charge exchange collisions with neutrals.

To simplify the equations for $F_i(x)$, we use a convention of comparing trapped and surface emission ion density to the plasma ion density as illustrated in fig. 3.3.1. Figure 3.3.1 shows the distribution of ion velocity at the sheath motive peak. The trapped ion region is limited by the lesser of Δx or x_E by definition; an ion is not trapped if it has an energy greater than this. Trapped and surface emission ion densities are denoted by f_{tr} and f_{sur}. When $f_{tr} = 1$ and $f_{sur} = 1$, the dotted curve representing a thermal equilibrium distribution (based on the density of plasma ions) is filled by the trapped and surface emission ions.

$F_i(x)$ is then

$$F_i(x) = F_{tr}(x) + F_{sur}(x) + F_{plasma}(x) \tag{1}$$

where

$$F_{tr}(x) = \frac{2 f_{tr} e^{x_E}}{\sqrt{\pi}} \int_{\sqrt{x_E - x}}^{\sqrt{min(\Delta x, x_E)}} e^{-u^2} \frac{u \, du}{\sqrt{u^2 - (x_E - x)}} \, , \tag{2}$$
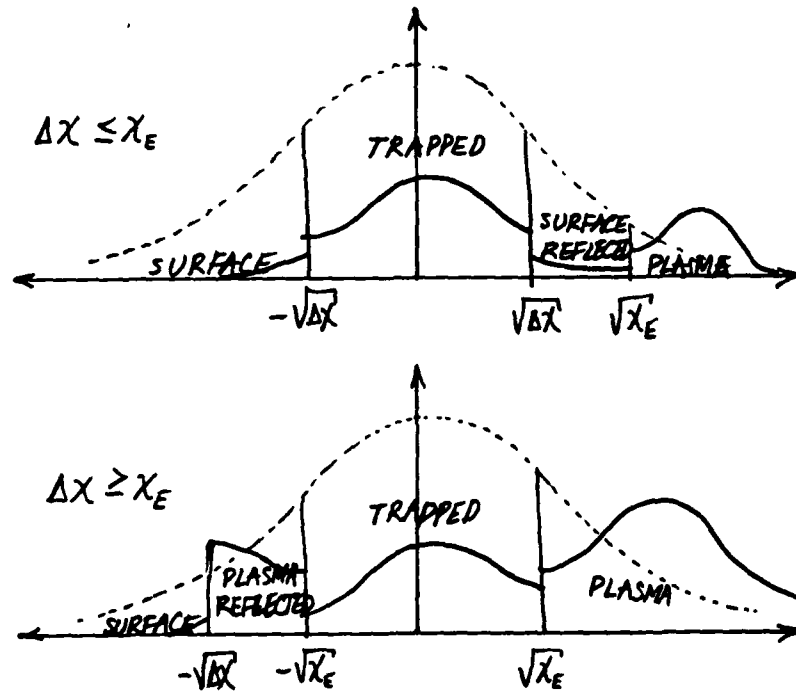
Figure 3.3.1 Trapped and Surface Emission Ions

at the Sheath Motive Peak

$$F_{sur}(\chi) = \frac{f_{sur}\,e^{\chi_E}}{\sqrt{\pi}}\left\{\int\limits_{max(\sqrt{\Delta\chi},\,\sqrt{\chi_E-\chi})}^{\infty} e^{-u^2}\frac{u\,du}{\sqrt{u^2-(\chi_E-\chi)}} + \int\limits_{max(\sqrt{\Delta\chi},\,\sqrt{\chi_E-\chi})}^{\sqrt{\chi_E}} e^{-u^2}\frac{u\,du}{\sqrt{u^2-(\chi_E-\chi)}}\right\}, \quad (3)$$

$$F_{plasma}(\chi) = \frac{f_{plasma}}{\sqrt{\pi}}\left\{\int\limits_{u_{cut}}^{\infty} e^{-(u-u_s)^2}\frac{u\,du}{\sqrt{u^2+\chi}} + \int\limits_{u_{cut}}^{\sqrt{\Delta\chi-\chi_E}} e^{-(u-u_s)^2}\frac{u\,du}{\sqrt{u^2+\chi}}\right\}. \quad (4)$$

In these equations two conventions have been used to simplify the notation:

1) if a square root has a negative argument, then it is zero

2) if an integral's upper limit is less than the lower limit, then the integral is zero.

This convention is followed for all integrals over distribution functions. As before the densities are nondimensionalized by total plasma density at the plasma-sheath interface. Finally the parameter f_{sur} is related to nondimensional emitted density by

$$f_{sur} = 2e^{\Delta \chi - \chi_E} F_{surface}. \tag{5}$$

Electron density, $F_e(\chi)$, is

$$F_e(\chi) = N_0^- \left\{ \frac{2}{\sqrt{\pi}} \int_{\sqrt{\frac{\chi}{\tau}}}^{\sqrt{\frac{\chi_E}{\tau}}} e^{-u^2} \frac{u\,du}{\sqrt{u^2 - \chi_E/\tau}} + \frac{2}{\sqrt{\pi}} \int_{\sqrt{\frac{\chi}{\tau}}}^{\infty} e^{-u^2} \frac{u\,du}{\sqrt{u^2 - \frac{\chi}{\tau}}} \right\}$$

$$+ N_E \left\{ \frac{2}{\sqrt{\pi}} \int_0^{\infty} e^{-u^2} \frac{u\,du}{\sqrt{u^2 + (\chi_E - \chi)}} \right\}. \tag{6}$$

The first term in this equation is the density of plasma electrons in the sheath. The second term is the density of emitted electrons in the sheath.

3. Integrals of $F_i(\chi)$ and $F_e(\chi)$

For the ions,

$$\int_0^\chi F_i(\chi)d\chi = \int_0^\chi F_{plasma}(\chi)d\chi$$

$$+ \int_0^\chi F_{tr}(\chi)d\chi \tag{7}$$

$$+ \int_0^\chi F_{sur}(\chi)d\chi$$

where

$$\int_0^\chi F_{plasma}(\chi)d\chi = \int_{u_{cut}}^\infty e^{-(u-u_s)^2} 2u\left(\sqrt{u^2+\chi} - u\right)du$$

$$+ \int_{u_{cut}}^{\sqrt{\Delta\chi-\chi_E}} e^{-(u-u_s)^2} 2u\left(\sqrt{u^2+\chi} - u\right)du, \tag{8}$$

$$\int_0^\chi F_{tr}(\chi)d\chi =$$

$$\frac{2f_{tr}}{\sqrt{\pi}} \left\{ e^\chi \int_0^{\sqrt{\chi+\Delta\chi-\chi_E}} e^{-u^2}du - e^{\chi_E-\Delta\chi}\sqrt{\chi+\Delta\chi-\chi_E} \right\},$$

$$\text{for} \quad \Delta\chi \leq \chi_E,$$

$$\tag{9}$$

$$= \frac{2f_{tr}}{\sqrt{\pi}} \left\{ e^\chi \int_0^{\sqrt{\chi}} e^{-u^2}du - \sqrt{\chi} \right\},$$

$$\text{for} \quad \Delta\chi \geq \chi_E,$$

$$\int_0^{\chi} F_{sur}(\chi)d\chi =$$
$$f_{sur}\left\{ \frac{1}{2}(e^{\chi}-1) + \frac{e^{\chi}}{\sqrt{\pi}} \left(\int_0^{\sqrt{\chi}} e^{-u^2}du - \sqrt{\chi}\, e^{-\chi} \right) \right\},$$

$$\text{for} \quad \Delta\chi \leq \chi_{\bar{E}},$$

$$= \frac{f_{sur}\, e^{\chi_E}}{\sqrt{\pi}} \left\{ \int_{\sqrt{\Delta\chi}}^{\infty} e^{-u^2}\, 2u \left(\sqrt{u^2 - \chi_E + \chi} - \sqrt{u^2 - \chi_E} \right) du \right\},$$

$$(10)$$

$$\text{for} \quad \Delta\chi \geq \chi_{\bar{E}}.$$

For the electrons,

$$\int_0^\chi F_e(\chi)d\chi =$$

$$N_0^- \left\{ \tau[1 - e^{-\chi/\tau}] + \tau \int_{\sqrt{\frac{\chi}{\tau}}}^{\sqrt{\frac{\chi}{\tau}}} \frac{2}{\sqrt{\pi}} e^{-u^2} 2u \left(u - \sqrt{u^2 - \frac{\chi}{\tau}}\right) du \right.$$

$$\left. + \tau \int_0^{\sqrt{2}\tau} e^{-u^2} 2u^2 du \right\}$$

(11)

$$+ N_E \left\{ \frac{2}{\sqrt{\pi}} \int_0^\infty e^{-u^2} \left(2u\sqrt{u^2 + \chi_E} - 2u\sqrt{u^2 + \chi_E - \chi}\right) du \right\}.$$

4. Equations

First, we have $F_i(0) = 1$ from eqs. 1,2,3 and 4,

$$1 = \frac{f_{sur}}{\sqrt{\pi}} \int_{\sqrt{\Delta\chi - \chi_E}}^\infty e^{-u^2} du +$$

$$\frac{f_{plasma}}{\sqrt{\pi}} \left\{ \int_{u_{cut}}^\infty e^{-(u-u_s)^2} du + \int_{u_{cut}}^{\sqrt{\Delta\chi - \chi_E}} e^{-(u-u_s)^2} du \right\}$$

(12)

A term for trapped ions does not appear in this equation because

trapped ions, by definition, do not exist at the plasma-sheath interface. And, we have $F_e(0) = 1$ from eq. 6,

$$
1 = N_0^- \left\{ 1 + \frac{2}{\sqrt{\pi}} \int_0^{\sqrt{\frac{\chi_E}{T}}} e^{-u^2} du \right\} \\
+ N_E \left\{ \frac{2}{\sqrt{\pi}} \int_0^{\infty} e^{-u^2} \frac{u \, du}{\sqrt{u^2 + \chi_E}} \right\}.
$$

(13)

The other two equations which apply in this section,

$$
min \left[\int_0^{\chi} F(x) dx , \ 0 \leq x \leq \chi_E \right] = 0,
$$

(14)

and,

$$
\int_0^{\chi_E} F(x) dx = 0
$$

(15)

are straight forward applications of the integrals of $F_i(x)$ and

$F_e(\chi)$. We will not write out the details of these equations since they cannot be solved analytically. The numerical solution of these is simple in principle: we have to solve four simultaneous equations in four variables, N_0^-, N_E, f_{plasma} and u_s where f_{sur}, f_{tr}, χ_E, $\Delta\chi$, u_{cut} and τ are given. And, the four equation can be reduced to two by using eqs. 12 and 13 in 14 and 15 to eliminate f_{plasma} and N_0^-. However, the actual solution for each case requires approximately 15 sec of CPU time on an IBM 370-3081.

5. Useful Resultant Quantities

The results of this sheath are presented in the same way as in 3.3(a)5 except that N_E is a dependent variable and the results now depend on f_{tr}, f_{sur} and $\Delta\chi$:

$$
\begin{aligned}
\bar{u} &= \bar{u}\,(\chi_E, \Delta\chi, \tau, f_{tr}, f_{sur}), \\
j &= j\,(\chi_E, \Delta\chi, \tau, f_{tr}, f_{sur}), \\
Q &= Q\,(\chi_E, \Delta\chi, \tau, f_{tr}, f_{sur}), \\
\alpha_0 &= \alpha_0(\chi_E, \Delta\chi, \tau, f_{tr}, f_{sur}), \\
N_E &= N_E(\chi_E, \Delta\chi, \tau, f_{tr}, f_{sur}).
\end{aligned}
\tag{16}
$$

d. single ion repelling sheath

1. Configuration
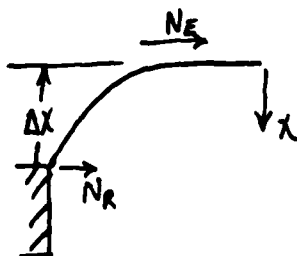
In this case, we have reversed the sense of X for convenience.

2. $F_i(X)$ and $F_e(X)$

The ion density, $F_i(X)$, is

$$F_i(X) = \frac{\int_{\sqrt{x}}^{\infty} e^{-(u-u_s)^2} \frac{u\,du}{\sqrt{u^2-x}} + \int_{\sqrt{x}}^{\sqrt{\Delta x}} e^{-(u-u_s)^2} \frac{u\,du}{\sqrt{u^2-x}} + f_s e^{-\Delta X} \int_0^{\infty} e^{-u^2} \frac{u\,du}{\sqrt{u^2+(\Delta-x)}}}{\int_0^{\infty} e^{-(u-u_s)^2}\,du + \int_0^{\sqrt{\Delta x}} e^{-(u-u_s)^2}\,du + f_s e^{-\Delta X} \int_0^{\infty} e^{-u^2} \frac{u\,du}{\sqrt{u^2+\Delta}}} \tag{1}$$

We have contracted this expression for ion density to eliminate N_i by using $F_i(0) = 1$ immediately. For this sheath configuration, there cannot be trapped ions.

The electron density, $F_e(X)$, is

$$F_e(X) = N_o^- \left\{ \frac{2}{\sqrt{\pi}} \int_0^{\infty} e^{-u^2} \frac{u\,du}{\sqrt{u^2 + x/\tau}} \right\}$$
$$+ N_E \left\{ 1 + \frac{2}{\sqrt{\pi}} \int_0^{\sqrt{x}} e^{-u^2}\,du \right\} e^X \tag{2}$$

where

$$F_e(0) = N_o^- + N_E = 1 \tag{3}$$

and

$$N_E = N_R e^{-\Delta X} \tag{4}$$

3. Integrals of $F_i(x)$ and $F_e(x)$

$$\int_0^x F_i(x) =$$

$$\frac{\int_0^\infty 2u^2 e^{-(u-u_s)^2} du + \int_0^{\sqrt{\beta x}} u^2 e^{-(u-u_s)^2} du - \int_{\sqrt{x}}^\infty 2u\sqrt{u^2-x}\, e^{-(u-u_s)^2} du - \int_{\sqrt{x}}^{\sqrt{\beta x}} 2u\sqrt{u^2-x}\, e^{-(u-u_s)^2} du}{\int_0^\infty e^{-(u-u_s)^2} du + \int_0^{\sqrt{\beta x}} e^{-(u-u_s)^2} du} \quad \text{----}$$ (5)

$$\frac{+ f_s e^{-\beta x} \int_0^\infty u e^{-u^2}\left(\sqrt{u^2+x}-u\right) du}{+ f_s e^{-\beta x} \int_0^\infty e^{-u^2}\frac{u\,du}{\sqrt{u^2+\beta x}}} \quad .$$

$$\int_0^x F_e(x)\, dx =$$

$$N_o^- \left[\frac{2}{\sqrt{\pi}} \int_0^\infty e^{-u^2}\, 2u\, \tau\left(\sqrt{u^2 + x/\tau} - u\right) du \right] \quad (6)$$

$$+ N_E \left[\frac{2}{\sqrt{\pi}}\left(e^x \int_0^{\sqrt{x}} e^{-u^2} du - \sqrt{x}\right) + \left(e^x - 1\right) \right]$$

4. Equations

Instead of presenting only the equations, in this case we can

produce an analytical result. We find, analytically, that the minimum for u_s is always less than zero for small Δx under certain easily satisfied conditions. Regardless of Δx, numerical calculation always supports $u_s = 0$.

To demonstrate that $u_s = 0$ for small Δx we assume $f_{sur} = 0$ for simplicity [*] and take the asymptotic expansion of the integrals for $u_s = 0$,

$$\int_0^{\chi} F(\chi)d\chi = \int_0^{\chi} F_i(\chi)d\chi - \int_0^{\chi} F_e(\chi)d\chi$$

$$= \left\{ \chi + \chi^{3/2}\left[\frac{2}{\sqrt{\pi}}\frac{2}{3} - \frac{2}{\sqrt{\pi}} \right] \right\} \tag{7}$$

$$- \left\{ \chi + \chi^{3/2}\left[\frac{4}{3\sqrt{\pi}}\left(1 - N_0^- - \frac{N_0^-}{T^{1/2}}\right) \right] \right\}.$$

The general solution condition then requires

$$N_0^- \leq \frac{3/2}{1 + T^{1/2}} \tag{8}$$

----

[*] In the cases that this sheath occurs, f_{sur} is always small (10^{-6}) and does not affect the numerical conclusion that $u_s = 0$.

We now show that for J >= 0 (positive net current density) eq. 8 is satified:

$$J = n_0 \left(\frac{N_E a_E}{2} - \frac{N_0^- a_e}{2} \right)$$

$$= n_0 \frac{a_E}{2} \left(1 - N_0^-(1 + \sqrt{T}) \right). \tag{9}$$

Then J >= 0 implies

$$N_0^- \leq \frac{1}{1 + \sqrt{T}} . \tag{10}$$

Therefore eq. 8 is satisfied for J >= 0 and $u_s = 0$ is a self-consistant solution.

5. Useful Resultant Quantities

The resultant quantities of this sheath must be presented to the rest the thermionic convertor formulation differently because there is no sheath height, x_E. In fact from eqs. 3 and 9 (charge neutrality and net current) we can immediately derive

$$j = \frac{Q(1 + \sqrt{T})}{Q + \sqrt{\frac{2}{T}}} . \tag{11}$$

The definitions of j and Q are as in 3.3(a) resultant quantities. Because of this, we present these sheath results in this case as

$$Q = Q(j, \tau),$$

$$u_s = 0, \tag{12}$$

e. collector sheath

1. Configuration
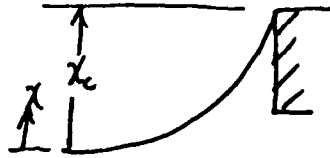
Since the collector is assumed to emit nothing, this case is particularly simple. As in all other cases, the electron distribution function is assumed to have no shift. However, as will be seen in section 4.2 the collector sheath height is usually small and goes to zero with ion reflection at the emitter. Because of this it may be of interest in further work to allow the electron distribution to have a shift and to simultaneously allow an ion repelling collector sheath.

2. $F_i(x)$ and $F_e(x)$

The ion density, $F_i(x)$, is

$$F_i(x) = \frac{\int_{u_{int}}^{\infty} e^{-(u-u_s)^2} \frac{u\,du}{\sqrt{u^2+x}}}{\int_{u_{int}}^{\infty} e^{-(u-u_s)^2}\,du} \tag{1}$$

and the electron density, $F_e(x)$, is

$$F_e(x) = e^{-x/\tau}\left[\frac{\frac{\sqrt{\pi}}{2} + \int_0^{\sqrt{\frac{x_c-x}{\tau}}} e^{-u^2}\,du}{\frac{\sqrt{\pi}}{2} + \int_0^{\sqrt{\frac{x_c}{\tau}}} e^{-u^2}\,du}\right] \tag{2}$$

3. Integrals of $F_i(x)$ and $F_e(x)$

In this case we do not list the integrals since local matching always suffices (because no trapped or surface emission ions exist).

4. Equations

To carry out local matching, we expand $F(x)$ and apply $F(x) >= 0$. $F_i(x)$ expanded is

$$F_i(x) = 1 - \left[\frac{\int_{u_{cut}}^{\infty} e^{-(u-u_s)^2} \frac{1}{2u^2} du}{\int_{u_{cut}}^{\infty} e^{-(u-u_s)^2} du} \right] x + O(x^2). \qquad (3)$$

And, $F_e(x)$ expanded is

$$F_e(x) = 1 - \left[\frac{1}{\tau} \frac{1}{\sqrt{\pi}} \sqrt{\frac{\tau'}{\chi_c}} \right] x + O(x^2). \qquad (4)$$

Therefore, the local matching condition is

$$\frac{1}{\tau} \sqrt{\frac{\tau'}{\pi \chi_c}} \geq \frac{\int_{u_{cut}}^{\infty} e^{-(u-u_s)^2} \frac{1}{2u^2} du}{\int_{u_{cut}}^{\infty} e^{-(u-u_s)^2} du} . \qquad (5)$$

This the classical Bohm criterion.

5. Useful Resultant Quantities

The results of this sheath are presented as:

$$\bar{u} = \bar{u}\,(\chi_c, \tau),$$
$$\alpha_1 = \alpha_1\,(\chi_c, \tau), \tag{6}$$

where α_1 is the fraction of electrons at the plasma-collector sheath interface moving toward the collector,

$$\alpha_1 = \frac{1}{1 + \frac{2}{\sqrt{\pi}} \int_0^{\sqrt{\frac{\chi}{\tau}}} e^{-u^2} du}. \tag{7}$$

3.4 Sheath Solutions

Again, we divide this section into subsections for each type of sheath. Most of the results in this section are on the double emitter sheath because its is the most complex case and contains the emitter sheath phenomena of interest - trapped ions and surface emission ions.

a. single electron repelling sheath

This sheath occurs at the emitter when the net current density, J, is greater than appoximately 75% of J_R. We do not present results for this case because they are expected to be similar to conventional theories.

b. and c. double sheath

This subsection on the double emitter sheath contains most of the results of interest. In this subsection, we first distinguish the results of the present full collisionless sheath theory from past approximate theories but still assuming no trapped or emitted ions. We then demonstrate the effect of trapped ions on the sheath. We make no mention of surface emission ions in this subsection because of their small amount and small effect in the convertor at the current densities we make calculations for. However, surface emission is fully included in all sheath results used in the thermionic convertor calculations.

The essential diferences in results of the present full collisionless theory and past approximate theories is illustrated in figs. 3.4.1, 3.4.2 and 3.4.3. Figure 3.4.1 demonstrates the relationship between sheath height, x_E, and normalized current, j. The first curve (to the right) is the simplest approximate, assuming that 1) the emitted electrons are monoenergetic at their average speed, 2) the plasma electrons are in a fully Boltzmann distribution despite a finite sheath height, and 3) the plasma ions are monoenergetic. The second curve removes the Boltzmann plasma electron assumption. The third curve removes the cold emitter electron assumption. And, the fourth curve removes the final assumption of cold plasma ions. The first two changes are unequivocal corrections to the sheath theory. However, the last correction, removal of the cold ion approximation requires the imposition of the cut-off of low energy ions. The cut-off, as discussed previously, is set at 10% of the monoenergetic Bohm
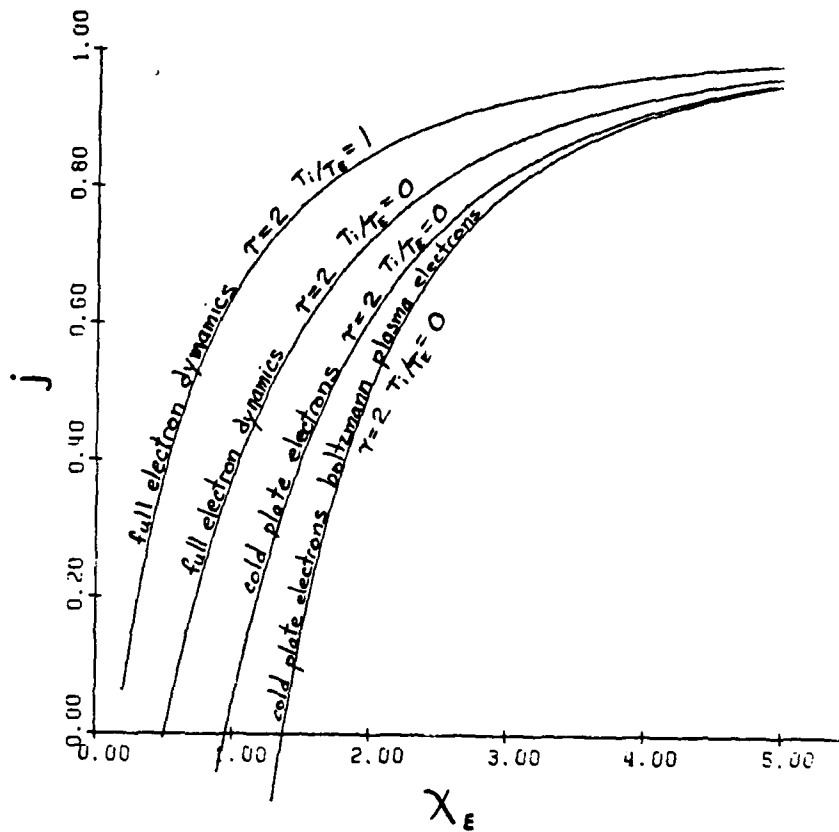
Figure 3.4.1 Net Current and Sheath Approximations

speed. Figure 3.4.2 shows the effect of these approximations on the ion distribution shift speed, u_s. It should be noted that u_s compares closely with the monoenergetic Bohm speed until the cold ion approximation is removed. Figure 3.4.3 shows the effect of the cut-off on shift speed, u_s, in the full sheath theory case. The weak variation of u_s is the justification for an arbitrary u_{cut}. We have made no mention of the back sheath height, ΔX, because its effect on the results is very small. However, this is not the case when surface emission ions or trapped ions are included.
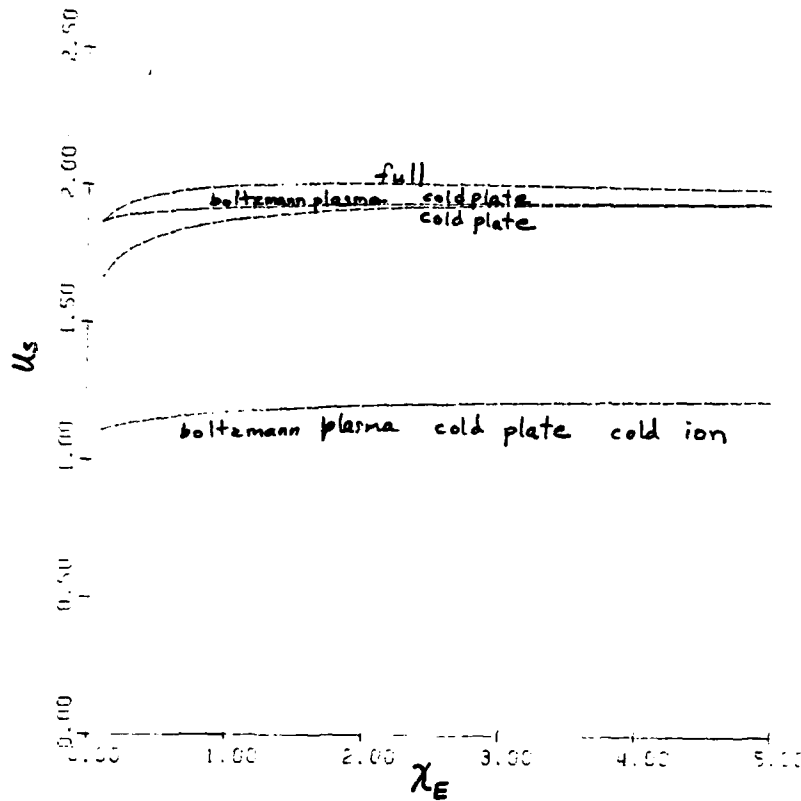
Figure 3.4.2   Shift Speed and Sheath Approximations

Trapped ions have a substantial effect on the sheath solution. Figure 3.4.4 shows the general solution condition for a double sheath with χ_E and for $f_{tr} = 0.0$ and for $f_{tr} = 0.2$. In the *no* trapped ion case ($f_{tr} = 0.0$) we have local matching in which the critical point occours at the plasma sheath interface ($\chi = 0$) As trapped ions are added, the critical point moves into the sheath ($f_{tr} = 0.2$). Figure 3.4.5 shows the sheath potential versus nondimensional position, $\xi = x/\lambda_D$. The two cases shown are for $f_{tr} = 0.0$ and $f_{tr} = 0.2$ corresponding to fig. 3.4.4. In the no trapped ion case the potential drops rapidly from its peak
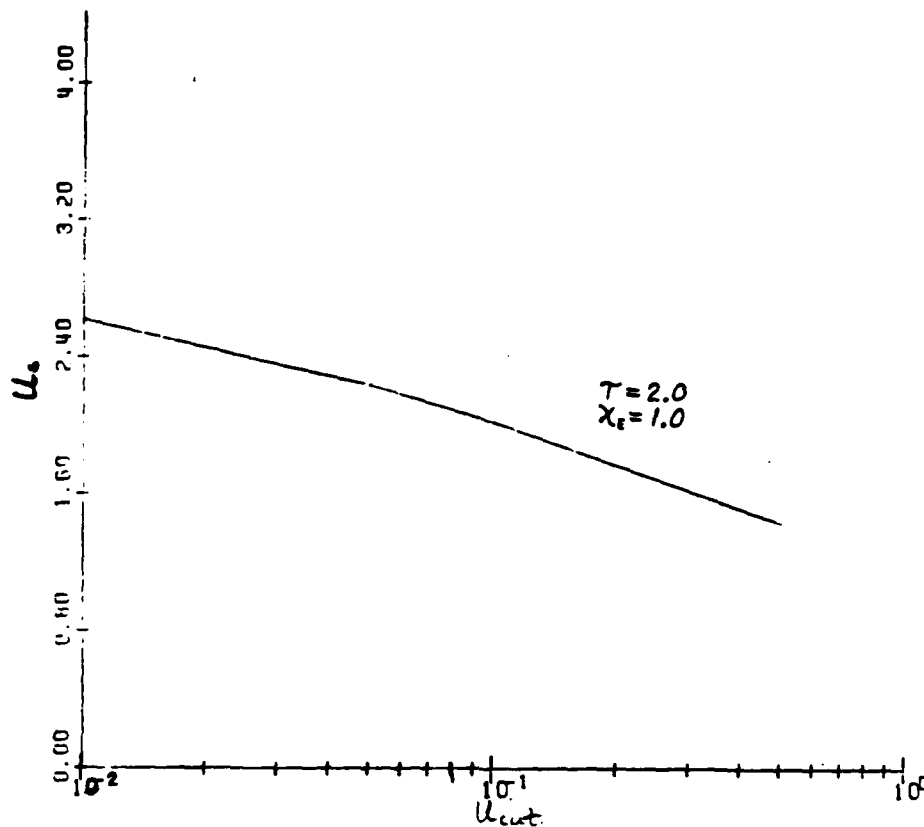
Figure 3.4.3 Effect of Cut-Off on Shift Speed

at χ_E = 2.0 to χ_E = 0.0. In the f_{tr} = 0.2 trapped case the
sheath drops rapidly to the critical matching point, where it
levels out asymptotically and then continues its drop to χ = 0.0.
This asymptotic region has a finite slope in fig. 3.4.5 because a
numerical factor has been added for display purposes. The
existence of this asymptotic "flat spot" is not troublesome
because a slight increase in u_s will remove it. Figure 3.4.6
shows the trapped ion effect on u_s for various χ_E. Only a
certain amount of trapped ions can be added before no sheath
solution exists. Trapped ions added for a given sheath height,
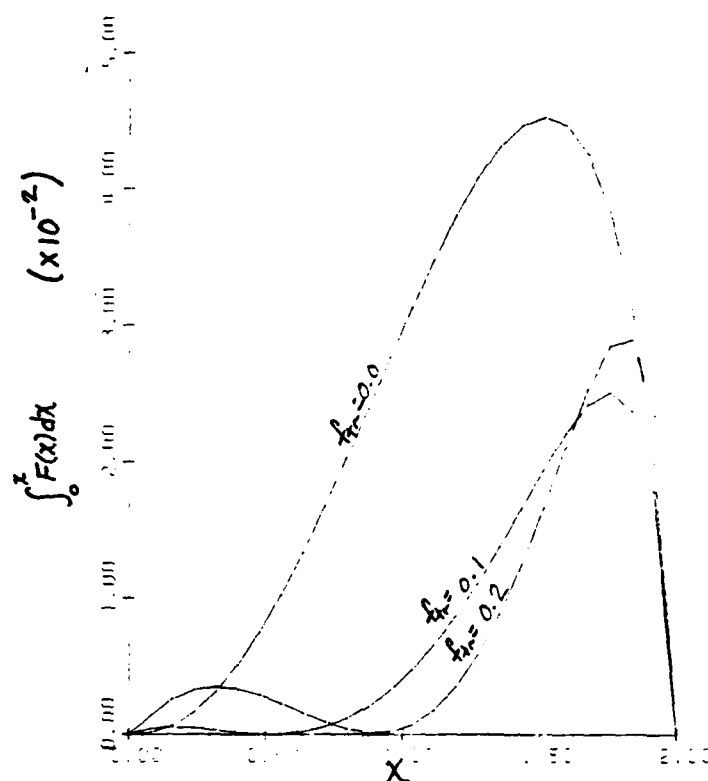
Figure 3.4.4 Solution Condition with Trapped Ions

x_E, require a larger n_E (emitted electrons) and a smaller N_0^- (

plasma electrons). The solution fails when the required N_0^- is

less than zero (a negative density of plasma electrons). The

failure point, in f_{tr}, decreases as x_E increases. This is

because the total density of trapped ions that corresponds to a

given f_{tr} rises exponentially with x_E. Figure 3.4.7 shows the

effect of trapped ions on nondimensional current density, j. The

essential feature here is that trapped ions reduce x_E for a given

j.
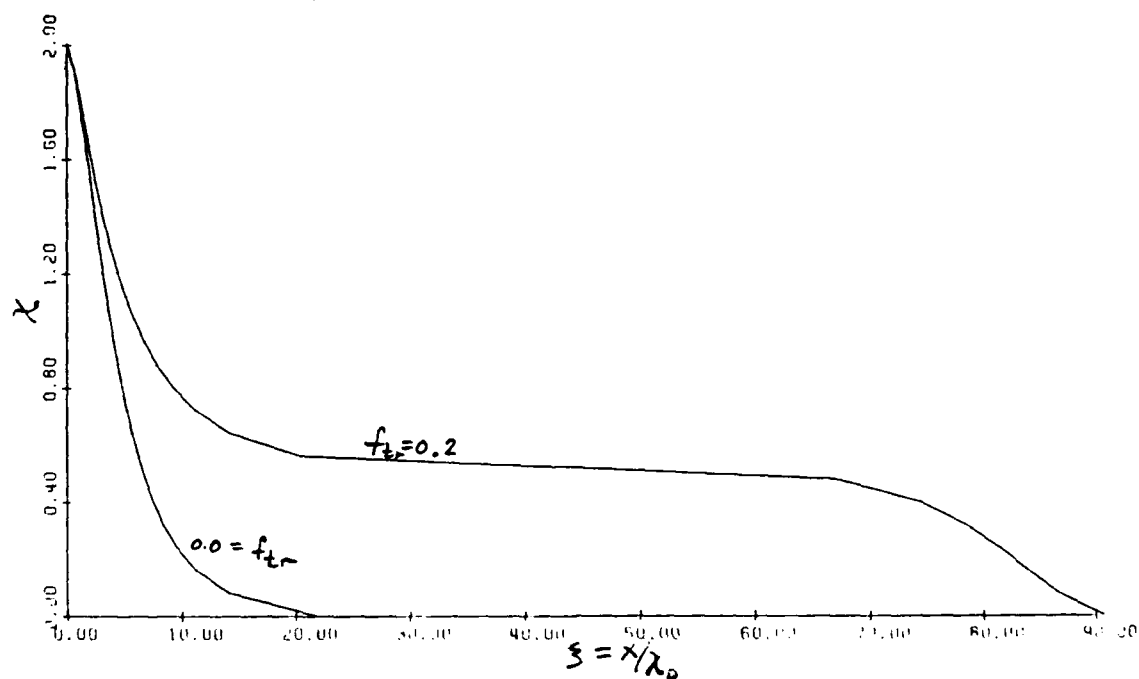
Figure 3.4.5 Sheath Structure with Trapped Ions

The sheath results on trapped ions so far have assumed $\Delta x_s \geq$ 0 (a reflective double sheath), in which case the effects of Δx_s (on all but the amount of ions reflected) are insignificant. However, when $\Delta x_s < 0$ the amount of trapped ions is controlled by the back sheath height, Δx, but the matching is controlled by local matching at the plasma-sheath interface. Figure 3.4.8 shows this effect on u_s for $x_E = 0.5$. When $\Delta x_s = -0.5$, back sheath height is zero. In this case the shift speed, $u_s = 1.95$, is the expected result corresponding to the no trapped ion case. However, as the back sheath height, Δx, increases from
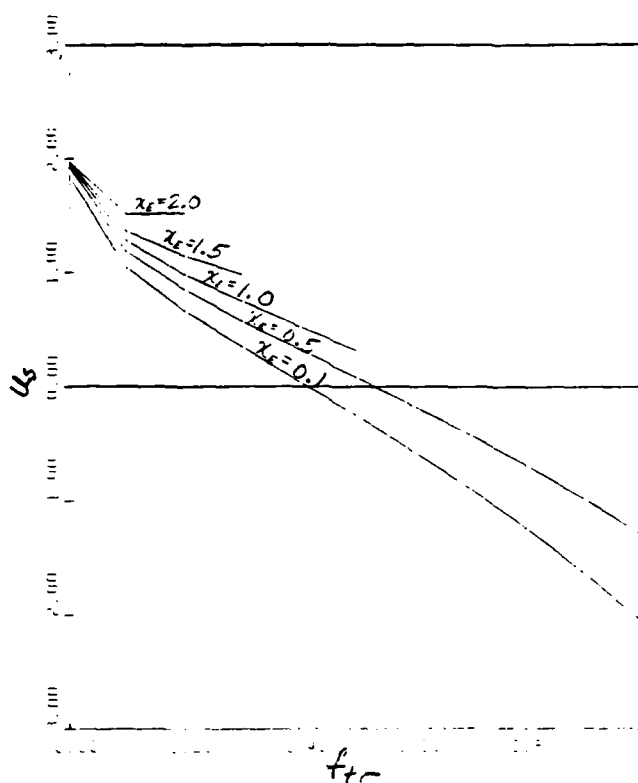
Figure 3.4.6 Shift Speed with Trapped Ions

zero the matching remains local while trapped ions accumulate in sheath peak. This causes u_s to rise and also causes j to rise (fig. 3.4.9). For display purposes u_s has been limited to 3 by the numerical routine. As can be seen u_s increases exponentially with Δx until $\Delta x = x_E$ where trapped ions begin to control matching. For the purpose of clarity, u_s is shown to have a finite slope at $\Delta x = x_E$ when in fact the slope is infinite. After $\Delta x = x_E$ is passed u_s drops to its value shown in fig. 3.4.6.
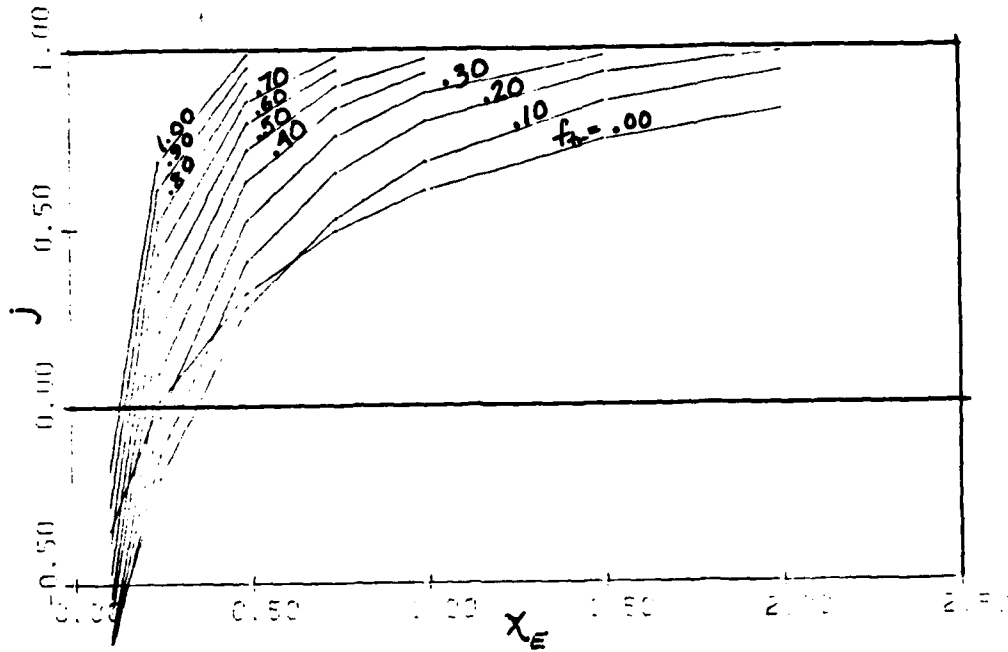
Figure 3.4.7 Nondimensional Current Density with Trapped Ions

d. single ion repelling sheath

The results in this case are very simple:

$$U_s = 0,$$

$$j = \frac{Q(1+\sqrt{T})}{Q + \sqrt{\frac{2}{\pi}}}, \qquad (1)$$

$$\chi_E = 0.$$
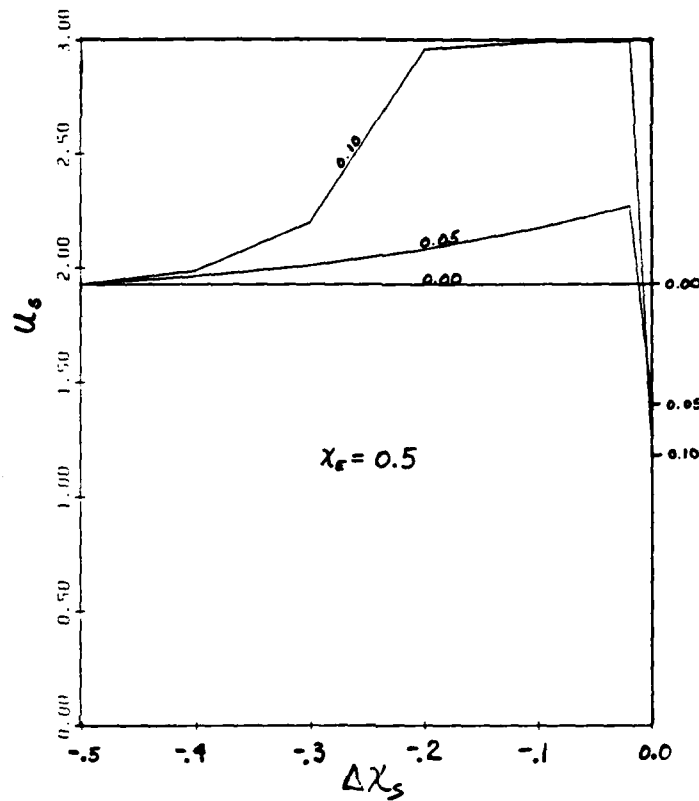
Figure 3.4.8 Effect of Back Sheath Height on Shift Speed

e. collector sheath

This is the classical Bohm matching case. Figure 3.4.10 shows
the collector shift speed, u_s, versus collector sheath height,
x_c. The curves shown are for various ion distribution cut-offs,
$u_{cut} = .1, .01, .001, .0001$. The notable feature here is that u_s
drops to negative infinity at a finite but small x_c. This is
expected because a small sheath should not have a pre-sheath
region capable of accelerating ions to a high speed.
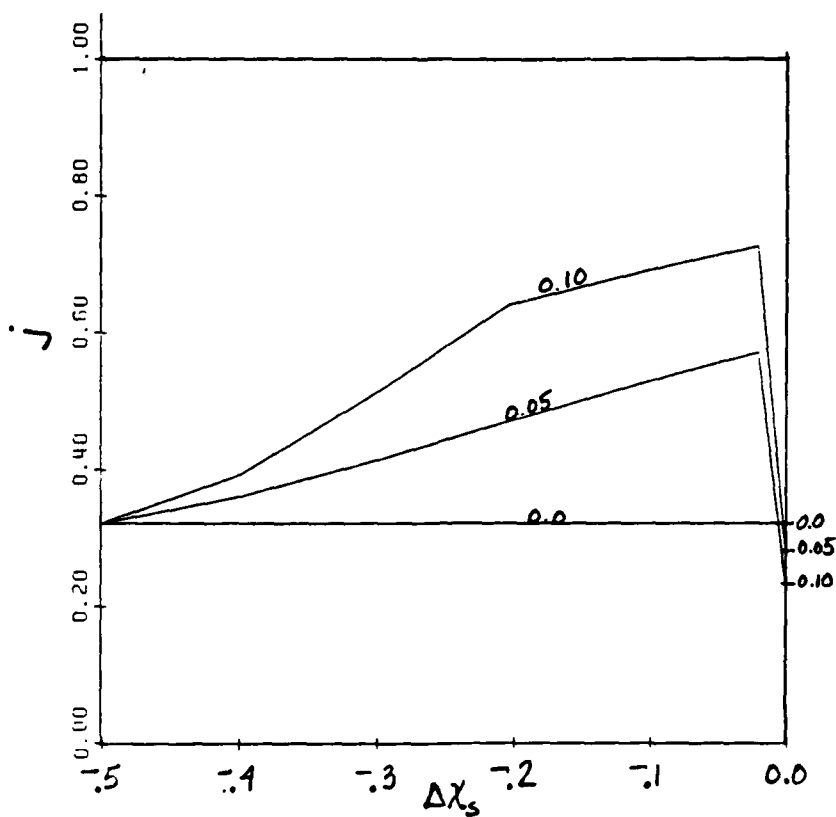
Figure 3.4.9 Effect of Back Sheath Height on j
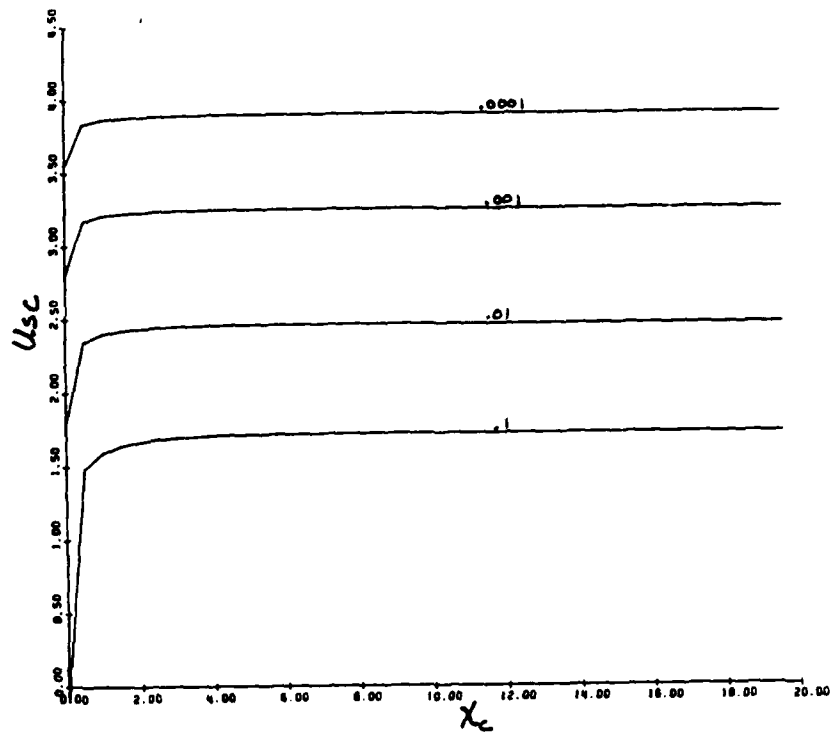
Figure 3.4.10 The Collector Sheath Shift Speed.

CHAPTER 4: ISOTHERMAL SOLUTIONS

4.1 Effects of Ion Reflection

4.2 Effects of Trapped Ions

4.3 Effects of Surface Emision

4.4 Comparison with Experimental Work

In this chapter we develop and discuss isothermal solutions for the thermionic convertor with the emitter sheath phenomena of ion reflection, trapped ions and surface emission ions included. All three of these phenomena increase in significance as net current density through the convertor is reduced. Each of the these reduces the net ion loss rate to the emitter and consequently increases arc-drop (therefore degrading performance at low current densities). This increase in arc-drop is in agreement with the same tendency in the experimental results. However, the experimental results also show a plateau (of low arc-drop) at low current density. This plateau occurs at a current density corresponding to significant surface ion emission and is therefore thought to occur as surface emission replaces

volume ionization as the dominant source of plasma ions. Unfortunately, the theoretical calculations cannot be carried into this region because the collisionless collector sheath matching (to the neutral plasma) fails.

To provide a realistic framework for presenting the results of this chapter, we consider the convertor conditions shown as case

---

CASE 1	CASE 2
T_E = 1500 K	T_E = 1750 K
T_C = 750 K	T_C = 750 K
p_{cs} = 1 torr	p_{cs} = 1 torr
d = 10 mil	d = 10 mil
ϕ_E = 2.12 eV	ϕ_E = 2.67 eV
ϕ_C = 1.60 eV	ϕ_C = 1.73 eV
J_R = 20 amp/cm^2	J_R = 7.57 amp/cm^2
J_{cs+} = 1.80 x 10^{-5} amp/cm^2	J_{cs+} = 2.10 x 10^{-3} amp/cm^2

Figure 4.1 Isothermal Solution Conditions

---

1 in fig. 4.1. Case 2 is shown because it has the largest surface emission of any typical thermionic convertor operating condition (because the work function is high and the temperature is also high). Instead of presenting case 2 seperately, we demonstrate the effects of surface emission in case 1 by increasing the surface emission by a factor of 100 thereby bringing it up to the level in case 2. The net current density at which surface emission becomes significant can be estimated by multiplying J_{cs+} by the square root of the ion to electron mass

ratio (approximately 500). In case 1 this means that surface
emission becomes significant at $J = .01$ amps/cm^2 while in case 2
significant surface emission begins at $J = 1.0$ amps/cm^2.

4.1 Effects of Ion Reflection

In this section we develop the isothermal results for case 1
with ion reflection, but without trapped ions and with the small
amount of surface emission ions of case 1. Figure 4.1.1 is the
C-V diagram for this case. The dotted line extending upward from
point A is the single electron repelling emitter sheath solution.
However, we have not taken recombination into account in this
isothermal calculation nor have we included the Schottky effect,
both of which are expected to become important at current
densities near J_R. Therefore the curve above point A should be
treated as qualitative and not quantitative.

The interest of this thesis begins at point A, where the
single sheath doubles over. Between points A and B, where the
back sheath height, Δx, is less than the sheath height, x_E, the
emitter sheath is non-reflecting. In this region the sheath
heights, x_E and x_C, remain constant while the plasma density is
proportional to net current, J (the *normalized plasma density*
nc/J is constant). Only the back sheath height, Δx, changes and
the C-V curve in this region is Boltzmann (the arc-drop is
constant). Beginning at point B and continuing to point C, the
double emitter sheath reflects plasma ions because the back
sheath is larger than the front sheath, in other words the
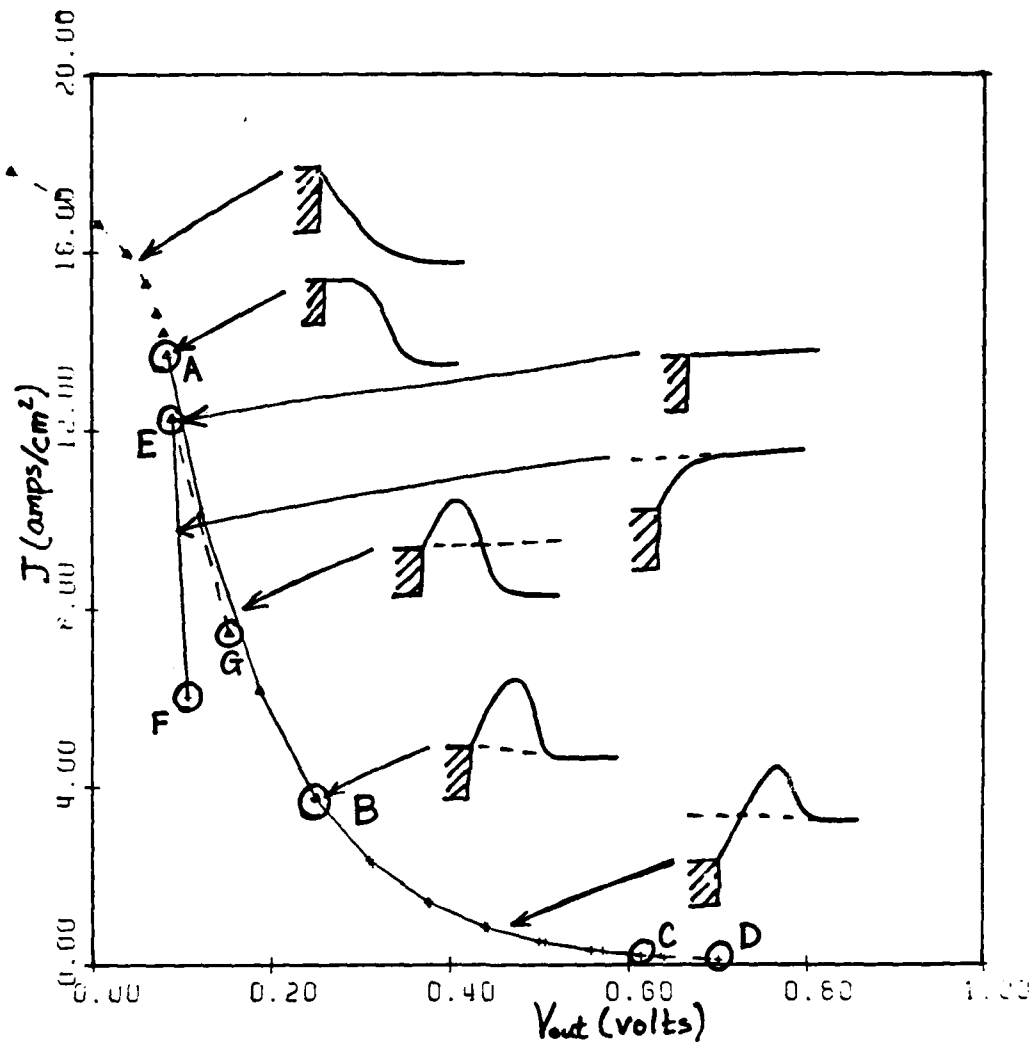
Figure 4.1.1 C-V Diagram with Ion Reflection for Case 1

reflective potential, $\Delta x_s = \Delta x - x_E$, is positive. The result is that net ion loss rate, u, decreases and that arc-drop increases. The dotted curve BD is the same double sheath except that it assumes no ions are reflected; therefore $\bar{u}$ is constant and arc-drop is constant. The two curves BC and BD are almost indistinguishable because the increase in arc-drop is small until the net current density is extremely small. The reason for this

END

FILMED

DTIC
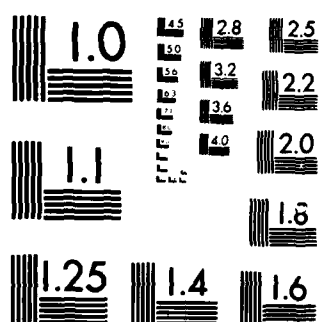
MICROCOPY RESOLUTION TEST CHART

NATIONAL BUREAU OF STANDARDS-1963-A

is that the shift speed is approximately $u_s = 2$ and therefore a large increase in reflective potential is required to change u significantly (the half reflection point is $\Delta x_s = 4.0$ or approximately $J = J_R e^{-4} = .4$ amp/cm^2).

The curve EF is the single electron repelling emitter sheath case. It is the limiting case for large amounts of trapped ions in which the double sheath peak has been completely suppressed by the trapped ions. As is explained in sections 3.3(d) and 3.4(d), the solution condition is satisfied by $u_s = 0$. This curve is not topologically connected to the curve ABC; it will be shown in section 4.2 that trapped ions move ABC toward the single ion repelling sheath case. Curve is much steeper (a faster increase in arc-drop) in this case because $u_s = 0$ (the half point in ion reflection is approximately $J = 8$ amp/cm^2). Curve EG is the single ion repelling case assuming no reflection and is therefore a Boltzmann line with constant arc-drop.

At points F and C the solutions fail at the collector. The explanation for this failure is best given by examining figs. 4.1.2, 4.1.3, 4.1.4 and 4.1.5. Figure 4.1.2 is the normalized plasma density through the convertor gap. The highest curve with no reflection, $\Delta x_s = 0$, has the largest plasma density at the collector but the lowest plasma density at the emitter. Ion reflection, which decreases the ion loss rate to the emitter, raises the plasma density at the emitter but lowers the plasma density at the collector. The lower plasma density at the collector forces a smaller collector sheath height to pass the
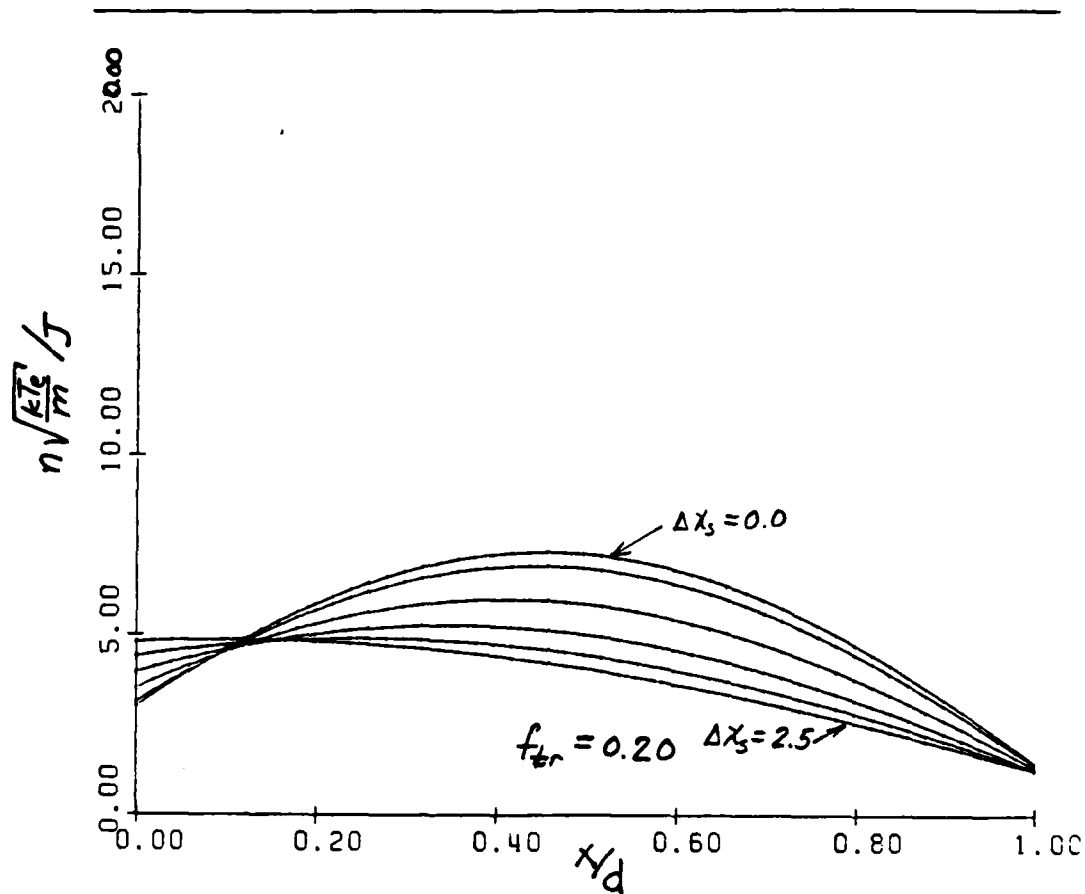
Figure 4.1.2 Normalized Plasma Density with Reflection

net current density. This can be seen from eq. 2.2.10. Figure

4.1.3 is the potential through the convertor under the same

reflection conditions as in fig. 4.1.2. In fig. 4.1.3 the first

two spaces on the left make up the double emitter sheath, and the

last space on the right is the collector sheath. The region

between the two sheaths is the neutral plasma region. In the no

reflection case, it can be seen that the potential has a

pronounced well in the middle. This is the result of the large

plasma density in the middle. As reflection increases, this well

disappears on the collector side of the plasma because resistive
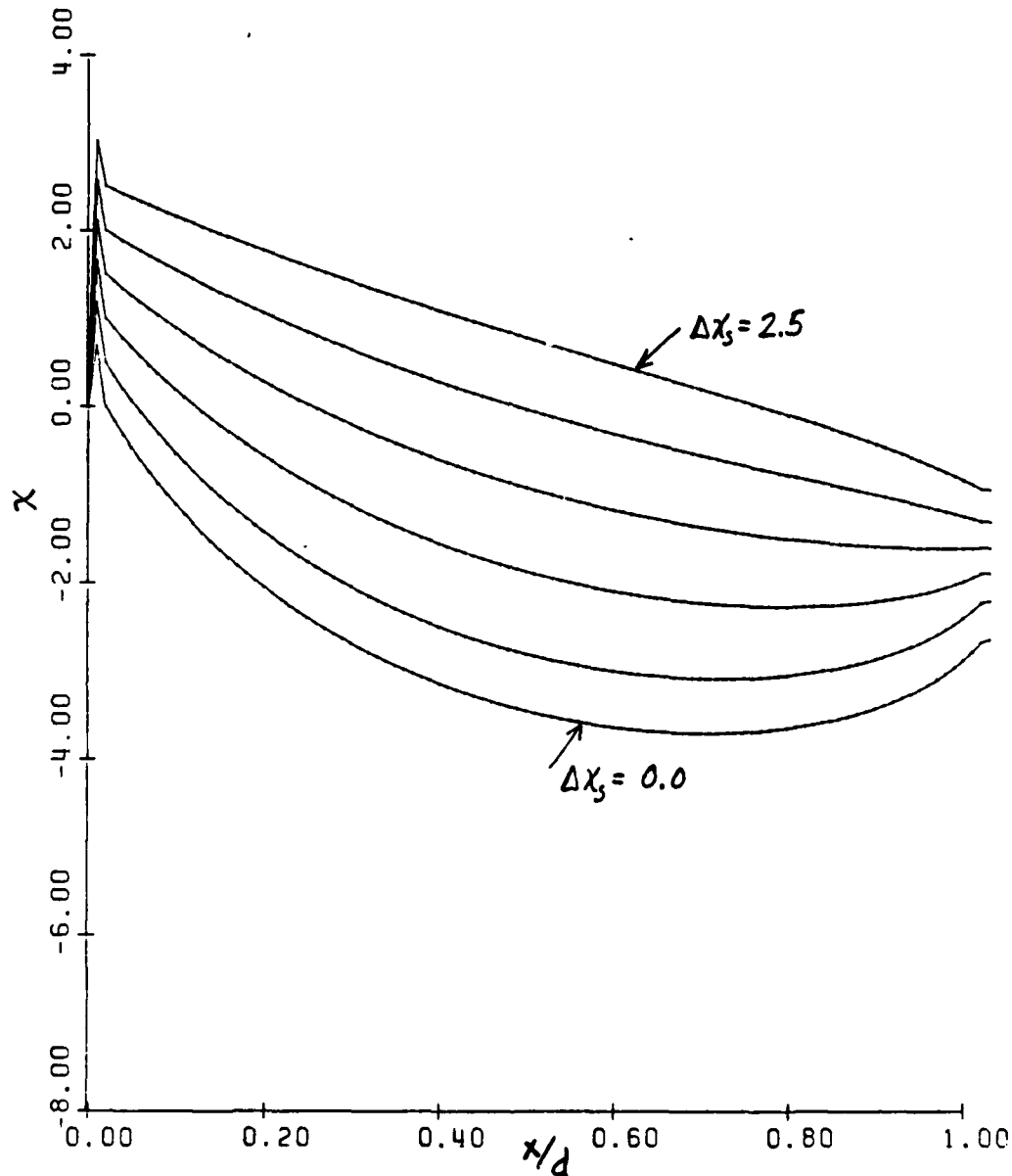
Figure 4.1.3 Potential Distribution in the Convertor

drop there (due to low plasma density) increases to the degree

that it is greater than the ambipolar rise (due decreasing

density toward the collector).   Simultaneously with plasma

potential gradient at the collector becoming negative, the collector sheath go toward zero height. Figure 4.1.4 shows the critical collector sheath quantities as the collector sheath
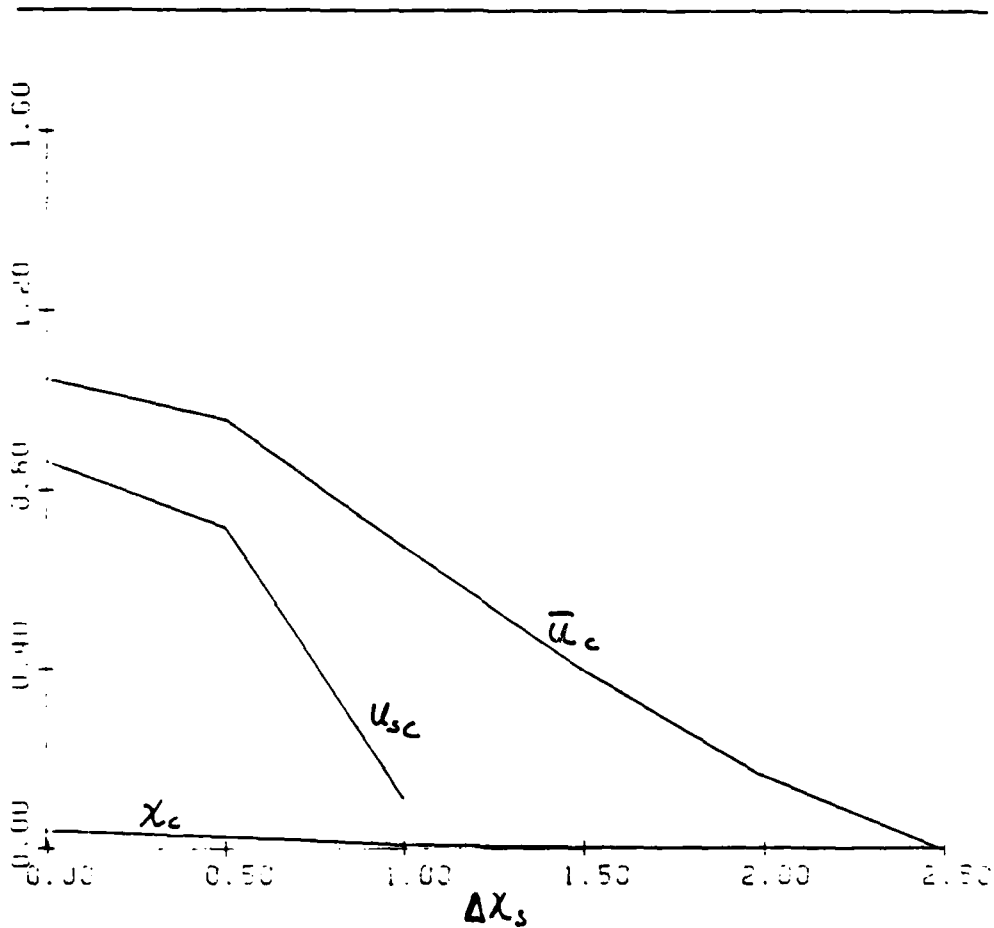
Figure 4.1.4 Collector Sheath Failure

failure occurs. Collector sheath height, χ_C goes toward zero, the shift speed, u_{sc}, goes toward negative infinity (see fig. 3.4.10), and the ion loss rate to the collector, $\overline{u}_c$, is driven to zero. Figure 4.1.5 shows the changes in the emitter sheath height, ion shift speed and ion loss rate. When the collector sheath failure occurs, the ion loss rate to the collector is zero
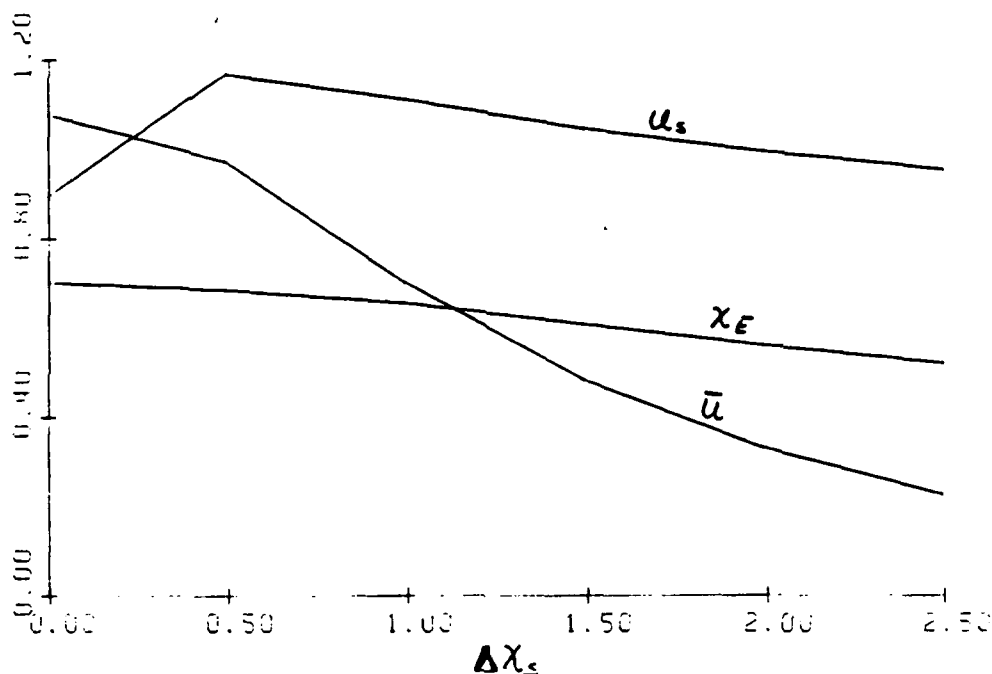
Figure 4.1.5 Emitter Sheath During Reflection

($\overline{u}_c = 0$) and the corresponding plasma ion distribution at the
collector is bunched at zero velocity ($u_{sc} = -\infty$). While the
mathematics hold self-consistantly until $\overline{u}_c = 0$, the physics is
clearly poor at this point because $\overline{u}_c = 0$ demands that the plasma
ions at the collector have zero energy (zero temperature and
zero mean velocity). An estimate of when the physics becomes
poor is $u_{sc} = 0$. At this point the net ion loss rate is close
to the thermal speed. A second physical difficulty that occurs
with collector sheath failure is that the electron Mach number
there, Q_c, (from eq. 2.2.10) becomes

$$Q_c = \sqrt{\frac{2}{\pi}}$$

because the collector sheath height approaches zero (actually about .001). In the present continuum formulation of the plasma region, it was assumed in eq. 2.1.13 that Q_c is small so that the electron momentum term, $u_e du_e/dx$ can be neglected.

One could take the solution below the collector sheath failure point if $\overline{u}_c$ could attain negative values or if Q_c could attain values larger than $\sqrt{(2/\pi)}$. There is no physical basis for assuming that $\overline{u}_c$ can become negative since the collector emits nothing. However, there is a physical basis for allowing Q_c to be larger than $\sqrt{(2/\pi)}$, (an electron distribution shift) as can be seen in fig. 4.1.3: the potential drop nearing the collector becomes progressively more electron accelerating as the collector sheath fails and therefore the electron distribution should be shifted as the ion distribution is in an electron repelling sheath. However, this would clearly invalidate the assumption that the electron momentum term is negligible. Therefore the momentum term must be added to explore further in this direction and this has not been done because of the resulting complexity in the equations.

Comparison of fig. 4.1.4. to fig. 4.1.5 at the collector sheath failure point ($\Delta x_s = 2.5$, $\overline{u}_c = 0$) shows that the ion loss rate to the emitter is positive. At this point the plasma is still ignited and generating ions as can be seen from figs. 4.1.6 and 4.1.7. The ionization coefficient, A, has dropped by 50%, but the plasma electron temperature has dropped by only 5%. Finally, we note in fig. 4.1.8 that the normalized plasma
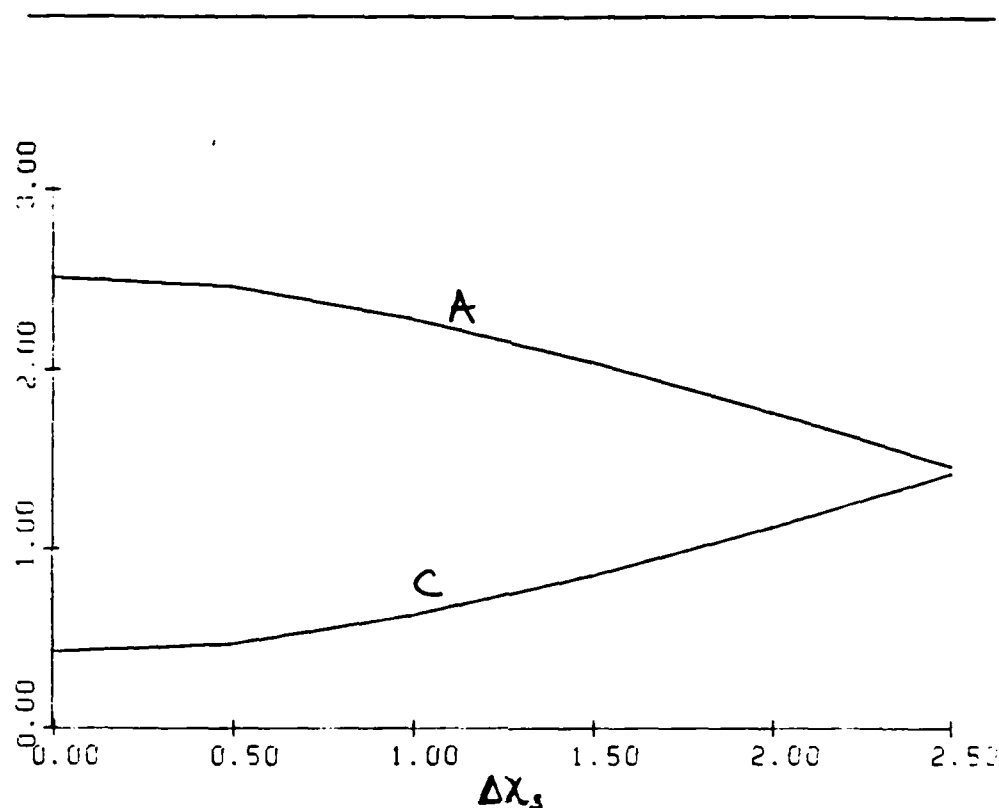
Figure 4.1.6 Ionization Coefficient A, and C

resistance, R, has risen by almost 100%. This is responsible for

the increase in arc-drop and the decrease in performance. Plasma

resistance increases in response to reflection because the loss

of plasma electron energy to the emitter is more important than

the loss of ionization energy to the emitter. Ion reflection at

the emitter increases the normalized plasma density there, and

consequently increases the normalized loss of plasma electron

energy there. The basis of this can be seen from conservation of

electron energy (eq. 2.2.22),
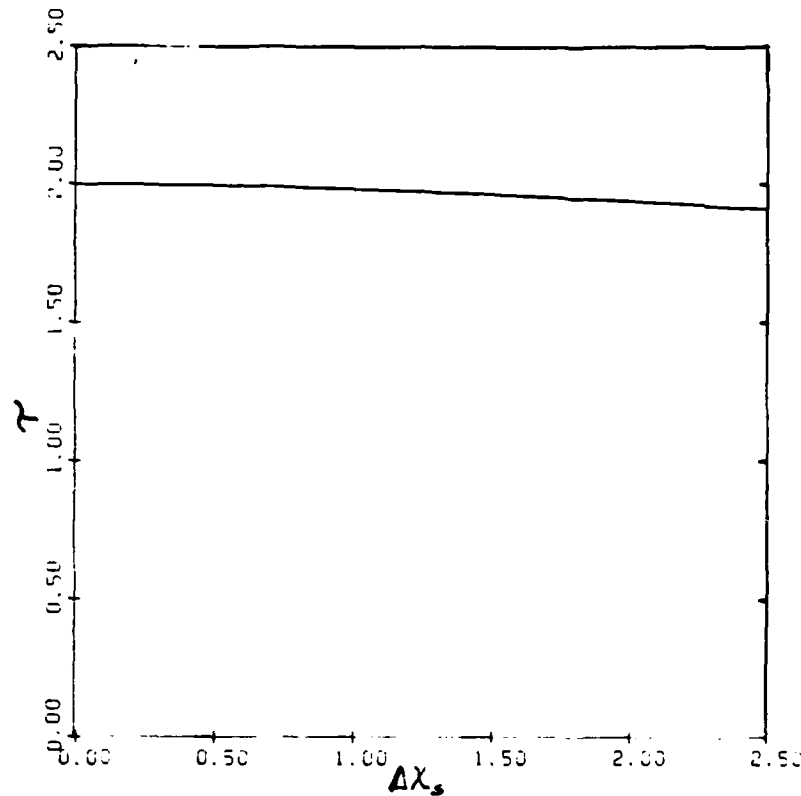
Figure 4.1.7 Plasma Electron Temperature

$$\tau = 1 - \frac{1}{2} j \, V_d - \frac{1}{2} j_i \, V_{f_i} \tag{1}$$

The ion energy loss term is generally small compared to the electron energy loss term:

$$\frac{\frac{1}{2} j_i \, V_{f_i}}{\frac{1}{2} j \, V_d} = \frac{J_i}{J} \frac{V_{f_i}}{V_d} \simeq O\left(\frac{1}{500} \frac{30}{3}\right) = O(.02). \tag{2}$$

Therefore, we take the the electron energy equation as:

$$\tau = 1 - \frac{1}{2} j \, V_d . \tag{3}$$

Since τ is nearly constant (because of the ionization kinetics
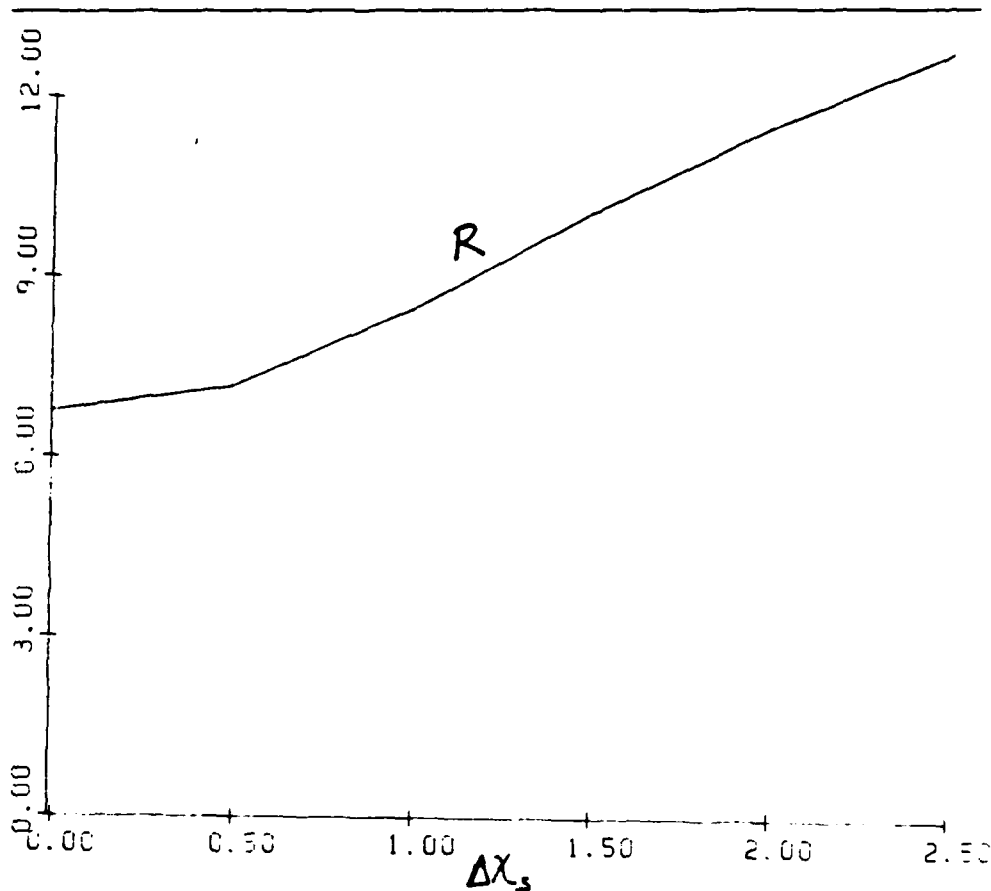
Figure 4.1.8 Normalized Plasma Resistance

), the product jV_d is nearly constant. Ion reflection decreases
j (because the normalized plasma density increases) and
therefore increases arc-drop, V_d (makes V_d a more negative
number.

If the equations are reformulated in such a way as to be valid
past the collector sheath failure point, then we can expect to
eventually see a decrease in arc-drop and a low current plateau
as the electron temperature approaches 1 (the ignited plasma is
extinguished and the ionization source is surface emission).

This can be seen from eq.1. However, as we see, the collector

failure occurs before τ has dropped more than 5%. Consequently

we do not see any plateau or decrease in arc-drop as net current

density is decreased in the present calculations.

4.2 Effects of Trapped Ions

Figure 4.2.1 shows the effect of trapped ions on the C-V
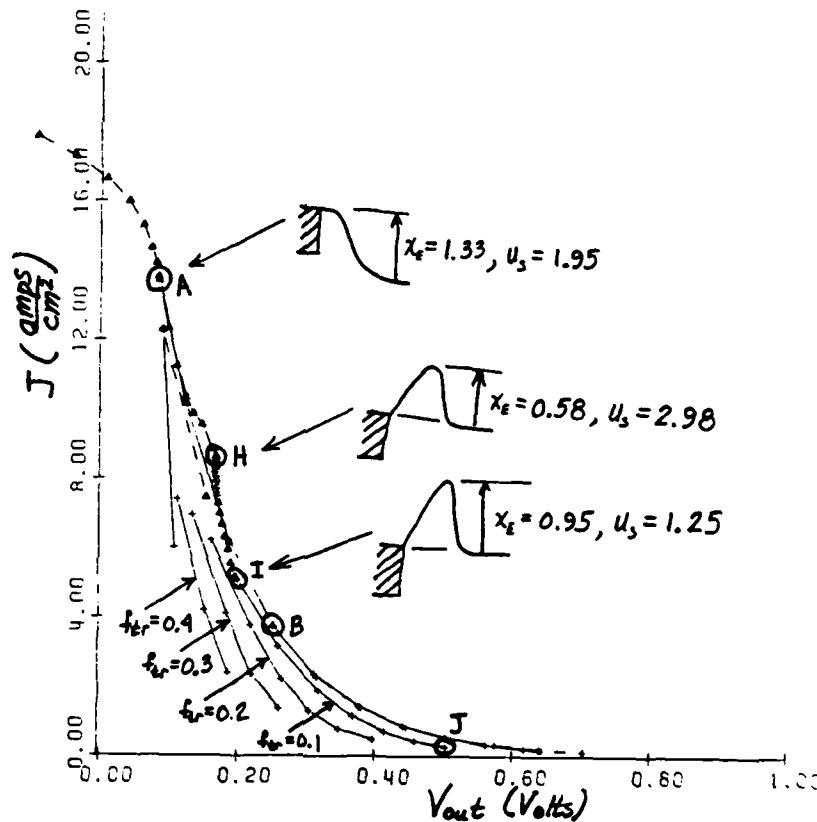
Figure 4.2.1 C-V Diagram with Trapped Ions

characteristics. (The amounts of trapped ions added in this

section are parameters as yet to be determined based of the

definition in section 3.3.) Curve AHIJ is the C-V characteristic

for f_{tr} = 0.10 At point A there cannot be any trapped ions since

the back sheath height, Δx, is zero. Therefore the trapped C-V

merges into the non-trapped curve there.   The actual amount of

trapped ions on the f_{tr} = 0.10 curve increases from zero at point

A to the full 10% of a thermal distribution at point H where the

back sheath height, Δx, is equal to the sheath height, x_E. The

shift speed increases on AH from 1.95 to 3.00. This correspondes

to what is seen in fig. 3.4.8 where $\Delta x < x_E$. The rise in shift

speed has been limited to 3.00 as in fig. 3.4.8. This limit is

placed on the shift speed because a sheath with height of about

1.0 should not have a pre-sheath region capable of shifting the

entire distribution so far. In fact limiting the shift speed is

equivalent   to   increasing   the   cut-off   speed   for   the   ion

distribution function. The arc-drop decreases as result of the

increase in u_s and the consequent increase in the net ion loss

rate to the emitter. A "hump" can be seen on AH where the shift

speed hits 3.00. The arc-drop is lowest on this "hump" because

the shift speed is at its maximum of 3.00. Between points H and

I the back sheath height remains equal to the sheath height, Δx -

$x_E = x_s = 0$. On this segment, u_s decreases to 1.25, therefore

increasing arc-drop. The drop in u_s at $\Delta x_s = 0$ can be seen in

fig. 3.4.8 also. From point I to point J, the shift speed

remains constant at 1.25 and the ion loss rate decreases because

of reflection. The other trapped cases, f_{tr} = 0.2, 0.3, and 0.4

have not been connected because they hit the 3.00 maximum shift

speed much sooner than in the f_{tr} = 0.1 case as can also be seen

from fig. 3.4.8. Point J is the collector sheath failure point.

Each of the f_{tr} = 0.2, 0.3 and 0.4 curves begins at Δx_s = 0 and

ends at the collector sheath failure point. It should be noted

that each of the trapped ion curves failes at a higher current

than the last because the shift speed is lower.

4.3 Effects of Surface Emission

In this section the effect of surface emission is discussed.
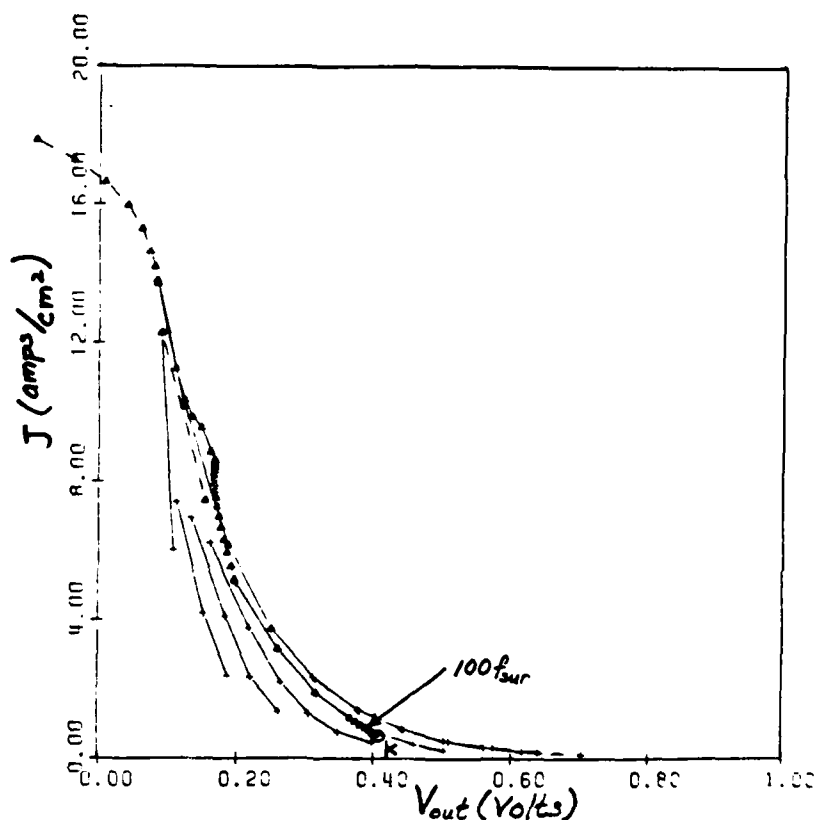
Figure 4.3.1 C-V Diagram with Surface Emission

and Trapped Ions

Figure 4.3.1 adds the effect of surface emission to fig. 4.2.1. On the f_{tr} = 0.10 curve, surface emission is added by multiplying the actual small amount of surface emission in case 1 by a factor of 100. This brings the surface emission up to the level in case 2, making it significant at J = 1.0 amp/cm^2. It can be seen that surface emission increases arc-drop; it does so in exactly the same way as reflection or trapped ions do - it decreases the net loss rate of ions to the emitter. Also the collector sheath failure occurs at point K in exactly the same way as in section 4.1.

4.4 Comparison with Experimental Work

Figure 4.4.1 puts the isothermal results of fig. 4.3.1 next to the experimental results of fig. 1.1.2. The point of this comparison is that the steepness of the C-V characteristic in the experimental convertors can be explained by a decreasing ion loss rate to the emitter. We have shown that all three of the expected emitter sheath phenomena decrease the ion loss rate to the emitter. We cannot calculate the amount of trapped ions in a collisionless sheath without knowledge of the collisional processes. However, the experimental C-V suggests that if the amount of trapped ions (f_{tr}) increases from 0% at J = 14 amps/cm^2 (the double sheath formation point) to 30% at J = 2 amps/cm^2 (the collector sheath failure at f_{tr} =0.30) then the steepness could result from trapped ions reducing the ion loss rate to the emitter. Since these percentages are based on a
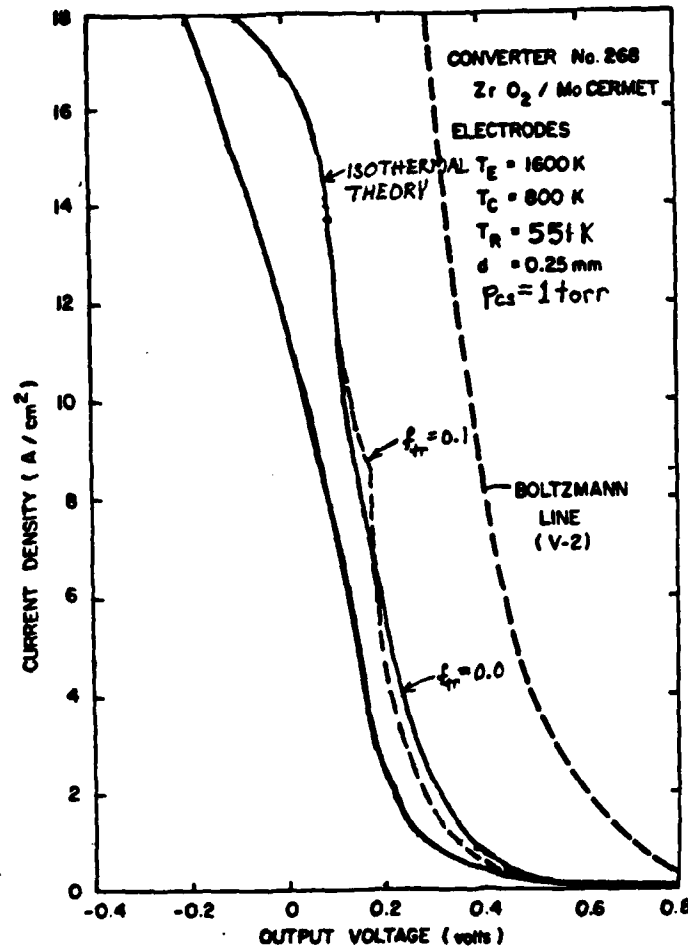
Figure 4.4.1 Isothermal versus Experimental C-V Diagrams

emitter. Since these percentages are based on a thermal distribution of ions, they seem physically reasonable. Unfortunately, the collector sheath failure prevents us from going to the point in the calculations where τ drops enough to make surface emission the source of ions.

The experimental curve is nearly a constant .05 volts below the isothermal result (f_{tr} = 0.10) except at high current densities and at the "hump". Comparison of the curves at high current density is not valid since neither the Schottky effect

effect nor recombination have been included. The Schottky effect

is important above 12 amps/cm^2 in this case because the emitter

sheath is single electron repelling (to the plasma) and

therefore puts a strong electric field against the emitter with

the appropriate sign. Recombination is also potentially

important because the plasma density scales with current density

and at high current densities the plasma density in the middle of

the convertor approaches the Saha density. The .05 volt

difference may or may not be explained by a discrepency in the

assumed collector work function. At 800 K the collector emits

essentially nothing and therefore any change in the collector

work function directly affects output voltage. If the collector

work function were in fact 1.65 volts instead of 1.60 volts then

the isothermal result would lie nearly on top of the experimental

result. We have not adjusted the assumed collector work function

so as to illustrate the importance it and therefore the

importance of the surface physics of the adsorbed cesium layer.

The "hump" should not be taken as an expected experimental result

since it results from the interaction of the trapped ions with

the plasma-emitter sheath interface (fig. 3.4.8). Instead it

should be taken as a second reason (in addition to the cut-off

of the ion distribution) for further study of the matching

region between the collisionless sheath and the neutral plasma.

CHAPTER 5: NON-ISOTHERMAL SOLUTIONS

5.1 The Implicit Computational Scheme

5.2 Non-Isothermal Results

The non-isothermal solution for the thermionic convertor is found by integrating (through time) the set of parabolic Partial Differential equations (eqs. 2.1.14 and 2.1.15):

$$\left(1 + \frac{\mu_i}{\mu_{ea}}\right)\frac{\partial n}{\partial t} = \frac{\partial}{\partial x}\left(\mu_i \frac{\partial P}{\partial x}\right) + \left(1 + \frac{\mu_i}{\mu_{ea}}\right)S^{(n)} + \Gamma_e \frac{\partial}{\partial x}\left(\frac{\mu_i}{\mu_{ea}}\right), \tag{1}$$

$$\frac{3}{2}n\frac{\partial}{\partial t}(kT_e) = \frac{\partial}{\partial x}\left(k_e \frac{\partial T_e}{\partial x}\right) - \frac{3}{2}\Gamma_e \frac{\partial}{\partial x}(kT_e) - nkT_e \frac{\partial}{\partial x}\left(\frac{\Gamma_e}{n}\right) + \frac{\Gamma_e^2}{n\mu_{ea}} + \Gamma_e \frac{\Gamma_e - \Gamma_i}{n\mu_{ei}}. \tag{2}$$

These equations can be marched forward in time with an explicit scheme by computing all of the quantities on the right at previous time step (Lawless). This, however, encounters a stability limit on Δt which slows the numerical solution excessively. The energy equation (eq. 2) has a time scale inherently 500 times faster than the diffusion equation (eq. 1) because the mass ratio of electron to ions is approximately 500. The stability limit for the faster energy equation:

$$\Delta t_{stab} = t_{elec} \left(\frac{\Delta x}{d} \right)^2 \qquad (3)$$

where Δx is the space step size, t_{elec} is the characteristic electron energy time scale and Δt_{stab} is the stability limit time step size. Since the energy equation is the faster of the two in the system, its stabilty limit controls the time step size for the set of both equations. It can be seen that if 10 space steps are used, then $\Delta t_{stab} = 100 t_{elec}$. Since we want to find a steady state solution, we need about $10 t_{diff}$, but $t_{diff} = 500 t_{elec}$ (approximately), therefore we would need about 5×10^5 time steps to achieve a steady state solution.

The implicit scheme does not have the stability limit and therefore needs only 5×10^3 time steps to achieve the steady state. Each time step requires about 10^4 floating point operations (flops) whether or not the implicit scheme is used (assuming 10 space steps). For the explicit scheme this would result in 5×10^9 flops while the implicit scheme would require only 5×10^7 flops. In both cases the estimate of 10^4 flops in each time step assumes that the sheath calculations are a negligible part of this. In fact the general sheath solution requires approximately 10^8 flops in its full form. This would result in 5×10^{15} flops. Therefore, running even the implicit non-isothermal scheme requires that a sheath model be used. Because of this, exploring thermionic convertor sheath effects with the non-isothermal theory is difficult and we demonstrate only the simple non-reflecting, non-trapped ion, non-surface

emission case in this chapter and compare it to the isothermal
result.

5.1 The Implicit Computational Scheme

The diffusion equation can be written as

$$\frac{\partial n}{\partial t} = a \frac{\partial^2 n}{\partial x^2} + b \frac{\partial n}{\partial x} + c + d \tag{1}$$

and the energy equation can be written as

$$\frac{\partial T}{\partial t} = e \frac{\partial^2 T}{\partial x^2} + f \frac{\partial T}{\partial x} + gT + h . \tag{2}$$

The quantities a through h are not constant but approximately so.
The explicit scheme is constructed as follows:

$$\frac{n_i^{j+1} - n_i^j}{\Delta t} = a \frac{n_{i+1}^j - 2n_i^j + n_{i-1}^j}{\Delta x^2} + b \frac{n_{i+1}^j - n_{i-1}^j}{2\Delta x} + cn_i^j + d \tag{3}$$

and

$$\frac{T_i^{j+1} - T_i^j}{\Delta t} = e \frac{T_{i+1}^j - 2T_i^j + T_{i-1}^j}{\Delta x^2} + f \frac{T_{i+1}^j - T_{i-1}^j}{2\Delta x} + gT_i^j + h \tag{4}$$

where j is the time index and i is the space index. If a and e
are the only non-zero coefficients (a and e dominate), then the
stability criteria are

$$\Delta t \leq \frac{1}{2} \frac{\Delta x^2}{a} \tag{5}$$

and

$$\Delta t \leq \frac{1}{2} \frac{\Delta x^2}{e} . \tag{6}$$

We will not analyse the stability criteria in any more detail,

but simply develop the implicit scheme which has no stability
limits.   The   implicit   scheme   is   constructed   by   taking   the
variables at the advanced time step in the right sides of eqs. 1
and 2:

$$\frac{n_i^{j+1} - n_i^j}{\Delta t} = a \frac{n_{i+1}^{j+1} - 2n_i^{j+1} + n_{i-1}^{j+1}}{\Delta x^2} + b \frac{n_{i+1}^{j+1} - n_{i-1}^{j+1}}{2\Delta x} + cn_i^{j+1} + d \quad (7)$$

and

$$\frac{\tau_i^{j+1} - \tau_i^j}{\Delta t} = e \frac{\tau_{i+1}^{j+1} - 2\tau_i^{j+1} + \tau_{i-1}^{j+1}}{\Delta x^2} + f \frac{\tau_{i+1}^{j+1} - \tau_{i-1}^{j+1}}{2\Delta x} + g\tau_i^{j+1} + h. \quad (8)$$

These equations can be written as

$$\left[a\frac{\Delta t}{\Delta x^2} + \frac{b}{2}\frac{\Delta t}{\Delta x} \right] n_{i+1}^{j+1} + \left[c\Delta t - \frac{2a\Delta t}{\Delta x^2} + 1 \right] n_i^{j+1} + \left[a\frac{\Delta t}{\Delta x^2} - \frac{b}{2}\frac{\Delta t}{\Delta x} \right]$$
$$(9)$$
$$= n_i^j \frac{\Delta t}{\Delta x} - d\Delta t$$

and

$$\left[e\frac{\Delta t}{\Delta x^2} + \frac{f}{2}\frac{\Delta t}{\Delta x} \right] \tau_{i+1}^{j+1} + \left[g\Delta t - \frac{2e\Delta t}{\Delta x^2} + 1 \right] \tau_i^{j+1} + \left[e\frac{\Delta t}{\Delta x^2} - \frac{f}{2}\frac{\Delta t}{\Delta x} \right] \tau_{i-1}^{j+1}$$
$$(10)$$
$$= \tau_i^j \frac{\Delta t}{\Delta x} - h\Delta t.$$

which   form   tridiagonal   matrices,   that   with   the   boundary
conditions, can be inverted in 3N operations where N is the
number of space steps.

5.2 <u>Non-Isothermal</u> <u>Results</u>

Figure   5.2.1   shows   the   electron   temperature   distribution
across the convertor gap for two cases: the non-isothermal case
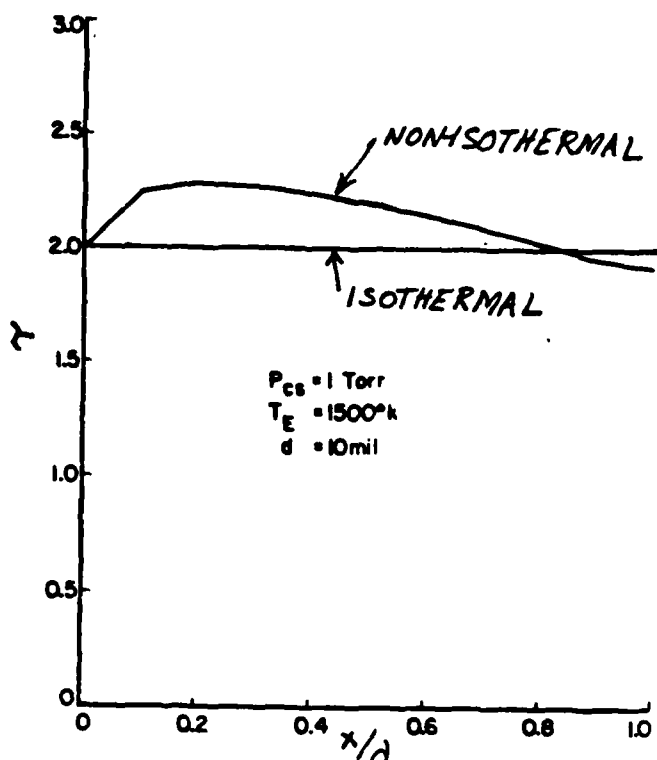
Figure 5.2.1 Non-Isothermal Electron Temperature

and the corresponding isothermal case at $\Delta x_s = 0$ and $J = 12$ amps/cm^2. The electron temperature remains close to 2 in the non-isothermal case. Figure 5.2.2 is the corresponding normalized plasma density. It can be seen that the plasma density in the isothermal case corresponds closely with the non-isothermal case. The seemingly large difference in plasma density in the middle of the gap not important since its contribution to total plasma resistance is small and all other effects of plasma density result from the plasma density at the emitter and collector.
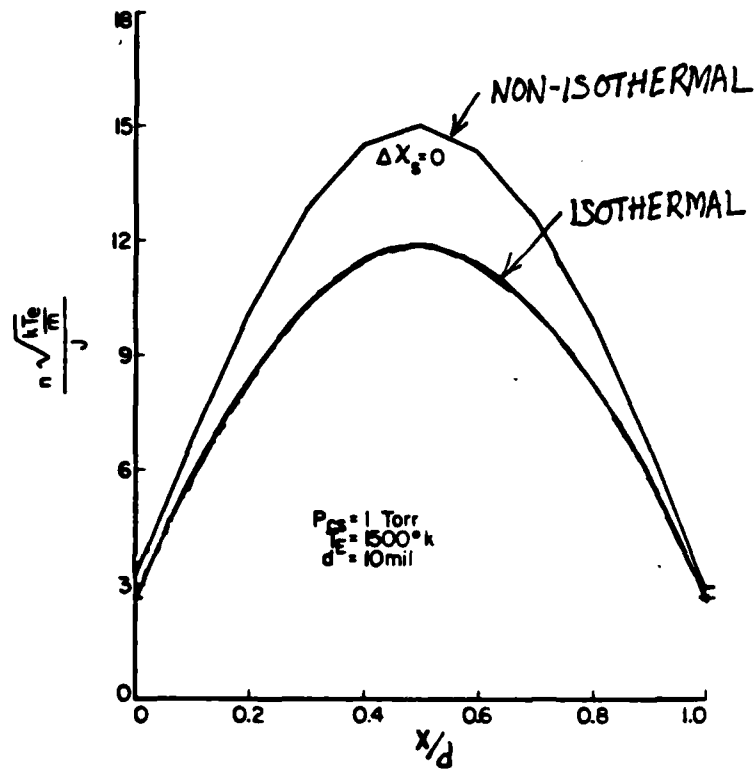
Figure 5.2.2 Non-Isothermal Plasma Density

CHAPTER 6: CONCLUSIONS AND RECOMMENDATIONS

6.1 Conclusions

6.2 Recommendations for Further Work

6.1 Conclusions

Using only a simple isothermal model, the emitter sheath effects of trapped ions, ion reflection and surface emission ions can explain the steep C-V characteristic of the thermionic convertor. Contrary to intuition, all three of these effects increase arc-drop in the thermionic convertor because they increase plasma density at the emitter and increase electron energy loss to the emitter to a greater degree than they decrease ionization energy loss. The low current density plateau observed in thermionic convertors may well still be explained by surface emission, however we cannot demonstate this because of our collector sheath failure.

6.2 Recommendations for Further Work

Four things should be done to carry this work forward: 1) the continuum equations should be generalized to include the convection of momentum terms, udu/dx, to allow the collector sheath failure to be overcome, 2) a collisional transition region between the neutral plasma and the collisionless sheath should be developed to determine the appropriate cut-off for the plasma ion distribution, 3) the collisional trapping mechanism should be explored, and 4) a fast comprehensive sheath model should be developed and inserted into the implicit non-isothermal computational scheme.

BIBLIOGRAPHY

Baksht, F.G. et al, Thermionic Converters and Low Temperature
     Plasma, Moscow, 1973. English Translation by U.S. D.O.E.,
     1978.

Bernstein, I.B. and Rabinowitz, I.N., Theory of Electrostatic
     Probes in a Low Density Plasma, Physics of Fluids, p.112,
     vol.2, No.2, 1959.

Bienkowski, G.K., Electrostatic Sheath in a Weakly Ionized Gas,
     Physics of Fluids, p.381, vol.10, No.2, 1967.

Bienkowski, G.K. and Chang, K-W, Asymptotic Theory of a
     Spherical Electrostatic Probe in a Stationary Weakly
     Ionized Plasma, Physics of Fluids, p.784, vol.11, No.4,
     1968.

Bohm, D., in Characteristics of Electrical Discharges in
     Magnetic Fields, edited by A. Guthrie and R. Wakerling,
     McGraw-Hill, New York, 1949.

Chung, P.M., Talbot, M. and Touryan, K.J., Electric Probes in
     Stationary and Flowing Plasmas: Theory and Application,
     Springer-Verlag, New York, 1975.

Cipolla, J.W. Jr. and Silevitch, M.B., On the Temporal
     Development of a Plasma Sheath, J. Plasma Physics,
     p.373, vol. 25, 1981.

Hansen, L.K., et al, Analytical Model for the Ignited Mode
     Thermionic Convertor, Topical Report, Rasor Associates,
     Sunnyvale, Calif., Aug. 1978.

Harrison, E.R. and Thompson, W.B., Proc. Phys. Soc. London,
     p.145, vol.74., 1959.

Hatsopoulis, G.N. and Gyftopoulos, E.P., Thermionic Energy
     Conversion, Vol. I: Processes and Devices, MIT Press,
     Cambridge, Mass., 1973.

Hochstim, A.R., ed., Kinetic Processes in Gases and Plasmas,
     Academic Press, New York, 1969.

Krall, N.A. and Trivelpiece, A.W., Principles of Plasma Physics,
     McGraw Hill, New York, 1973.

Lam, S.H., Unified Theory for the Langmuir Probe in a Collisionless
     Plasma, Physics of Fluids, p.73, vol.8, No.1, 1965.

Lam, S.H., Preliminary Report on Plasma Arc-Drop in Thermionic
     in Thermionic Energy Converters. Princeton Unversity,

1976.

Lam, S.H., Theory of Langmuir Probes at Moderate Pressures,
    Proc. International Atomic Energy Agency Conference
    on Phenomena in Ionized Gases, Vienna, p.545, 1968.

Lawless, J.L., The Plasma Dynamics and Ionization Kinetics of
    Thermionic Energy Conversion, Ph.D. Thesis, Princeton
    University, 1981.

Montgomery, D.C. and Tidman, D.A., Plasma Kinetic Theory,
    McGraw Hill, New York, 1964.

Persson, K-B, Inertial-Controlled Ambipolar Diffusion, Physics
    of Fluids, p.1625, vol.3, No.12, 1962.

Su, C.H. and Lam, S.H., Continuum Theory of Spherical Electrostatic
    Probes, Physics of Fluids, p.1479, vol.6, No.10, 1963.

Su, C.H., Kinetic Theory of a Highly Negative Langmuir Probe,
    Proc. International Atomic Energy Agency Conference
    on Phenomena in Ionized Gases, Vienna, p.569, 1968.

Swift, J.D. and Schwar M.J.R., Electrical Probes for Plasma
    Diagnostics, Elsevier, New York, 1969.

Thermo-Electron Corp., DOE Advanced Thermionic Technology
    Program, Progress Report No.46, Waltham, Mass.,
    March 1981.

Thermo-Electron Corp., DOE Advanced Thermionic Technology
    Program, Progress Report No.48, Waltham, Mass.,
    Sept. 1981.

Wu, T-Y, Kinetic Equations of Gases and Plasmas, Addison-Wesley,
    1966.

APPENDIX A: ASYMTOTIC EXPANSIONS

A.1 Particle Density in an Accelerating Potential

A.2 Particle Density in an Decelerating Potential

In this appendix we develop the asymptotic expansions for the integrals

$$F_i(\chi) = \int_0^\infty f_i(u) \frac{u\, du}{\sqrt{u^2 + \chi}} \tag{1}$$

and

$$F_e(\chi) = \int_{\sqrt{\chi}}^\infty f_e(u) \frac{u\, du}{\sqrt{u^2 - \chi}} \ . \tag{2}$$

These are needed (in chap. 3) to develop the Bohm criterion correctly and to demonstrate the necessity of a general (as opposed to a local) matching condition. The expansion of these integrals is non-trivial because the taylor expansions of

$$\frac{u}{\sqrt{u^2 + \chi}} \quad and \quad \frac{u}{\sqrt{u^2 - \chi}}$$

are not uniformly valid at $u = 0$ and $u = \sqrt{\chi}$ respectively; therefore we cannot use the simple method of expanding the

integrand.

A.1 <u>Particle Density</u> <u>in</u> <u>an</u> <u>Accelerating</u> <u>Potential</u>

The expansion of this integral,

$$F(\chi) = \int_0^\infty f(u) \frac{u\,du}{\sqrt{u^2 + \chi}} \tag{1}$$

is done by splitting the domain of integration at a small fixed non-zero point, k. On the lower part of the domain the function, f(u), is expanded into a taylor series (for the distribution functions of interest this is always possible) and on the upper part of the domain, $u/\sqrt{(u^2 + \chi)}$ is expanded (uniformly because k is greater than zero):

$$F(\chi) = \int_0^k f(u) \frac{u\,du}{\sqrt{u^2 + \chi}} + \int_k^\infty f(u) \frac{u\,du}{\sqrt{u^2 + \chi}}$$

$$= \int_0^k \left\{ \sum_{n=0}^\infty f^{(n)}(0) \frac{u^n}{n!} \right\} \frac{u\,du}{\sqrt{u^2 + \chi}}$$

$$\hspace{6cm}(2)$$

$$+ \int_k^\infty f(u) \left\{ 1 - \frac{1}{1!} \frac{1}{2} \frac{1}{u^2} \chi + O(\chi^2) \right\} du.$$

The expansion of the upper part is complete and we need to determine the asymptotic expansion of the lower part. We will find the asymptotic expansions of the infinite series of integrands and regroup the terms by order in χ and then show that

the result is independent of k as it should be. Finally, we will take the limit as k goes to zero and we will then have the result.

The asymptotic expansions of the infinite series can be found recursively starting with the first four integrals:

$$\int_0^k \frac{u\,du}{\sqrt{u^2+\chi}} = k - \chi^{1/2} + \frac{1}{2k}\chi + O(\chi^2),$$

$$\int_0^k \frac{u^2\,du}{\sqrt{u^2+\chi}} = \frac{k^2}{2} + \frac{\chi}{4}\ln\chi + \chi\left(\frac{1}{4} - \frac{\ln 2k}{2}\right) + O(\chi^2),$$

$$\int_0^k \frac{u^3\,du}{\sqrt{u^2+\chi}} = \frac{k^3}{3} - \frac{k}{2}\chi + O(\chi^{3/2}), \tag{3}$$

$$\int_0^k \frac{u^4\,du}{\sqrt{u^2+\chi}} = \frac{k^4}{4} - \frac{k^2}{4}\chi + O(\chi^2 \ln\chi).$$

The remainder of the terms are found by integration by parts:

$$\int_{\sqrt{\chi}}^{\sqrt{k^2+\chi}} (v^2 - \chi)^{\frac{m-1}{2}}\,dv = \frac{1}{m}\sqrt{k^2+\chi}\, k^{m-1} - \chi\,\frac{m-1}{m}\int_{\sqrt{\chi}}^{\sqrt{k^2+\chi}} (v^2-\chi)^{\frac{m-3}{2}}\,dv, \quad m \geq 5 \tag{4}$$

which results in

$$\int_0^k \frac{u^m\,du}{\sqrt{u^2+\chi}} = \frac{k^m}{m} - \chi\frac{k^{m-2}}{2(m-2)}, \quad m \geq 5. \tag{5}$$

Adding and regrouping these terms produces:

$$\int_0^\infty f(u) \frac{u\,du}{\sqrt{u^2+\chi}} = \sum_{n=0}^\infty \frac{f^{(n)}(0)}{n!} \int_0^k \frac{u^{n+1}\,du}{\sqrt{u^2+\chi}} + \int_k^\infty f(u)\left\{1 - \frac{1}{2u^2}\chi + O(\chi^2)\right\} \tag{6}$$

$$= \sum_{n=2}^\infty \frac{f^{(n)}(0)}{n!}\left[\frac{k^{n+1}}{n+1} - \chi\frac{k^{n-1}}{2(n-1)}\right] + f^{(0)}(0)\left[k - \chi^{1/2} + \frac{\chi}{2k}\right]$$

$$+ f^{(1)}(0)\left[\frac{k^2}{2} + \frac{\chi}{4}\ln\chi + \chi\left(\frac{1}{4} - \frac{\ln 2k}{2}\right)\right] \tag{7}$$

$$+ \int_k^\infty f(u)\,du - \frac{\chi}{2}\int_k^\infty f(u)\frac{du}{u^2} + O(\chi^{3/2})$$

$$= \int_0^\infty f(u)\,du + \chi^{1/2}\left[-f(0)\right] + \chi\ln\chi\left[\frac{f^{(1)}(0)}{4}\right]$$

$$+ \chi\left[\frac{f^{(0)}(0)}{2k} + f^{(1)}(0)\left(\frac{1}{4} - \frac{\ln 2k}{2}\right) - \int_k^\infty f(u)\frac{1}{2u^2}\,du - \sum_{n=2}^\infty \frac{f^{(n)}(0)}{n!}\frac{k^{n-1}}{2(n-1)}\right] \tag{8}$$

$$+ O(\chi^{3/2}).$$

Now we demonstrate that this result is independent of k. The only term in eq. 8 containing k is the χ term; therefore we take the derivative of this term with respect to k:

$$\frac{d}{dk}\left[\frac{f(0)}{2k} + f^{(1)}(0)\left(\frac{1}{4} - \frac{\ln 2k}{2}\right) - \int_k^\infty f(u)\frac{1}{2u^2}\,du - \sum_{n=2}^\infty \frac{f^{(n)}(0)}{n!}\frac{k^{n-1}}{2(n-1)}\right]$$

$$= \left[f(k) - \sum_{n=0}^\infty \frac{f^{(n)}(0)}{n!}k^n\right]\frac{1}{2k^2} = 0 \tag{9}$$

Since f(u) is assumed to be expandable as a taylor series on (0,k) the expression in brackets is zero.

We now take the limit of eq. 8 as k goes to zero. Through integration by parts

$$\left[\frac{f^{(\prime)}(0)}{2k} + f^{\prime\prime}(0)\left(\frac{1}{4} - \frac{\ln 2k}{2} \right) - \int_k^\infty f(u) \frac{1}{2u^2} du - \sum_{n=2}^\infty \frac{f^{(n)}(0)}{n!} \frac{k^{n-1}}{2(n-1)} \right]$$

$$= \left[\frac{f^\prime(0)}{4} - \frac{1}{2} \int_0^\infty f^{\prime\prime\prime}(u) \, u \ln 2u \, du \right], \tag{10}$$

therefore we have the final result:

$$\int_0^\infty f(u) \frac{u \, du}{\sqrt{u^2 + \chi}} = \int_0^\infty f(u) \, du \ - \ \chi^{1/2} \left[f(0) \right]$$

$$+ \chi \ln \chi \left[\frac{f^{(\prime)}(0)}{4} \right]$$

$$+ \chi \left[\frac{f^{(\prime)}(0)}{4} - \frac{1}{2} \int_0^\infty f^{\prime\prime\prime}(u) \, u \ln 2u \, du \right] \tag{11}$$

$$+ O(\chi^{3/2}).$$

The $\chi^{1/2}$ term and the $\chi \ln \chi$ term in eq.11 depend only on the distribution function zero. If the distribution function has its

low energy tail cut off (as in chap. 3), then the $\chi^{1/2}$ and $\chi \ln \chi$ terms are zero and the χ term can be reduced (by integration by parts) to:

$$\int_{u_{cut}}^\infty f(u) \frac{u \, du}{\sqrt{u^2 + \chi}} = \int_{u_{cut}}^\infty f(u) \, du \tag{12}$$

$$- \chi \left[\int_{u_{cut}}^\infty f(u) \frac{1}{2u^2} du \right]$$

$$+ O(\chi^2).$$

A.2 Particle Density in an Decelerating Potential

The expansion of this integral,

$$F(\chi) = \int_{\sqrt{\chi}}^{\infty} f(u) \frac{u \, du}{\sqrt{u^2 - \chi}}, \tag{1}$$

is done by splitting the domain of integration at a small fixed non-zero point, k. On the lower part of the domain the function, f(u), is expanded into a taylor series (for the distribution functions of interest this is always possible) and on the upper part of the domain, $u/\sqrt{(u^2 - \chi)}$ is expanded (uniformly because k is greater than zero):

$$F(\chi) = \int_{\sqrt{\chi}}^{k} f(u) \frac{u \, du}{\sqrt{u^2 - \chi}} + \int_{k}^{\infty} f(u) \frac{u \, du}{\sqrt{u^2 - \chi}}$$

$$= \int_{\sqrt{\chi}}^{k} \left\{ \sum_{n=0}^{\infty} f^{(n)}(0) \frac{u^n}{n!} \right\} \frac{u \, du}{\sqrt{u^2 - \chi}} \tag{2}$$

$$+ \int_{k}^{\infty} f(u) \left\{ 1 + \frac{1}{1!} \frac{1}{2u^2} \chi + O(\chi^2) \right\}.$$

The expansion of the upper part is complete and we need to determine the asymptotic expansion of the lower part. We will find the asymptotic expansions of the infinite series of integrands and regroup the terms by order in χ and then show that the result is independent of k as it should be. Finally, we will take the limit as k goes to zero and we will then have the result.

The asymptotic expansions of the infinite series can be found recursively starting with the first four integrals:

$$\int_{\sqrt{x}}^{k} \frac{u\,du}{\sqrt{u^2-x}} = k - \frac{x}{2k} + O(x^2),$$

$$\int_{\sqrt{x}}^{k} \frac{u^2\,du}{\sqrt{u^2-x}} = \frac{k^2}{2} - \frac{x\ln x}{4} - x\left(\frac{1}{4} - \frac{\ln 2k}{2}\right) + O(x^2),$$

$$\int_{\sqrt{x}}^{k} \frac{u^3\,du}{\sqrt{u^2-x}} = \frac{k^3}{3} + \frac{xk}{2} + O(x^2), \tag{3}$$

$$\int_{\sqrt{x}}^{k} \frac{u^4\,du}{\sqrt{u^2-x}} = \frac{k^4}{4} + \frac{xk^2}{4} + O(x^2\ln x).$$

The remainder of the terms are found by integration by parts:

$$\int_{0}^{\sqrt{k^2-x}} (v^2+x)^{\frac{m-1}{2}}\,dv = \frac{1}{m}\sqrt{k^2-x}\,k^{m-1} + x\int_{0}^{\sqrt{k^2-x}} (v^2+x)^{\frac{m-3}{2}}\,dv, \quad m\geq 5 \tag{4}$$

which results in

$$\int_{\sqrt{x}}^{k} \frac{u^m\,du}{\sqrt{u^2-x}} = \frac{k^m}{m} + \frac{k^{m-2}}{2(m-2)}x + O(x^2). \tag{5}$$

Adding and regrouping these terms produces:

$$\int_{\sqrt{x}}^{\infty} f(u)\frac{u\,du}{\sqrt{u^2-x}} = \sum_{n=0}^{\infty} \frac{f^{(n)}(0)}{n!}\int_{\sqrt{x}}^{k} \frac{u^{n+1}\,du}{\sqrt{u^2-x}} \tag{6}$$

$$+ \int_{k}^{\infty} f(u)\left\{1 + \frac{1}{1!}\frac{1}{2u^2}x + O(x^2)\right\}$$

$$= \sum_{n=2}^{\infty} \frac{f^{(n)}(0)}{n!} \left[\frac{k^{n+1}}{n+1} + \frac{k^{n-1}}{2(n-1)} \chi \right] + f(0) \left(k - \frac{\chi}{2k} \right)$$

$$+ f^{(1)}(0) \left[\frac{k^2}{2} - \frac{\chi \ln \chi}{4} - \chi \left(\frac{1}{4} - \frac{\ln 2k}{4} \right) \right] \qquad (7)$$

$$+ \int_k^{\infty} f(u) \, du + \chi \int_k^{\infty} f(u) \frac{1}{2u^2} \, du + O(\chi^2)$$

$$= \int_0^{\infty} f(u) \, du + \chi \ln \chi \left[-\frac{f^{(1)}(0)}{4} \right] \qquad (8)$$

$$+ \chi \left\{ -\frac{f(0)}{2k} - f^{(1)}(0) \left(\frac{1}{4} - \frac{\ln 2k}{2} \right) + \sum_{n=2}^{\infty} \frac{f^{(n)}(0)}{n!} \frac{k^{n-1}}{2(n-1)} + \int_k^{\infty} f(u) \frac{1}{2u^2} \, du \right. .$$

Now we demonstrate that this result is independent of k. The only term in eq. 8 containing k is the χ term; therefore we take the derivative of this term with respect to k:

$$\frac{d}{dk} \left[-\frac{f(0)}{2k} - f^{(1)}(0) \left(\frac{1}{4} - \frac{\ln 2k}{2} \right) + \sum_{n=2}^{\infty} \frac{f^{(n)}(0)}{n!} \frac{k^{n-1}}{2(n-1)} + \int_k^{\infty} f(u) \frac{1}{2u^2} \, du \right]$$

$$= \frac{1}{2k^2} \left[\sum_{n=0}^{\infty} \frac{f^{(n)}(0) k^n}{n!} - f(k) \right] = 0 . \qquad (9)$$

Since f(u) is assumed to be expandable as a taylor series on (0,k) the expression in brackets is zero.

We now take the limit of eq. 8 as k goes to zero. Through integration by parts

$$\left[-\frac{f(0)}{2k} - f^{(1)}(0)\left(\frac{1}{4} - \frac{\ln 2k}{2}\right) + \sum_{n=2}^{\infty} \frac{f^{(n)}(0)}{n!} \frac{k^{n-1}}{2(n-1)} + \int_k^{\infty} f(u) \frac{1}{2u^2} du \right] \quad (10)$$

$$= \left[-f^{(1)}(0)\frac{1}{4} + \frac{1}{2}\int_0^{\infty} f'''(u)\, u\ln 2u\, du \right]$$

therefore we have the final result:

$$\int_{\sqrt{x}}^{\infty} f(u)\frac{u\,du}{\sqrt{u^2 - x}} = \int_0^{\infty} f(u)\,du + x\ln x\left[-\frac{f^{(1)}(0)}{4} \right]$$

$$+ x\left[-\frac{f^{(1)}(0)}{4} + \frac{1}{2}\int_0^{\infty} f'''(u)\, u\ln 2u\, du \right] \quad (11)$$

$$+ O(x^2).$$

The $x\ln x$ term in eq.11 depends only on the distribution function zero. If the distribution function has its low energy tail cut off (as in chap. 3), then the $x\ln x$ term is zero and the x term can be reduced (by integration by parts) to:

$$\int_{u_{cut}}^{\infty} f(u)\frac{u\,du}{\sqrt{u^2 - x}} = \int_{u_{cut}}^{\infty} f(u)\,du \quad (12)$$

$$+ x\left[\int_{u_{cut}}^{\infty} f(u)\frac{1}{2u^2}\,du \right]$$

$$+ O(x^2).$$

APPENDIX B: ISOTHERMAL PROGRAMS

B.1 ISOTHER: Computes the Isothermal Solution

B.2 SHIFT: Computes the General Sheath Solution

B.3 CAL3:   Computes the Sheath Solution given Ushift
             and Computed the Sheath Solution for no
             Trapped and no Surface Emission

B.1 <u>ISOTHER</u>: <u>Computes</u> <u>the</u> <u>Isothermal</u> <u>Solution</u>

```
ISOTHER:PROC OPTIONS(MAIN);
    DCL (T,DELT,X,DELX,FT,FX,DF1DT,DF1DX,DF2DT,DF2DX,
         DELTIN,DELXIN,ERSH,NEWSH,DUM,
         JR,TE,PHIW,NCS,NCSP,NPO,SURMULT,
         B1,DBDT,CHITEM,UZERO,SMR,LOSSION,
         CCHI,ACHI,OCHI,A1A0,TAU,RTAU,TAUIN,NO,N1,
         DELCHII,DELCHIF,DELCHIS,VD,VOUT,JJR,RATIO,
         TIN,XIN,BOTEM,B1TEM,QTEM,QCTEM,RTEM,ATEM,CTEM,ABTEM,
         A0,A1,VION,SMALLJ,DELCHI,DELTAT,DELTAX,
         ERROR1,ERROR2) FLOAT BIN(31);
    DCL (FLAGCOL,ISOL,IPLASMA,IPLATE,ISINGLE,ISPEED,
         ISUR) EXT FIXED BIN(31);
    DCL (I,J,ICASE,ICASEST,INERTIA,IDELCHI,IONIZA,IA1A0) FIXED BIN(31);
    DCL (CUTOFF,TRAPPED,SURFACE,UIN,VIONC,UCSHIFT,CCUT,
         MUI,MUEA,KN,LAMDAR) EXT FLOAT BIN(31);
    DCL (ABINV,A,RQ,Q,BETA0,BETA1,SHIFT,INVB1) EXT ENTRY
         RETURNS(FLOAT BIN(31) );
    CCUT=CUTOFF;
    SMR=1./492.2;
    IPLASMA=0;IPLATE=0;
    SURMULT=1.;
    GET FILE(ISODAT) DATA;
    ICASE=ICASEST-1;
    LOOP:DO DELCHI=DELCHII TO DELCHIF BY DELCHIS;
    ICASE=ICASE+1;

    SHIFTLP:DO J=1 TO 3;

    IF(FLAGCOL=0) THEN BEGIN;

    /* SET INITIAL ITERANTS IF FIRST CASE */
    IF (ICASE=ICASEST) THEN BEGIN;
      T=TIN;X=XIN;
      TAU=TAUIN;
    END;
    FT=F1(T,X);FX=F2(T,X);
    CON:DO I= 1 TO 20;
      DELTIN=.05;
      DELXIN=.05;
      DELT=(EXP(DELTIN)-1.)*T;
      DELX=(EXP(DELXIN)-1.)*X;
      DF1DT=(F1(T+DELT,X)-FT)/DELTIN;
      DF1DX=(F1(T,X+DELX)-FT)/DELXIN;
      DF2DT=(F2(T+DELT,X)-FX)/DELTIN;
      DF2DX=(F2(T,X+DELX)-FX)/DELXIN;
      DELTAT=(FX*DF1DX-FT*DF2DX)/(DF1DT*DF2DX-DF1DX*DF2DT);
      DELTAX=(FT*DF2DT-FX*DF1DT)/(DF1DT*DF2DX-DF1DX*DF2DT);
      T=EXP(DELTAT)*T;
```

```
X=EXP(DELTAX)*X;
FT=F1(T,X);
FX=F2(T,X);
IF(ABS(FT)<=ERROR1 & ABS(FX)<=ERROR2) THEN GO TO FIN;
END CON;
PUT FILE(ISOPRT) SKIP LIST('FAILED TO CONVERGE');
PUT FILE(ISOPRT) SKIP DATA;
STOP;
END;
ELSE BEGIN;
T=0.0;
/* SET INITIAL ITERANTS IF FIRST CASE */
IF (ICASE=ICASEST) THEN BEGIN;
  X=XIN;
  TAU=TAUIN;
END;
FX=F2(T,X);
CON2:DO I= 1 TO 20;
 DELXIN=.05;
 DELX=(EXP(DELXIN)-1.)*X;
 DF2DX=(F2(T,X+DELX)-FX)/DELXIN;
 DELTAX=-FX/DF2DX;
 X=X*EXP(DELTAX);
 FX=F2(T,X);
 IF(ABS(FX)<=ERROR2) THEN GO TO FIN;
END CON2;
PUT FILE(ISOPRT) SKIP LIST('FAILED TO CONVERGE');
PUT FILE(ISOPRT) SKIP DATA;
STOP;
END;
FIN:
  IF(FLAGCOL¬=0) THEN BEGIN;
  T=.001;
  B1TEM=-ATEM*COS(ATEM+CTEM)/SIN(ATEM+CTEM);
  IF(FLAGCOL¬=2) THEN BEGIN;
  B1=BETA1(TAU,T,QCTEM)-B1TEM;
  CON3:DO I = 1 TO 20;
   DBDT=(BETA1(TAU,T+DELT,QCTEM)-B1TEM-B1)/DELT;
   DELTAT=-B1/DBDT;
   T=T+DELTAT;
   B1=BETA1(TAU,T,QCTEM)-B1TEM;
   IF(ABS(B1)<=ERROR2)  THEN GO TO FIN1;
  END CON3;
  PUT FILE(ISOPRT) LIST('B1 LOOP FAILED TO CONVERGE');
  STOP;
  END;
  ELSE BEGIN;
  DUM=INVB1(TAU,B1TEM);
  END;
  END;
  FIN1:

  NEWSH=SHIFT(TAU,X,CHITEM,TRAPPED,SURFACE);
  ERSH=NEWSH-UIN;
```

```
          UIN,UZERO=NEWSH;

          END SHIFTLP;

          PUT FILE(ISOPRT) SKIP DATA;
          PUT FILE(ISOPLOT) SKIP(2) EDIT('DELCHI(',ICASE,
          ')=',DELCHI,',')
          (A(7),F(2),A(2),E(13,5),A(1));
          PUT FILE(ISOPLOT) EDIT('R(',ICASE,
          ')=',RTEM,',')
          (A(2),F(2),A(2),E(13,5),A(1));
          PUT FILE(ISOPLOT) EDIT('MACHE(',ICASE,
          ')=',QTEM,',')
          (A(6),F(2),A(2),E(13,5),A(1));
          PUT FILE(ISOPLOT) SKIP EDIT('BETA0(',ICASE,
          ')=',BOTEM,',')
          (A(6),F(2),A(2),E(13,5),A(1));
          PUT FILE(ISOPLOT) EDIT('BETA1(',ICASE,
          ')=',B1TEM,',')
          (A(6),F(2),A(2),E(13,5),A(1));
          PUT FILE(ISOPLOT) EDIT('A(',ICASE,
          ')=',ATEM,',')
          (A(2),F(2),A(2),E(13,5),A(1));
          PUT FILE(ISOPLOT) SKIP EDIT('SMALLJ(',ICASE,
          ')=',SMALLJ,',')
          (A(7),F(2),A(2),E(13,5),A(1));
          PUT FILE(ISOPLOT) EDIT('ECHI(',ICASE,
          ')=',X,',')
          (A(5),F(2),A(2),E(13,5),A(1));
          PUT FILE(ISOPLOT) EDIT('TAU(',ICASE,
          ')=',TAU,',')
          (A(4),F(2),A(2),E(13,5),A(1));
          VD=-2*(TAU-1.)/SMALLJ;
          IF(IONIZA¬=0) THEN VD=VD-LOSSION;
          PUT FILE(ISOPLOT) SKIP EDIT('VD(',ICASE,
          ')=',VD,',')
          (A(3),F(2),A(2),E(13,5),A(1));
          JJR=SMALLJ*EXP(-X-DELCHI);
          PUT FILE(ISOPLOT) EDIT('JJR(',ICASE,
          ')=',JJR,',')
          (A(4),F(2),A(2),E(13,5),A(1));
          VOUT=X+DELCHI+VD;
          IF(T<0.) THEN VOUT=VOUT+T;
          PUT FILE(ISOPLOT) EDIT('VOUT(',ICASE,
          ')=',VOUT,',')
          (A(5),F(2),A(2),E(13,5),A(1));
          ACHI=TAU*LOG(SIN(ATEM+CTEM)/SIN(CTEM));
          PUT FILE(ISOPLOT) SKIP EDIT('ACHI(',ICASE,
          ')=',ACHI,',')
          (A(5),F(2),A(2),E(13,5),A(1));
          OCHI=SMALLJ*RTEM;
          PUT FILE(ISOPLOT) EDIT('OCHI(',ICASE,
          ')=',OCHI,',')
          (A(5),F(2),A(2),E(13,5),A(1));
```

```
        PUT FILE(ISOPLOT) EDIT('CCHI(',ICASE,
        ')=',T,',')
        (A(5),F(2),A(2),E(13,5),A(1));
        PUT FILE(ISOPLOT) SKIP EDIT('A0(',ICASE,
        ')=',A0,',')
        (A(3),F(2),A(2),E(13,5),A(1));
        PUT FILE(ISOPLOT) EDIT('A1(',ICASE,
        ')=',A1,',')
        (A(3),F(2),A(2),E(13,5),A(1));
        PUT FILE(ISOPLOT) EDIT('C(',ICASE,
        ')=',CTEM,',')
        (A(2),F(2),A(2),E(13,5),A(1));
        PUT FILE(ISOPLOT) SKIP EDIT('VAVE(',ICASE,
        ')=',VION,',')
        (A(5),F(2),A(2),E(13,5),A(1));
        PUT FILE(ISOPLOT) EDIT('UZERO(',ICASE,
        ')=',UZERO,',')
        (A(6),F(2),A(2),E(13,5),A(1));
        PUT FILE(ISOPLOT) EDIT('CUTOFF(',ICASE,
        ')=',CUTOFF,',')
        (A(7),F(2),A(2),E(13,5),A(1));
        PUT FILE(ISOPLOT) SKIP EDIT('TRAPPED(',ICASE,
        ')=',TRAPPED,',')
        (A(8),F(2),A(2),E(13,5),A(1));
        PUT FILE(ISOPLOT) EDIT('SURFACE(',ICASE,
        ')=',SURFACE,',')
        (A(8),F(2),A(2),E(13,5),A(1));
        PUT FILE(ISOPLOT) EDIT('ISOL(',ICASE,
        ')=',ISOL,',')
        (A(5),F(2),A(2),F(2),A(1));
        PUT FILE(ISOPLOT) EDIT('IONIZA(',ICASE,
        ')=',IONIZA,',')
        (A(7),F(2),A(2),F(2),A(1));
        N0=1./QTEM;
        PUT FILE(ISOPLOT) SKIP EDIT('N0(',ICASE,
        ')=',N0,',')
        (A(7),F(2),A(2),E(13,5),A(1));
        PUT FILE(ISOPLOT) EDIT('VIONC(',ICASE,
        ')=',VIONC,',')
        (A(6),F(2),A(2),E(13,5),A(1));
        PUT FILE(ISOPLOT) EDIT('UCSHIFT(',ICASE,
        ')=',UCSHIFT,',')
        (A(8),F(2),A(2),E(13,5),A(1));
        N1=1./QCTEM;
        PUT FILE(ISOPLOT) SKIP EDIT('N1(',ICASE,
        ')=',N1,',')
        (A(7),F(2),A(2),E(13,5),A(1));
        PUT FILE(ISOPLOT) EDIT('ERSH(',ICASE,
        ')=',ERSH,',')
        (A(5),F(2),A(2),E(13,5),A(1));
        PUT FILE(ISOPLOT) SKIP EDIT('FLAGCOL(',ICASE,
        ')=',FLAGCOL,',')
        (A(8),F(2),A(2),E(13,5),A(1));
    END LOOP;
```

```
                RETURN;
                F1:PROC(CX,XX) RETURNS(FLOAT BIN(31));
                  DCL (CX,XX,F1X) FLOAT BIN(31);
                  IF(IDELCHI=0) THEN CHITEM=0.;
                  ELSE CHITEM=DELCHI;
                  QTEM=Q(TAU,XX,CHITEM,SMALLJ,VION,UZERO);

                 /* SURFACE EMISSION */
                  TE=1500.;PHIW=1.60;JR=20.;
                  JJR=SMALLJ*EXP(-XX-CHITEM);
                  NCS=6.44E+15*(1500./TE);
                  NCSP=NCS/2./(1.+2.*EXP((3.89-PHIW)*11600./TE));
                  NPO= (JJR*JR)*2.925E+11/QTEM*(1500./TE);
                  SURFACE=NCSP/NPO*2.*EXP(CHITEM);
                  SURFACE=SURFACE*SURMULT;
                  IF (ISUR=0) THEN SURFACE=0.;

                  BOTEM=BETA0(TAU,XX,QTEM,VION);
                  QCTEM=SQRT(2./3.14159)*EXP(-CX/TAU)/C1(CX/TAU);
                  IF(FLAGCOL=0) THEN BEGIN;
                     B1TEM=BETA1(TAU,CX,QCTEM);
                  END;
                  ATEM=A(BOTEM,B1TEM,QTEM,CTEM);
                  TAU=ABINV(ATEM);
                  A0=SQRT(3.1415927/2.)*QTEM*(1./SMALLJ-1.)*EXP(XX/TAU);
                  IF(CX/TAU<=0.) THEN
                  A1=1.;
                  ELSE
                  A1=1./C1(CX/TAU);
                  A1A0=A1/A0;
                  IF (IA1A0=0) THEN A1A0=1.;
                  F1X=CX-XX-TAU*LOG(SIN(ATEM+CTEM)/SIN(CTEM))
                      -TAU*LOG(A1A0)-TAU*LOG(1./SMALLJ-1.);
                  RETURN(F1X);
                END F1;
                F2:PROC(CX,XX) RETURNS(FLOAT BIN(31));
                  DCL (CX,XX,RQTEM,F2X) FLOAT BIN(31);
                  IF( IDELCHI=0) THEN CHITEM=0.;
                  ELSE CHITEM=DELCHI;
                  QTEM=Q(TAU,XX,CHITEM,SMALLJ,VION,UZERO);

                 /* SURFACE EMISSION */
                  TE=1500.;PHIW=1.60;JR=20.;
                  JJR=SMALLJ*EXP(-XX-CHITEM);
                  NCS=6.44E+15*(1500./TE);
                  NCSP=NCS/2./(1.+2.*EXP((3.89-PHIW)*11600./TE));
                  NPO= (JJR*JR)*2.925E+11/QTEM*(1500./TE);
                  SURFACE=NCSP/NPO*2.*EXP(CHITEM);
                  SURFACE=SURFACE*SURMULT;
                  IF (ISUR=0) THEN SURFACE=0.;

                  BOTEM=BETA0(TAU,XX,QTEM,VION);
                  QCTEM=SQRT(2./3.14159)*EXP(-CX/TAU)/C1(CX/TAU);
                  IF(FLAGCOL=0) THEN BEGIN;
```

```
      B1TEM=BETA1(TAU,CX,QCTEM);
    END;
    ATEM=A(B0TEM,B1TEM,QTEM,CTFM);
    TAU=ABINV(ATEM);
    A0=SQRT(3.1415927/2.)*QTEM*(1./SMALLJ-1.)*EXP(XX/TAU);
    RQTEM=RQ(ATEM,CTEM);
    RTEM=RATIO*RQTEM*QTEM/SMALLJ*TAU*
                    4./SQRT(2.*3.1415927);
    IF(CX/TAU<=0.) THEN
    A1=1.;
    ELSE
    A1=1./C1(CX/TAU);
    A1A0=A1/A0;
    IF(IA1A0=0) THEN A1A0=1.;
    F2X= 2.*(1.-TAU)/SMALLJ + SMALLJ*RTEM
        +TAU*LOG(SIN(ATEM+CTEM)/SIN(CTEM))+XX-CX;
    IF(INERTIA¬=0) THEN BEGIN;
    F2X=F2X
        -TAU*QTEM**2/2.*(1.-(SIN(CTEM)/SIN(ATEM+CTEM))**2);
    END;
    IF(IONIZA¬=0) THEN BEGIN;
    LOSSION=SMR*(VION+VIONC*SIN(ATEM+CTEM)/SIN(CTEM))/
        QTEM*3.896/8.609E-05/TE;
    F2X=F2X-LOSSION;
    END;
    RETURN(F2X);
  END F2;
  C1:PROC(XX) RETURNS(FLOAT BIN(31));
    DCL (XX,C1X) FLOAT BIN(31);
    IF(XX<=0.) THEN C1X=1.;
    ELSE C1X=1.+ERF(SQRT(XX));
    RETURN(C1X);
  END C1;
  C2:PROC(XX) RETURNS(FLOAT BIN(31));
    DCL (XX,C2X) FLOAT BIN(31);
    C2X=EXP(XX)*(1.-ERF(SQRT(XX)));
    RETURN(C2X);
  END C2;
END ISOTHER;
```

B.2 <u>SHIFT</u>: <u>Computes</u> <u>the</u> <u>General</u> <u>Sheath</u> <u>Solution</u>

```
SHIFT:PROC(CE,PHIM,R,TRAPPED,SURFACE) RETURNS(FLOAT BIN(31));
     DCL(BETA,BETATEM,CI,SCI,CE,R,UR,
         NEB,NPLASMA,
         C1,C2,C5,C6,PHIM,
         PLASMA,SURFACE,
         CHI,
         URL,URH,MURM,URM,
         TEM1,TEM2,TEM3,TEM4,TEM5,TEM6,TEM7)
         FLOAT BIN(31);
     DCL( I,ICASE) FIXED BIN(31);
     DCL(FIB,FID,FII)
         EXT ENTRY(FLOAT BIN(31),FLOAT BIN(31),
         FLOAT BIN(31),FLOAT BIN(31),FLOAT BIN(31))
         RETURNS( FLOAT BIN(31));
     DCL (FEB,FIJ) EXT ENTRY(FLOAT BIN(31),FLOAT BIN(31),
         FLOAT BIN(31),FLOAT BIN(31))
         RETURNS( FLOAT BIN(31) );
     DCL (TRAPPED) FLOAT BIN(31);
     DCL (M) FIXED BIN(31) EXT;
     M=20;
       CI=1.;BETATEM=.1;
       SCI=SQRT(CI);
       BETA=BETATEM*SQRT(CE/2.);
URH=3.;URL=-3.;
LOOPUR:DO I = 1 TO 10;
  URM=(URL+URH)/2.;
  MURM=MININT(URM);
  IF(MURM<=-0.00000001) THEN URL=URM;
                        ELSE URH=URM;
END LOOPUR;
FINUR:UR=URM*SQRT(2./CE);
RETURN(UR);

   MININT:PROC(URTEM) RETURNS( FLOAT BIN(31));
           DCL (URTEM,FNETMIN,TEMP) FLOAT BIN(31);
           DCL J FIXED BIN(31);
           CHI=PHIM;NEB=(EA(URTEM,R)-K3(CHI))/K4(CHI);
           CHI=0.;FNETMIN=EA(URTEM,R)-K3(CHI)-K4(CHI)*NEB;
           LOOP:DO J=1 TO 25;
               CHI=J*PHIM/25.;
               TEMP=EA(URTEM,R)-K3(CHI)-K4(CHI)*NEB;
               FNETMIN=MIN(FNETMIN,TEMP);
           END LOOP;
           LOOP2:DO J=1 TO 10;
               CHI=J*PHIM/250.;
               TEMP=EA(URTEM,R)-K3(CHI)-K4(CHI)*NEB;
               FNETMIN=MIN(FNETMIN,TEMP);
           END LOOP2;
```

```
                RETURN(FNETMIN);
        END MININT;

            EA:PROC(TUZERO,TR) RETURNS(FLOAT BIN(31));
            DCL(TUZERO,TR,TEMEA,TPHIM,TPHIZ,SQZM,SQPI,
                IOXZM,IZMXX,IOM,
                SQZX,IZXI,IOX,IZMXI,SQXZM,IZI,IZMI)
            FLOAT BIN(31);
            TPHIM=PHIM;TPHIZ=(PHIM+TR);
            IF(TPHIZ>=TPHIM) THEN BEGIN;

            SQZM=SQRT(TPHIZ-TPHIM);
            SQZX=SQRT(TPHIZ-CHI);

            IZMI=(1.-ERF(SQZM))*SQRT(3.1415926)/2.;
            IOM=ERF(SQRT(TPHIM))*SQRT(3.1415926)/2.;
            IZXI=(1.-ERF(SQZX))*SQRT(3.1415926)/2.;
            IOX=ERF(SQRT(CHI))*SQRT(3.1415926)/2.;
            IZI=(1.-ERF(SQRT(TPHIM)))*SQRT(3.1415926)/2.;
            IZMXI=(1.-ERF(SQRT(TPHIZ-TPHIM+CHI)))*SQRT(3.1415926)/2.;
            PLASMA=(SQRT(3.1415926)-SURFACE*IZMI)/
                    (FID(BETA/SCI,1000000.,1.,TUZERO,0.) +
                     FID(BETA/SCI,SQZM,1.,TUZERO,0.) );
        TEMEA=2.*PLASMA*
          ( FII(BETA/SCI,1000000.,1.,TUZERO,
                SQRT(CHI)) -
            FII(BETA/SCI,1000000.,1.,TUZERO,
                0.) +
            FII(BETA/SCI,SQZM,1.,TUZERO,
                SQRT(CHI)) -
            FII(BETA/SCI,SQZM,1.,TUZERO,
                0.))
        + TRAPPED*
          ( 2.*EXP(CHI)*IOX-2.*SQRT(CHI) )
        +SURFACE*
          ( EXP(TPHIM-TPHIZ)*SQRT(TPHIZ-TPHIM+CHI)
          +EXP(CHI)*IZMXI
          -SQRT(TPHIZ-TPHIM)*EXP(TPHIM-TPHIZ)
          -IZMI );

        TEMEA=TEMEA/SQRT(3.1415926);
        END;
        ELSE BEGIN;
            SQPI=SQRT(3.1415926);
            PLASMA=SQPI*(1.-SURFACE/2.)/
                    FID(BETA/SCI,1000000.,1.,TUZERO,0.);
            TEMEA=
                    2.*PLASMA*(FII(BETA/SCI,1000000.,1.,TUZERO,
                                SQRT(CHI))-
                            FII(BETA/SCI,1000000.,1.,TUZERO,
                                0.)    )/SQPI;
          IF(CHI<=TPHIM-TPHIZ) THEN BEGIN;
            IOX=ERF(SQRT(CHI))*SQPI/2.;
            TEMEA=TEMEA + SURFACE*
```

```
                        (SQPI/2.*(EXP(CHI)-1.)
                        +EXP(CHI)*IOX-SQRT(CHI))/SQPI;
            END;
            ELSE BEGIN;
            , SQXZM=SQRT(CHI+TPHIZ-TPHIM);
             IOXZM=SQPI*ERF(SQXZM)/2.;
             IZMXI=(1.-ERF(SQRT(TPHIZ-TPHIM+CHI)))*SQPI/2.;
             IZMXX=( ERF(SQRT(CHI))
                        -ERF(SQRT(TPHIZ-TPHIM+CHI)) )*SQPI/2.;
               TEMEA=TEMEA + SURFACE*
                        (SQRT(TPHIZ-TPHIM+CHI)*EXP(TPHIM-TPHIZ)*2.
                        +EXP(CHI)*IZMXI
                        -SQPI/2.-SQRT(CHI)+EXP(CHI)*IZMXX)/SQPI
                    +TRAPPED*(2.*EXP(CHI)*IOXZM -
                            2.*EXP(TPHIM-TPHIZ)*SQXZM)/SQPI;
            END;

            END;
    RETURN(TEMEA*CI);
    END EA;

    K3:PROC(CHITEM) RETURNS( FLOAT BIN(31));
        DCL(CHITEM) FLOAT BIN(31);
        TEM1=SQRT(3.1415926)/2.;
        TEM3=SQRT(3.1415926)/2.*ERF(SQRT(PHIM/CE));

        C1=(TEM1+TEM3)/(TEM1);
        C5=  (1.-EXP(-CHITEM/CE))+  EXP(-CHITEM/CE)*(
          2*FII(0.,SQRT((PHIM-CHITEM)/CE),1.,0.,SQRT(CHITEM/CE))-
          2*FII(0.,SQRT((PHIM-CHITEM)/CE),1.,0.,0.) )*
             2./SQRT(3.1415926)+
          2*FII(0.,SQRT(CHITEM/CE),1.,0.,0.)*2./SQRT(3.1415926);

        RETURN(C5*CE/C1);
    END K3;

    K4:PROC(CHITEM) RETURNS( FLOAT BIN(31));
        DCL(CHITEM) FLOAT BIN(31);
        TEM1=SQRT(3.1415926)/2.;
        TEM2=TEM1;
        TEM3=SQRT(3.1415926)/2.*ERF(SQRT(PHIM/CE));
        TEM4=FID(0.,1000000.,1.,0.,SQRT(PHIM));
        TEM6=2*FII(0.,1000000.,1.,0.,SQRT(PHIM));
        TEM7=2*FII(0.,1000000.,1.,0.,SQRT(PHIM-CHITEM));

        C1=(TEM1+TEM3)/(TEM1);
        C2=TEM4/TEM2;
        C5=  (1.-EXP(-CHITEM/CE))+  EXP(-CHITEM/CE)*(
          2*FII(0.,SQRT((PHIM-CHITEM)/CE),1.,0.,SQRT(CHITEM/CE))-
          2*FII(0.,SQRT((PHIM-CHITEM)/CE),1.,0.,0.) )*
             2./SQRT(3.1415926)+
          2*FII(0.,SQRT(CHITEM/CE),1.,0.,0.)*2./SQRT(3.1415926);
        C6=(TEM6-TEM7)/TEM2;
```

```
            RETURN(C6-C2*C5*CE/C1);
        END K4;
    END SHIFT;
```

B.3 <u>CAL3</u>: <u>Computes the Sheath Solution given Ushift</u> and Computed the Sheath Solution for no Trapped and no Surface Emission

```
CAL3:PROC(ECHI,PHIZ,CE,CI,BETATEM,MR,ERROR,UZERO,BNEB,BJNET,VAVE);
        DCL(BETA,BETATEM,CI,SCI,CE,ALPH,BET,R,UR,
            NEB,NEP,BNEB,BJNET,JNET,VAVE,
            C1,C2,C3,C4,C5,C6,H,PHIM,ECHI,
            F0,F1,F2,UR0,UR1,UR2,
            K1,K2,K3,K4,
            JION,JEE,RZ,
            JEP,PLASMA,
            DELX,DELTAX,X,HX,DHDX,
            UP,MR,ATEM,
            ERROR,PHIZ,TEM1,
            TEM2,TEM3,TEM4,TEM5,TEM6,TEM7,UZERO)
            FLOAT BIN(31);
        DCL(FIB,FID,FII)
            EXT ENTRY(FLOAT BIN(31),FLOAT BIN(31),
            FLOAT BIN(31),FLOAT BIN(31),FLOAT BIN(31))
            RETURNS( FLOAT BIN(31));
        DCL (FEB,FIJ) EXT ENTRY(FLOAT BIN(31),FLOAT BIN(31),
            FLOAT BIN(31),FLOAT BIN(31))
            RETURNS( FLOAT BIN(31) );
        DCL(I,J) FIXED BIN(31);
        DCL(M,ISOL,ISINGLE,ISPEED,IPLASMA,IPLATE) FIXED BIN(31) EXT;
        DCL (TRAPPED,SURFACE,INTERR,NENO,UIN) FLOAT BIN(31) EXT;
/**********************************************************************/
/*                                                          */
/*              EXTERNAL VARIABLE INPUTS                     */
/* ISOL   = 0 FOR CUTOFF ION DISTRIBUTION BOHM              */
/*        = 1 SQRT(CHI) MATCHING                            */
/* ISINGLE= 0 FOR DOUBLE SHEATH                             */
/*        = 1 SINGLE SHEATH                                 */
/* ISPEED = 0 MATCHED SHEATH                                */
/*        = 1 VSHIFT INPUT                                  */
/*        = 2 VSHIFT = VAVERAGE                             */
/* IPLASMA= 0 FOR FULL PLASMA ELECTRON DYNAMICS            */
/* IPLATE = 0 FOR FULL PLATE ELECTRON DYNAMICS             */
/*                                                          */
/**********************************************************************/
            PHIM=ECHI;
            R=(PHIZ-PHIM)/CI;
            SCI=SQRT(CI);
            BETA=BETATEM*SQRT(CE/2.);
            TEM1=SQRT(3.1415926)/2.;
            TEM2=TEM1;
            TEM3=SQRT(3.1415926)/2.*ERF(SQRT(PHIM/CE));
            TEM4=FID(0.,1000000.,1.,0.,SQRT(PHIM));
    /*      TEM4=SQRT(3.1415926)/2.*EXP(PHIM)*(1.-ERF(SQRT(PHIM))); */
```

```
                    TEM5=FEB(0.,1000000.,1.,PHIM);
           /*       TEM5=1./SQRT(PHIM)-2.*EXP(PHIM)*SQRT(3.1415926)/2.*
                       (1.-ERF(SQRT(PHIM)));                               */
                    TEM6=2*FII(0.,1000000.,1.,0.,SQRT(PHIM));
                    TEM7=2*FII(0.,1000000.,1.,0.,0.);

                    C1=(TEM1+TEM3)/(TEM1);
                    C2=TEM4/TEM2;
                    C3=2.*(TEM1+TEM3)/TEM1+SQRT(CE/PHIM)*EXP(-PHIM/CE)/TEM1;
                    C4=TEM5/TEM2;
                    C5=( TEM3-SQRT(PHIM/CE)*EXP(-PHIM/CE)+
                        SQRT(3.1415926)/2.*(1.-EXP(-PHIM/CE)) )/
                       (TEM1);
                    C6=(TEM6-TEM7)/TEM2;
                    IF (IPLASMA¬=0) THEN BEGIN;
                    C1=2.;
                    C3=4.;
                    C5=2.*(1.-EXP(-PHIM/CE));
                    END;
                    IF(IPLATE¬=0) THEN BEGIN;
                    C2=1./SQRT(1.+3.14159*PHIM);
                    C4=3.14159/2./(1.+3.14159*PHIM)**(1.5);
                    C6=2./3.14159*(SQRT(1.+3.14159*PHIM)-1.);
                    END;

                    K1=C3/CE/C1;
                    K2=C4+C2*C3/CE/C1;
                    K3=C5*CE/C1;
                    K4=C6-C2*C5*CE/C1;

        IF(ISPEED=0) THEN BEGIN;
        IF(ISOL=0) THEN BEGIN;
        UR0=2.0;F0=F(UR0);
        UR1=2.1;F1=F(UR1);
        END;
        ELSE BEGIN;
        UR0=1.0;F0=F(UR0);
        UR1=1.1;F1=F(UR1);
        END;
        CON:DO I= 1 TO 20;
            UR2=UR1-(UR1-UR0)/(F1-F0)*F1;
            F2=F(UR2);
            IF(ISOL=0) THEN BEGIN;
            IF(ABS(F2)<=ERROR) THEN GO TO FIN;
            END;
            ELSE BEGIN;
            IF(ABS(F2)<=ERROR*TRAPPED) THEN GO TO FIN;
            END;
            UR0=UR1;F0=F1;
            UR1=UR2;F1=F2;
        END CON;
        PUT FILE(AUXPRT) SKIP LIST('FAILED TO CONVERGE');
        STOP;
        F:PROC(XX) RETURNS(FLOAT BIN(31));
```

```
            DCL (FX,XX) FLOAT BIN(31);
            IF(ISOL=0) THEN BEGIN;
            ALPH=(K1-BA(XX,R))/K2;
            BET=(EA(XX,R)-K3)/K4;
            IF( ISINGLE=0) THEN
            FX=ALPH-BET;
            ELSE
            FX=ALPH-NENO;
            END;
            ELSE BEGIN;
            BETA=0.;
            IF(R>=0.) THEN BEGIN;
            FX=2.*TRAPPED-EXP(-XX**2)/
                (FID(BETA/SCI,1000000.,1.,XX,0.) +
                 FID(BETA/SCI,SQRT(R),1.,XX,0.)          );
            END;
            ELSE BEGIN;
            FX=SURFACE-EXP(-XX**2)/
                (FID(BETA/SCI,1000000.,1.,XX,0.) );
            END;
            END;
            RETURN(FX);
        END F;
        END;

        IF(ISPEED=1) THEN BEGIN;
        UR2=UIN*SQRT(CE/2./CI);
        END;

        IF(ISPEED=2) THEN BEGIN;
         IF(R<=0.) THEN UR2=UIN;
         ELSE UR2=UIN*EXP(-R)*SQRT(CE/2./CI);
        END;

        FIN:UR=UR2;
          IF(ISOL¬=0) THEN
          ALPH,BET=(EA(UR,R)-K3)/K4;
          NEB=(BET+ALPH)/2.;
          IF(ISINGLE¬=0) THEN
          NEB=NENO;
          INTERR=NEB-BET;
          NEP=(1.-C2*NEB)/C1;
          IF R>0. THEN
          UP=MAX(BETA,SQRT(R)*SCI,0.);
          ELSE UP = MAX(BETA,0.);
          IF R<=0. THEN RZ=0.;
          ELSE RZ=R;

          ATEM=( FIJ(UP/SCI,1000000.,1.,UR) - SURFACE*.5*EXP(-R) )/
          ( FID(BETA/SCI,1000000.,1.,UR,0.) + FID(BETA/SCI,UP/SCI,1.,UR,0.)
          + SURFACE*SQRT(3.1415926)/2.*(1.-ERF(SQRT(RZ))) );

          JION=SQRT(CI/MR)*ATEM;
          VAVE=SQRT(2.*CI/CE)*ATEM;
```

```
        JEE= -NEB/SQRT(3.1415926);
        JEP= -(1-C2*NEB)/C1/SQRT(3.1415926)*SQRT(CE)*
             EXP(-PHIM/CE);
        JNET=-JEE+JEP;
        BNEB=NEB;
        BJNET=JNET/SQRT(CE/2.);
        UZERO=UR*SQRT(2.*CI/CE);
  PUT FILE(REFPRT) SKIP DATA(C1,C2,C3,C4,C5,C6,NEB);
        RETURN;

            BA:PROC(TUZERO,TR) RETURNS(FLOAT BIN(31));
              DCL(TUZERO,TR,SQTR,TEMBA,B1,B2,B3,B4) FLOAT BIN(31);
                   B1=FIB(BETA/SCI,1000000.,1.,TUZERO,0.);
                   B3=CI*FID(BETA/SCI,1000000.,1.,TUZERO,0.);
                IF(TR>(BETA/SCI)**2) THEN BEGIN;
                   SQTR=SQRT(TR);
                   B2=FIB(BETA/SCI,SQTR,1.,TUZERO,0.);
                   B4=CI*FID(BETA/SCI,SQTR,1.,TUZERO,0.);
                   TEMBA=(B1+B2)/(B3+B4);
                END;
                ELSE
                   TEMBA=B1/B3;
            RETURN(TEMBA);
            END BA;

            EA:PROC(TUZERO,TR) RETURNS(FLOAT BIN(31));
              DCL(TUZERO,TR,TEMEA,TPHIM,TPHIZ,SQZM,SQZ,SQM,SQPI,
                   IZI,IZMI,IOM,IOZ,IZM)
              FLOAT BIN(31);
              TPHIM=PHIM/CI;TPHIZ=TPHIM+TR;
              IF(TPHIZ<=0.) THEN TPHIZ=0.;
              IF(TPHIZ>=TPHIM) THEN BEGIN;
              SQZM=SQRT(TPHIZ-TPHIM);
              IZMI=(1.-ERF(SQZM))*SQRT(3.1415926)/2.;
              IOM=ERF(SQRT(TPHIM))*SQRT(3.1415926)/2.;
              IZI=(1.-ERF(SQRT(TPHIM)))*SQRT(3.1415926)/2.;
              PLASMA=(SQRT(3.1415926)-SURFACE*IZMI)/
                     (FID(BETA/SCI,1000000.,1.,TUZERO,0.) +
                      FID(BETA/SCI,SQZM,1.,TUZERO,0.) );
              TEMEA=2.*PLASMA*
                ( FII(BETA/SCI,1000000.,1.,TUZERO,
                     SQRT(TPHIM)) -
                  FII(BETA/SCI,1000000.,1.,TUZERO,
                     0.) +
                  FII(BETA/SCI,SQZM,1.,TUZERO,
                     SQRT(TPHIM)) -
                  FII(BETA/SCI,SQZM,1.,TUZERO,
                     0.))
              + TRAPPED*
                ( 2.*EXP(TPHIM)*IOM-2.*SQRT(TPHIM) )
              + SURFACE*
                ( EXP(TPHIM)*IZI+EXP(TPHIM-TPHIZ)*SQRT(TPHIZ)
                 -IZMI-SQZM*EXP(TPHIM-TPHIZ) );
              TEMEA=TEMEA/SQRT(3.1415926);
```

```
                END;
                ELSE BEGIN;
                     SQZ=SQRT(TPHIZ);
                     SQM=SQRT(TPHIM);
                 ,   SQPI=SQRT(3.1415926);
                     IOZ=SQPI*ERF(SQZ)/2.;
                     IZI=SQPI/2.-IOZ;
                     IZM=SQPI/2.*(ERF(SQM)-ERF(SQZ));
                     PLASMA=SQPI*(1.-SURFACE/2.)/
                            FID(BETA/SCI,1000000.,1.,TUZERO,0.);
                     TEMEA=SURFACE*(EXP(TPHIM)*(IZI+IZM)
                                   +2.*SQZ*EXP(TPHIM-TPHIZ)
                                   -SQM-SQPI/2.)/SQPI
                          +TRAPPED*(2.*EXP(TPHIM)*IOZ -
                                   2.*EXP(TPHIM-TPHIZ)*SQZ)/SQPI
                          +2.*PLASMA*(FII(BETA/SCI,1000000.,1.,TUZERO,
                                        SQRT(TPHIM))-
                                        FII(BETA/SCI,1000000.,1.,TUZERO,
                                        0.)      )/SQPI;
                     END;
                RETURN(TEMEA*CI);
                END EA;
        END CAL3;
```

APPENDIX C: NON-ISOTHERMAL PROGRAMS

C.1 PREDCOR: Computes the Unsteady
             Non-Isothermal Solution

C.2 SHEATH: Computes the Sheath Model Solution

C.1 PREDCOR: Computes the Unsteady Non-Iosthermal Solution

```
/*    PREDCOR FOR FULL TEC                                    */
/*    APRIL 27, 1980: REVISED TO INCLUDE YEN FACTOR           */
/*    MAY 4, 1980: REVISED TO INCLUDE IVD, FINAL DOT, ELOSSB, */
/*                 AND CORRECT MURS IN BC.                    */
PREDCOR:PROC( T1, T2, TAU, NEB, NSTEPS, TE, TC, ENR, CNR,
              TDOT1, NDOT1,
              PN, SMR, LAMDAR, KN, NR, ARECN, TCHAR, EGNDB, RE,
              N,I, AN, AT, BN, BT, CN, CT) REORDER;
    DECLARE
      SUMV ENTRY((*) FLOAT DEC(16),FIXED BIN(31),FIXED BIN(31))
           RETURNS(FLOAT DEC(16)),
      SQRT BUILTIN,
    /*THE FOLLOWING TIME VARIABLES ARE NOND BY TCHAR.          */
      (T1,T2,                          /*START & FINISH TIMES.      */
       DT,                             /*ACTUAL TIME STEP USED.     */
       TIME,


       AN,AT,BN,BT,CN,CT,              /*PRED-COR ALPHA,BETA,GAMMA  */

       IVD EXT,                        /*PLASMA POWER GAIN          */
     (LAMTAU,LAMNEB)EXT,
      /*THE FOLLOWING VARIABLES REFER TO THE MOST RECENT TIME   */
        TAU(*),                        /*E- TEMPERATURE (NOND BY TE). */
        NEB(*),                        /*ELECTRON DENSITY (NOND BY NR)*/
        TDOT1(*), NDOT1(*),            /*PREDICTOR STEP TIME DERIV.S  */
      ((ENE,CNE) INIT(0.8),            /*E & C EMITTED DENSITY, NE.   */
       (ECHI,CCHI) INIT(3),            /*EMITTER & COLLECTOR DROPS     */
       (EALPHA,CALPHA) INIT(0.5)       /*E & C ION SPEED PARAMETERS   */
           ) STATIC EXTERNAL,
      /*THE FOLLOWING ARE CONSTANT DURING THIS PROGRAM          */
        MUI(0:N+1),                    /*ION MOBILITY               */
        ONE INIT(1),
        I,                             /*CURRENT (NOND BY REF DIFF C) */
        DZ,                            /*ZETA INCREMENT BETWEEN PTS   */
        TCHAR,                         /*AN ELECTRON TRANSIT TIME     */
        ERR,                           /*ACCURACY PARAM FOR SHEATH    */
        TE,TC,                         /*EMITTER & COLLECTOR TEMPERATU*/
        DTAUNDZ,
        PN,                            /*NEUTRAL PRESSURE (TORR)      */
        ENR,CNR,                       /*E. & C. RICHARSON DENSITIES. */
        NR,                            /*REFERENCE ELECTRON DENSITY   */
        EGNDB,                         /*E(0)/KT(E). NON-D BINDING E  */
        ELOSSB EXT,                    /*ENERGY LOSS PER IONIZATION   */
        RE,                            /*Q(E-A) =Q0 * E**-RE          */
        SMR,                           /*SQRT OF ELECTRON/ION MASS RAT*/
        LAMDAR,                        /* MFP RATIO,  =RMUR/SMR       */
        RMUR,                          /*MU RATIO,  =SMR*LAMDAR       */
        KN,                            /*KNUDSEN NUMBER               */
```

```
        NNR,                            /*REFERENCE NEUTRAL DENSITY.   */
        ARECN,                          /*COEFFICIENT OF RECOMBINATION */
        PI,                             /*  3.14159...                 */
        CA,CSAHA,                       /*CONSTANTS IN MSOURCE EQN     */

    /*THE FOLLOWING ARE VECTORS (0:N+1).                               */
      (NNB,TAUN,                        /*NEUTRAL DENSITY & TEMP.       */
                                        /*   NON-D BY EMITTER VALUES    */
        MSOURCE,                        /*E- PRODUCTION RATE (NOND)     */
        ESOURCE,                        /*ENERGY SOURCE TERM (NOND)     */
        CV,
        MUEA,                           /*E- MOBILITY AMONG ATOMS.      */
        NDOT2,TDOT2,
        TTILDA,NTILDA)
          (0:N+1) ) FLOAT DEC(16),
        CFIX BIT(1) EXT,                /*DID C-SHEATH REQUIRE FIX?     */
        EFIX BIT(1) EXT,
        (NSTEPS,
        N,                              /*# OF GRID PTS, E TO C INCL.   */
        J,
        COUNT)                          /*PRESENT                       */
          FIXED BIN(31);
   DCL IDEN FIXED BIN(31) EXT;
/*HANDLE EXCEPTIONAL CONDITIONS.                                       */
   ON FINISH PUT SKIP(5) DATA;

   PI=3.1415926 + 5.3589793E-8;
   DZ=ONE/(N-1);
   DT=(T2-T1)/NSTEPS;
   CFIX,EFIX='0'B;
   ERR=1E-3;
/*SET NEUTRAL TEMPERATURE AND DENSITY.                                 */
   IF TE=TC THEN TAUN=1;
      ELSE DO J=0 TO N+1;
              TAUN(J)=1 + (TC/TE-1)*(J-1)/(N-1);
              END;
   NNR=965.5E16*PN/TE;
   NNB=1/TAUN;
   DTAUNDZ=TAUN(N)-TAUN(1);
/*SET TRANSPORT PARAMETERS.                                            */
   RMUR=LAMDAR*SMR;
   MUI=SQRT(TAUN);
/*SET IONIZATION AND SAHA PARAMETERS.                                  */
   CA=0.41283*ARECN*TCHAR*(NR/1E14)**2 * (TE/1500)**-4.5;
   CSAHA=LOG( (1.4027E20*NNR/NR/NR) * (TE/1500)**1.5 );

   DO COUNT=0 TO NSTEPS-1;
      TIME=T1+COUNT*DT;
      /*PREDICTOR STEP                                                 */
      CALL DOT(NDOT1,TDOT1,NEB,TAU);
      NTILDA=NEB + AN*DT*NDOT1;
      TTILDA=TAU + AT*DT*TDOT1;
      /*CORRECTOR STEP                                                 */
IF( AN=0. & AT=0. ) THEN BEGIN;
```

```
                NDOT2=0.;TDOT2=0.;GO TO NOCOR;END;
                     CALL DOT(NDOT2,TDOT2,NTILDA,TTILDA);
                NOCOR:
                     NEB=NEB + DT*( BN*NDOT1+CN*NDOT2 );
                     TAU=TAU + DT*( BT*TDOT1+CT*TDOT2 );
                     END;
                /*UPDATE TIME DERIV.S, IMAGE POINTS, AND FIND PLASMA POWER GAIN*/
                  CV(0),CV(N+1)=0;
                  ESOURCE(0),ESOURCE(N+1)=0;
                  CALL DOT(NDOT1,TDOT1,NEB,TAU);
                  IVD=   0.5*( ESOURCE(1)-CV(1)*TDOT1(1) )
                        + SUMV( ESOURCE-CV*TDOT1, 2, N-1)
                        +0.5*( ESOURCE(N)-CV(N)*TDOT1(N) );
                  IVD=DZ*IVD+ 2*I*(TAU(1)-TAU(N)) - (NEB(1)*ENE/KN)*(TAU(1)-1);
        1

            /*   DOT: RETURNS WITH NEW NEBDOT AND TAUDOT.                    */
            /***********************************************************************/
            /*                                                              */
            /*     COLLECTOR EMISSION IS NEGLECTED.                         */
            /*                                                              */
            /*     THERMAL DIFFUSION RATIO IS INCLUDED.                     */
            /*                                                              */
            /*     APRIL 2, 1980,  (B.C. BASED ON MARCH 1, 1980 VERSION)    */
            /***********************************************************************/
        DOT:   PROC(NEBDOT, TAUDOT, NEB, TAU) REORDER;
               DECLARE
                  CHKDOT BIT(1) EXT INIT('0'B),/*IF 1 PRINT DIAGNOSTIC INFO */
                  SHEATH ENTRY(DEC(16),DEC(16),DEC(16),DEC(16),DEC(16),
                     DEC(16),DEC(16),DEC(16),DEC(16),DEC(16)),
                  (TAUDOT(*),
                   NEBDOT(*),
                   NEB(*),
                   TAU(*),
                   PC(0:N+1),                   /*CHARGED PARTICLE PRESSURE    */
                   F(15) EXT INIT(5.74E-3, 1.4E-3, 2.3, .2, .027, .00574,
                            .0424, 3.2, 61.893, 11.607, 15473, 27.04),

                /*SHEATH VARIABLES                                           */
                   NCMIN,                       /*MINIMUM NEB(N) TO ALLOW I.  */
                   U,GU,DELU,DGDU,DELTAU,
                /*TRANSPORT VARIABLES                                        */
                   FYEN EXT INIT(1),            /*YEN THERMAL CONDUCTIVITY FACT*/
                   K(0:N+1),                    /*THERMAL CONDUCTIVITY       */
                   MNS,                         /*SUM OF MUI*NEB AT J & J+1   */
                   MUIS,MURS,                   /*SUM OF MUI & MUR AT J,J+1   */
                /*CONSERVATION EQUATION VARIABLES                            */
                   EN_Z,CN_Z,                   /*SPATIAL NEB DERIVS         */
                   ET_ETA,ET_Z,CT_ETA,CT_Z,     /*SPATIAL DERIVS OF TAU      */
                   EDETA,CDETA,                 /*ETA XPACING BETWEEN GRID-PTS */
                   EPC_Z,CPC_Z,                 /*PC GRADIENT FROM B.C.      */
                   MURSOLD,MNSOLD,MUISOLD,
              NBCOA,TBCOA,NBCOB,TBCOB,NBCOC,TBCOC,
              NBC1A,TBC1A,NBC1B,TBC1B,NBC1C,TBC1C,
              NEBA(0:N+1),NA(0:N+1),NEBB(0:N+1),NB(0:N+1),
```

```
NEBC(0:N+1),NC(0:N+1),NEBV(0:N+1),ND(0:N+1),
NS(0:N+1),TAUA(0:N+1),TA(0:N+1),TAUB(0:N+1),
TB(0:N+1),TAUC(0:N+1),TC(0:N+1),TAUV(0:N+1),TS(0:N+1),
NEBU(0:N+1),TAUU(0:N+1),
ALPHA(0:N+1),BETA(0:N+1),

   /*TEMPORARY ENERGY EQUATION VARIABLES                        */
     QKM,QKP,
     DETA,DETAP,                    /*GRID PT SPACING IN ETA      */
     KDE,                           /*THERMAL COND X D ETA AVE     */
     CONVECTN,
     POHMIC,
     PB,PBP,                        /*ENERGY STORED IN EXCITED STAT*/
     SIGMA)
        FLOAT DEC(16),

   /*TEMPORARY DENSITY EQUATION VARIABLES                       */
     (GAMMAM,GAMMAP,
     D1B,D21B,D32B,PO,IB,NUE,    /*PARAMETERS FOR MSOURCE         */
     A,
     NES2)
        FLOAT DEC(16),
     (J,IJ) FIXED BIN(31);
   ON FINISH PUT SKIP(5) DATA;

/*SET THERMAL & ELECTRICAL CONDUCTIVITIES AT 0+ (E) &, 1- (C). */
   IF TAU(1)<0.1 THEN DO; TAU(1)=0.1; EFIX='1'B; END;
   IF TAU(N)<0.1 THEN DO; TAU(N)=0.1; CFIX='1'B; END;
   IF         RE=0.5 THEN MUEA=TAUN;
     ELSE IF RE=0.0 THEN MUEA=TAUN/SQRT(TAU);
     ELSE IF RE=-.5 THEN MUEA=TAUN/TAU;
     ELSE                 MUEA=TAUN*( TAU**(RE-0.5) );
   K=( (RE+2)/FYEN )*MUEA*NEB*TAU;
   PC=NEB*(TAU+TAUN);
   DETA,DETAP=LOG(K(2)/K(1)) * DZ/(K(2)-K(1));
/*DETERMINE EMITTER SHEATH                                      */
   CALL SHEATH(ECHI,ENE,I*KN/NEB(1),TAU(1),ENR/NEB(1),
                  TE, SMR, EALPHA, 0.8, ERR);
   IF ECHI<=1E-5 | ECHI>=20 THEN EFIX='1'B;
/*FIND EMITTER (0+) DERIVATIVES FROM B.C.                       */
   ET_ETA=(TAU(1)-1)*ENE*NEB(1)/KN - I*(ECHI-TAU(1)/2);
   ET_Z=ET_ETA/K(1);
   EPC_Z=(SQRT(PI/8/EALPHA)/LAMDAR/KN)*NEB(1)/MUI(1)
           - I/MUEA(1);
   EN_Z=( EPC_Z-NEB(1)*(ET_Z+DTAUNDZ) )/( TAU(1)+TAUN(1) );
/*SOLVE COLLECTOR SHEATH                                        */
   CALPHA=1/TAU(N);
   CNE=0;
    U=1.0;GU=G(U);DELU=.01;
    CON:DO IJ=1 TO 50;
        DGDU=(G(U+DELU)-GU)/DELU;
        DELTAU=-GU/DGDU;
        U=U+DELTAU;
        GU=G(U);
```

```
               IF(ABS(GU)<=.0001) THEN GO TO FIN;
          END CON;
PUT SKIP LIST(' COLLECTOR SHEATH FAILED TO CONVERGE');
STOP;
          CCHI=0; CFIX='1'B;
          GO TO FIN2;
          G:PROC(UX) RETURNS(DEC(16));
          DCL(UX,GX,SQX) DEC(16);
          IF (UX<=0.) THEN SQX=0.;
          ELSE SQX=SQRT(UX);
          GX=EXP(UX)*(1.+ERF(SQX))*2.
              -NEB(N)*SQRT(TAU(N))/I/KN;
          RETURN(GX);
          END G;
          FIN:CCHI=U*TAU(N);
          FIN2:
     /*DETERMINE DERIVATIVES AT COLLECTOR (1-) FROM B.C.              */
       CT_ETA=-I*(CCHI-TAU(N)/2);
       CT_Z=CT_ETA/K(N);
       CPC_Z=(-SQRT(PI/8/CALPHA)/LAMDAR/KN)*NEB(N)/MUI(N)
                - I/MUEA(N);
       CN_Z=( CPC_Z-NEB(N)*(CT_Z+DTAUNDZ) ) / ( TAU(N)+TAUN(N) );
       CDETA=LOG(K(N)/K(N-1)) * DZ/(K(N)-K(N-1));

     NBCOA=TAU(1)+TAUN(1);
     NBCOB=SQRT(PI/EALPHA/8.)/LAMDAR/KN/MUI(1)-ENE*NEB(1)/K(1)*
             (TAU(1)-1.)-DTAUNDZ;
     NBCOC=I*NEB(1)/K(1)*(ECHI-TAU(1)/2.)-I/MUEA(1);
     NBC1A=TAU(N)+TAUN(N);
     NBC1B=-SQRT(PI/CALPHA/8.)/LAMDAR/KN/MUI(N)-CNE*NEB(N)/K(N)*
             (TAU(N)-1.)+DTAUNDZ;
     NBC1C=-I*NEB(N)/K(N)*(CCHI-TAU(N)/2.)-I/MUEA(N);
     TBCOA=1.;
     TBCOB=ENE*NEB(1)/KN+I/2.;
     TBCOC=-ENE*NEB(1)/KN-I*ECHI;
     TBC1A=-1.;
     TBC1B=CNE*NEB(N)/KN-I/2.;
     TBC1C=-CNE*NEB(N)/KN+I*CCHI;

     NEBA(0)=(NBCOA*LAMNEB)/(2.*DZ);
     NEBB(0)=-LAMNEB*NBCOB;
     NEBC(0)=-NBCOA*LAMNEB/(2.*DZ);
     NEBV(0)=NBCOB*(1.-LAMNEB)*NEB(1)+NBCOC-(1.-LAMNEB)*
         NBCOA*(NEB(2)-NEB(0))/(2.*DZ);
     TAUA(0)=TBCOA*LAMTAU/(2.*DETAP);
     TAUB(0)=-LAMTAU*TBCOB;
     TAUC(0)=-TBCOA*LAMTAU/(2.*DETAP);
     TAUV(0)=TBCOB*(1.-LAMTAU)*TAU(1)+TBCOC-(1.-LAMTAU)*
         TBCOA*(TAU(2)-TAU(0))/(2.*DETAP);

     NEBA(N+1)=(NBC1A*LAMNEB)/(2.*DZ);
     NEBB(N+1)=-LAMNEB*NBC1B;
     NEBC(N+1)=-NBC1A*LAMNEB/(2.*DZ);
     NEBV(N+1)=NBC1B*(1.-LAMNEB)*NEB(N)+NBC1C-(1.-LAMNEB)*
```

```
                NBC1A*(NEB(N+1)-NEB(N-1))/(2.*DZ);
TAUA(N+1)=TBC1A*LAMTAU/(2.*CDETA);
TAUB(N+1)=-LAMTAU*TBC1B;
TAUC(N+1)=-TBC1A*LAMTAU/(2.*CDETA);
TAUV(N+1)=TBC1B*(1.-LAMTAU)*TAU(N)+TBC1C-(1.-LAMTAU)*
    TBC1A*(TAU(N+1)-TAU(N-1))/(2.*CDETA);

 /*INITIALIZE GAMMAP & QKP FOR LOOP.                         */
   MNS=MUI(1)*NEB(1)+MUI(2)*NEB(2);
   MURS=MUI(2)/MUEA(2) + MUI(1)/MUEA(1)*( 1 -2*DZ*(
                   (0.5-RE)*ET_Z/TAU(1) - 0.5*DTAUNDZ/TAUN(1)) );
   GAMMAP=   0.5*( ( (MUI(1)+MUI( 2 ))*(PC( 1 )-PC(0))
               )/DZ +I*MURS );
   QKP=(TAU(1)-TAU(0))/DETA;
   MUIS=MUI(1)+MUI(2);

   DO J=1 TO N;
      /*UPDATE FOR NEW J.                                    */
      GAMMAM=GAMMAP;
      QKM=QKP;
      DETA=DETAP;
       MNSOLD=MNS;
       MUISOLD=MUIS;
       MURSOLD=MURS;
      IF J¬=N
         THEN DO;
            DETAP=LOG(K(J+1)/K(J)) * DZ/(K(J+1)-K(J));
            MNS=MUI(J)*NEB(J)+MUI(J+1)*NEB(J+1);
            MUIS=MUI(J)+MUI(J+1);
            MURS=MUI(J)/MUEA(J) + MUI(J+1)/MUEA(J+1);
            END;
         ELSE
            MURS=MURS +2*DZ*(MUI(N)/MUEA(N))*((.5-RE)*CT_Z/TAU(N)
                               - 0.5*DTAUNDZ/TAUN(N));
      /*FIND AMBIPOLAR FLUX AT J+1/2.                         */
      GAMMAP=0.5*( ( MUIS*(PC(J+1)-PC(J))
               )/DZ +I*MURS );
      /*FIND MASS SOURCE AT J.                                */
      A=CA/TAU(J)**4.5;
      NES2=NNB(J) * TAU(J)**1.5 * EXP( CSAHA-EGNDB/TAU(J) );
      D21B=F(7)*(1+F(8)/TAU(J));
      D32B=F(2)*EXP(F(3)/TAU(J));
      IB=A*NES2*( 1+F(1)/NEB(J) )/( 1+D21B*(1+D32B/NEB(J))/NEB(J)
                               );
      P0=1+( F(4)/NEB(J) )*( 1+F(5)/NEB(J) )/( 1+F(6)/NEB(J) );
      NUE=NEB(J)*NEB(J)/NES2;
      MSOURCE(J)=NEB(J)*IB*( 1-P0*NUE );
    IF(IDEN=1) THEN
      MSOURCE(J)=NEB(J)*A*NES2;

      NEBDOT(J)=RMUR*(GAMMAP-GAMMAM)/DZ + MSOURCE(J);

NA(J)=RMUR*MUIS*(TAU(J+1)+TAUN(J+1))/2./DZ**2;
NB(J)=RMUR*(MUIS+MUISOLD)*(TAU(J)+TAUN(J))/2./DZ**2;
```

```
NC(J)=RMUR*MUISOLD*(TAU(J-1)+TAUN(J-1))/2./DZ**2;
ND(J)=I*(MURS-MURSOLD)*RMUR/DZ/2.;
NS(J)=IB*(1.-PO*NUE);
IF(IDEN=1) THEN
 NS(J)=A*NES2;


NEBA(J)=-DT*NA(J)*LAMNEB;
NEBB(J)=1.+DT*NB(J)*LAMNEB-DT*NS(J)*LAMNEB;
NEBC(J)=-DT*NC(J)*LAMNEB;
NEBV(J)=NEB(J)+DT*NA(J)*(1.-LAMNEB)*NEB(J+1)-DT*NB(J)*
     (1.-LAMNEB)*NEB(J)+DT*NC(J)*(1.-LAMNEB)*NEB(J-1)+
    DT*ND(J)+DT*NS(J)*(1.-LAMNEB)*NEB(J);

    KDE=K(J)*(DETA+DETAP)/2;
    QKP=(TAU(J+1)-TAU(J))/DETAP;

    CONVECTN=-(1.5)*I*(DETA*QKP+DETAP*QKM)/(2*KDE);
    SIGMA=NEB(J)*MUEA(J);
    POHMIC=I*( I/SIGMA + TAU(J)*( NEB(J+1)-NEB(J-1) )
                                  / (2*DZ*NEB(J)));
    PBP=( F(9)*NNR/NR )*EXP( -F(10)/TAU(J) );
    PB=( F(11)*NNR/NR )*EXP( -F(12)/TAU(J) );
    CV(J)=1.5*NEB(J) + NNB(J)*(F(10)*PBP+F(12)*PB*NUE)
                                  / (TAU(J)*TAU(J));
    ESOURCE(J)=-ELOSSB*MSOURCE(J)
                    - NNB(J)*PB*( 2*NUE*NEBDOT(J)/NEB(J) );

    TAUDOT(J)=( (QKP-QKM)/KDE + CONVECTN + POHMIC + ESOURCE(J) )
          / CV(J);

TA(J)=1./(DETAP*KDE*CV(J));
TB(J)=(1./DETAP+1./DETA)/KDE/CV(J);
TC(J)=1./DETA/KDE/CV(J);
TS(J)=(CONVECTN+POHMIC+ESOURCE(J))/CV(J);
TAUA(J)=-DT*LAMTAU*TA(J);
TAUB(J)=1.+DT*LAMTAU*TB(J);
TAUC(J)=-DT*LAMTAU*TC(J);
TAUV(J)=TAU(J)+DT*(1.-LAMTAU)*TA(J)*TAU(J+1)
     -DT*(1.-LAMTAU)*TB(J)*TAU(J)
     +DT*(1.-LAMTAU)*TC(J)*TAU(J-1)
     +TS(J)*DT;


    IF CHKDOT THEN PUT SKIP(2) DATA(NEB(J),TAU(J),MSOURCE(J),
         J,PB,PBP,A,
            D21B,D32B,PO,IB,NUE,NES2,QKP,GAMMAP,DETAP,MURS);
    END;


NEBC(0)=NEBC(0)-NEBC(1)*NEBA(0)/NEBA(1);
NEBB(0)=NEBB(0)-NEBB(1)*NEBA(0)/NEBA(1);
NEBV(0)=NEBV(0)-NEBV(1)*NEBA(0)/NEBA(1);
NEBA(0)=NEBB(0);
NEBB(0)=NEBC(0);
```

```
NEBA(N+1)=NEBA(N+1)-NEBA(N)*NEBC(N+1)/NEBC(N);
NEBB(N+1)=NEBB(N+1)-NEBB(N)*NEBC(N+1)/NEBC(N);
NEBV(N+1)=NEBV(N+1)-NEBV(N)*NEBC(N+1)/NEBC(N);
NEBC(N+1)=NEBB(N+1);
NEBB(N+1)=NEBA(N+1);

TAUC(0)=TAUC(0)-TAUC(1)*TAUA(0)/TAUA(1);
TAUB(0)=TAUB(0)-TAUB(1)*TAUA(0)/TAUA(1);
TAUV(0)=TAUV(0)-TAUV(1)*TAUA(0)/TAUA(1);
TAUA(0)=TAUB(0);
TAUB(0)=TAUC(0);
TAUA(N+1)=TAUA(N+1)-TAUA(N)*TAUC(N+1)/TAUC(N);
TAUB(N+1)=TAUB(N+1)-TAUB(N)*TAUC(N+1)/TAUC(N);
TAUV(N+1)=TAUV(N+1)-TAUV(N)*TAUC(N+1)/TAUC(N);
TAUC(N+1)=TAUB(N+1);
TAUB(N+1)=TAUA(N+1);

ALPHA(0)=-NEBA(0)/NEBB(0);
LOOP1:DO J=1 TO N;
    ALPHA(J)=-NEBA(J)/(NEBC(J)*ALPHA(J-1)+NEBB(J));
END LOOP1;
ALPHA(N+1)=0.;
BETA(0)=NEBV(0)/NEBB(0);
LOOP2:DO J=1 TO (N+1);
 BETA(J)=(NEBV(J)-NEBC(J)*BETA(J-1))/(NEBC(J)*ALPHA(J-1)+NEBB(J));
END LOOP2;
NEBU(N+1)=BETA(N+1);
LOOP3:DO J=N TO 0 BY(-1);
      NEBU(J)=ALPHA(J)*NEBU(J+1)+BETA(J);
END LOOP3;

ALPHA(0)=-TAUA(0)/TAUB(0);
LOOP4:DO J=1 TO N;
    ALPHA(J)=-TAUA(J)/(TAUC(J)*ALPHA(J-1)+TAUB(J));
END LOOP4;
ALPHA(N+1)=0.;
BETA(0)=TAUV(0)/TAUB(0);
LOOP5:DO J=1 TO (N+1);
 BETA(J)=(TAUV(J)-TAUC(J)*BETA(J-1))/(TAUC(J)*ALPHA(J-1)+TAUB(J));
END LOOP5;
TAUU(N+1)=BETA(N+1);
LOOP6:DO J=N TO 0 BY(-1);
      TAUU(J)=ALPHA(J)*TAUU(J+1)+BETA(J);
END LOOP6;

NEBDOT=(NEBU-NEB)/DT;

TAUDOT=(TAUU-TAU)/DT;
   IF CHKDOT THEN PUT SKIP(3) DATA;
   END DOT;
   END PREDCOR;
```

C.2 SHEATH: Computes the Sheath Model Solution

```
SHEATH:PROC(OUTCHI,OUTNE,INCUR,INTAU,INNRNP,INTE,INMEMI,
      OUTALP,INDUM,INERR);
    DCL(JBAR,INCUR,CE,INTAU,NRP,INNRNP,TE,INTE,SMR,INMEMI,ERR,
      UZERO,
      PHIZ,INDUM,INERR,CI,PHIM,OUTCHI,NEB,OUTNE,OUTALP,VI)
      DEC(16);
    UZERO=2.1;
    CE=INTAU;
    JBAR=INCUR*2./SQRT(3.14159)*SQRT(2./CE);
    NRP=INNRNP;
    TE=INTE;
    SMR=INMEMI;   /* SQUARE ROOT OF MASS RATIO */
    ERR=INERR;
    CI=1.;

    PHIM=REPHIM(JBAR,CE,CI);
    NEB=RENEB(JBAR,PHIM,CE,CI);
    PHIZ=LOG(INNRNP/NEB);
    VI=REVI(UZERO,PHIZ,PHIM,CE,CI);
    IF(VI<=.001) THEN VI=.001;

    OUTCHI=PHIM;
    OUTNE=NEB;
    OUTALP=1./CE/(VI)**2;

    RETURN;

      REPHIM:PROC(TJBAR,TCE,TCI) RETURNS( DEC(16));
      DCL(TJBAR,TCE,TCI,TPHIM,TA,TB) DEC(16);
       TA=(.5000*SQRT(2.)-.2900*SQRT(1.))/
          (SQRT(2.)-SQRT(1.));
       TB=(.5000-.2900)/(SQRT(1./1.)-SQRT(1./2.));
       TPHIM=(TB/(TA-TJBAR) )**2 *TCE/2.1;
      RETURN(TPHIM);
      END REPHIM;

      RENEB:PROC(TJBAR,TPHIM,TCE,TCI) RETURNS( DEC(16));
      DCL(TJBAR,TCE,TCI,TNEB,TPHIM,SQRTPI,SQRTCE,SQPHCE,
          C1,C2,EXPHCE) DEC(16);
        SQRTPI=SQRT(3.1415926);
        SQRTCE=SQRT(TCE);
        SQPHCE=SQRT(TPHIM/TCE);
        C1=1.+ERF(SQPHCE);
        IF(TPHIM>10.) THEN
             C2=0.;
        ELSE
             C2=EXP(TPHIM)*( 1. - ERF(SQRT(TPHIM)) );
        EXPHCE=EXP(-TPHIM/TCE);
```

```
    TNEB=(TJBAR*SQRT(TCE/2.)+SQRTCE/C1*EXPHCE/SQRTPI)/
       (1./SQRTPI+SQRTCE/SQRTPI*C2/C1*EXPHCE);
RETURN(TNEB);
END RENEB;

REVI:PROC(TUZERO,TPHIZ,TPHIM,TCE,TCI) RETURNS( DEC(16));
DCL(TUZERO,TPHIZ,TPHIM,TCE,TCI,TVI,R) DEC(16);
R=0.;
IF(TPHIZ-TPHIM>0.) THEN R=SQRT((TPHIZ-TPHIM)/TCI);
TVI=SQRT(2.*TCI/TCE)*( TUZERO*SQRT(3.14)/2.*(1.-ERF(R-TUZERO))
     + EXP(-(R-TUZERO)**2)/2. )/( SQRT(3.14)/2.*(1-ERF(-TUZERO)));
RETURN(TVI);
END REVI;

END SHEATH;
```

END

FILMED

3-85

DTIC